BULLETIN OF THE EARTHQUAKE RESEARCH INSTITUTE,
UNIVERSITY OF TOKYO. Vol. 39, Part 1. March, 1961.

東京大学
地震研究所彙報

第39号　第1冊

昭和36年3月

目次

論文及報告

頁
1. 日本周辺の海洋底をつたわるレーリー波の分散（第三報）一東南太平洋の地殻構造一（英文）……三東哲夫 1
2. 微動について（英文）……赤松敬 23
3. 観測による土地の脈動の研究 続報（英文）……岸上冬彦 77
4. 強震動スペクトルに関する実験式（英文）……金井清 85
5. 常時微動について 第8報（英文）……金井清・田中貞二 97

(The titles in occidental languages are given on the back cover.)

地震研究所彙報は，年4回定期に（ただし，第1号より第6号までは不定期に，第7号は3冊として刊行された），彙報別冊は不定期に刊行される．

この彙報に載せられた論文及び報告についての責任は，すべてその著者のみにある．

この彙報についての照会通信は，すべて東京大学地震研究所長にあてられたい．

The Bulletin is published quarterly. (Vols. 1–6 were published at irregular intervals and Vol. 7 consisted of three parts.)
Supplementary Volume is published at irregular interval.

The authors of the papers alone are responsible for the statements and opinions contained in their respective papers.

All communications relating to this Bulletin should be addressed to the Director of the Earthquake Research Institute, University of Tokyo, Japan.

Earthquake Research Institute, University of Tokyo
Address:
No. 1, Motofuji-cho, Bunkyo-ku,
Tokyo Metropolis, Japan.
Telephone: 921-3161-Extension 6506
Cable address: ZISINKEN, TOKYO.

東京大学地震研究所
所在地
東京都文京区本富士町一番地
電話　小石川 921—3161（代）構内 6506
電略　ブンケウ　トウダイ　ヂシン

BULLETIN OF THE EARTHQUAKE RESEARCH INSTITUTE
Vol. 39 (1961), pp. 1-22

1. *Rayleigh Wave Dispersions across the Oceanic Basin around Japan (Part III).*

—On the Crust of the South-Western Pacific Ocean—

By Tetsuo A. SANTÔ,

Earthquake Research Institute.

(Read Oct. 18, 1960.—Received Dec. 26, 1960.)

1. Introduction

In the two previous papers,[1),2)] the writer studied the dispersion of Rayleigh waves which travelled along various oceanic paths to reach Japan. One of the important facts we obtained was that the dispersive character of Rayleigh waves changes gradually from an oceanic to a continental one when the travelling paths change northwest to south around Japan. Geographically speaking, the dispersive characteristics were almost uniform and purely oceanic for the paths across the region where neither oceanic island nor atoll exists, while they showed a slight difference from the oceanic when the path runs through the Polinesia or Micronesia region which contains " the rashes " given above. Further, when a section of the path entered the western side, the continental side of the " Andesite line ",[3)] the departure of the dispersive character of Rayleigh waves from the oceanic became marked and at last they became purely continental for the westernmost path, from Sumatra Island to Japan. The abundant dispersion data were classified into seven groups, numbered from 1 to 7 in the order from the purely oceanic to the continental type. From the geographical and the geological point of view, the following two factors seem to bring about a decrease in the group velocities of Rayleigh waves and therefore change the dispersion curves from oceanic to continental ones; that is, (i) the ex-

---

[1)] T. A. SANTÔ, " Observation of Surface Waves by Columbia-type Seismograph Installed at Tsukuba Station, Japan (Part I).—Rayleigh Wave Dispersions across the Oceanic Basin—," *Bull. Earthq. Res. Inst.*, **38** (1960), 237.

[2)] T. A. SANTÔ, " Rayleigh Wave Dispersions across the Oceanic Basin around Japan (Part II)," *Bull. Earthq. Res. Inst.*, **38** (1960), 385.

[3)] H. H. HESS, " Major Structural Features of the Western North Pacific. An Interpretation of H. O. 5485, Bathymetric Chart. Korea to New Guinea," *Bull. Geol. Soc. Amer.*, **59** (1948), 417.

istence of " the rashes " on the ocean floor such as oceanic islands, atolls or Guyots, and (ii) the continental crustal structure in the western side of the " Andesite line " in the western Pacific Ocean.

These suggestions may be affirmed by re-examining the dispersion data obtained by J. E. Oliver et al.[4] They studied the dispersions of Rayleigh waves which travelled along various paths to Hawaii. Plotting their data on our group velocity ∼ period diagram (our velocity scale to period scale is ten times larger than that in their paper), it was clarified up that these data also lead to the same conclusions (Fig. 1). That is, the Rayleigh waves which travelled the non-island region from the Marianas, Kuriles or Chile to Honolulu show the No. 1 dispersive characteristics according to our characteristic numbers, while they show the No. 2 characteristics owing to the shocks of the Solomons, Tongas or southern Japan, the paths of which contain oceanic islands. Rayleigh waves owing to the Formosa or Luzon shocks give Honolulu Station such dispersive characteristics as No. 3 or No. 4 according to our characteristic numbers, the paths of which enter deeply the continental side of the " Andesite line."

Then, what kind of crustal conditions at or around the " rashes " on the oceanic basin or around the " Andesite line " bring about a lowering in the group velocities of Rayleigh waves ?

The main purpose of this third paper is to discuss this point, and to give some information about the crustal conditions in the western side of the " Andesite line ", especially in and around the Philippine basin and Melanesia region, which is one of the most anomalous structures and has been inaccessible to geophysical research.

2. The relation between the sea depth and the dispersive feature of Rayleigh waves

In order to compare our observed dispersion data with the theoretical curves for some crustal models, it is desirable to know the average depths of the sea water which covers the crust along each path.

For this purpose, topographies of the sea bed along all of the travelling paths were examined. Some examples are shown in Fig. 2. The average sea depths ($\overline{D}$) along the paths were measured from these

---

[4] J. E. OLIVER, M. EWING and F. PRESS, "Crustal Structure and Surface-Wave Dispersion, Part IV. Atlantic and Pacific Ocean Basins," *Bull. Geol. Soc. Amer.*, **66** (1955), 913.

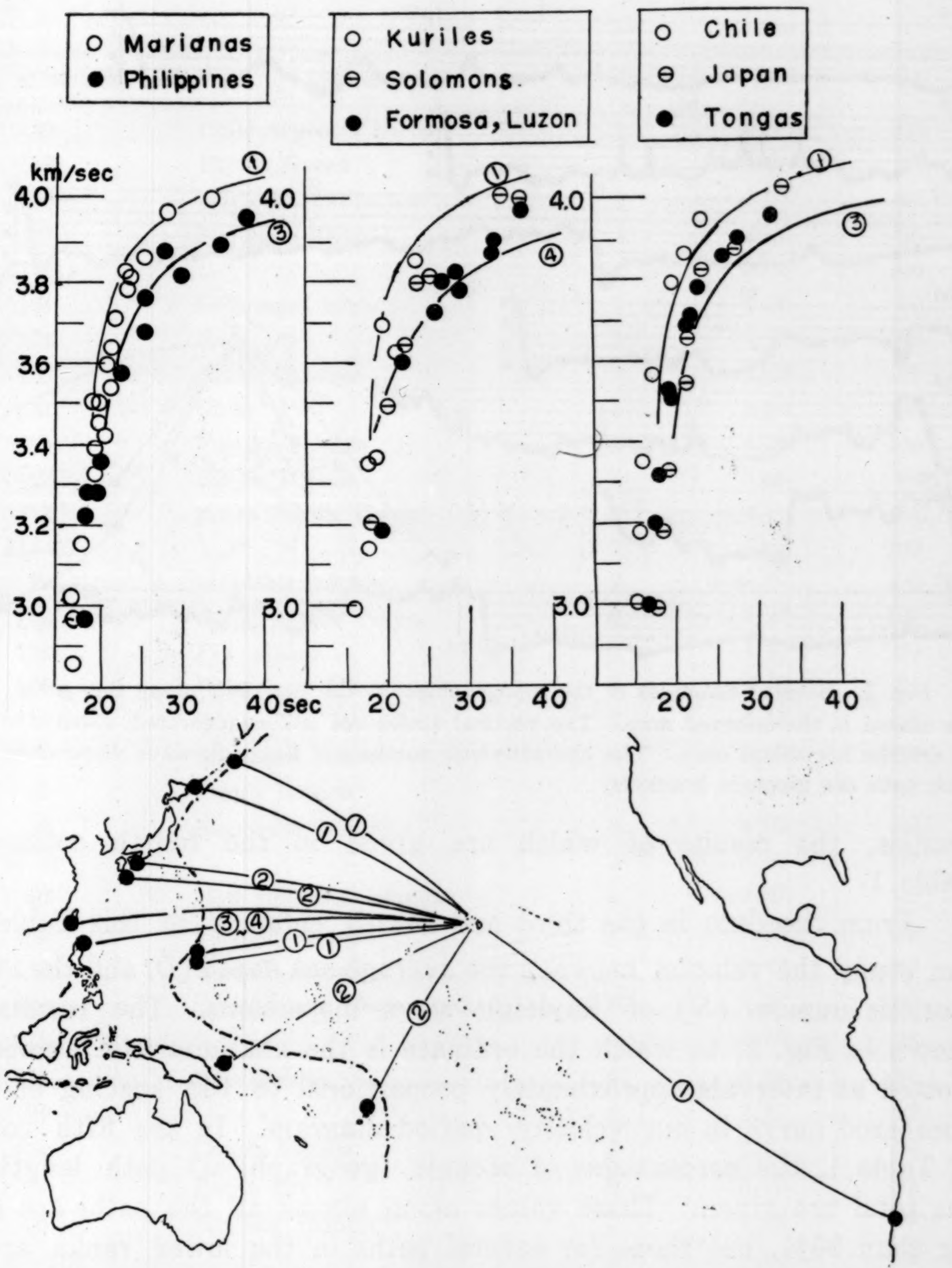

Fig. 1. Dispersive features of Rayleigh waves observed at Hawaii by J. Oliver et al. Original data were re-plotted on the new diagrams in which the ratio of the velocity scale to the period scale is ten times larger than the original one. Our classified dispersion curves and their corresponding characteristic numbers are given for comparison.

·—·—·— Andesite line.

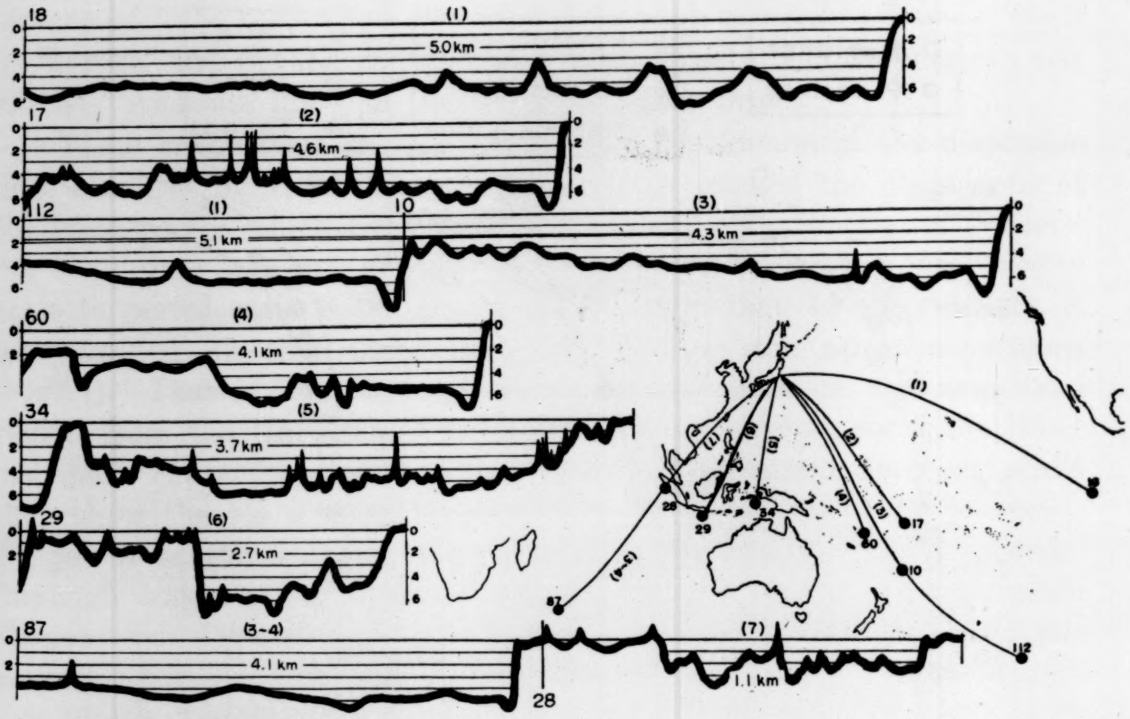

Fig. 2. Several examples of the topographies of the sea bed along the paths which are shown in the annexed map. The vertical scales are all exaggerated about 170 times as are the horizontal ones. The characteristic numbers of Rayleigh wave dispersions along each path are given in brackets.

profiles, the results of which are given in the fourth column of Table 1.

From the data in the third and fourth columns in this Table, we can study the relation between the average sea depth ($\overline{D}$) and the characteristic number (N) of Rayleigh wave dispersions. The results are shown in Fig. 3, in which the ordinate is the characteristic number N plotted at intervals approximately proportional to the spacing of each numbered curve in our velocity$\sim$period diagram. In the fifth column of Table 1, the percentages of oceanic (geographical) path lengths to the total are given. These values along almost all the paths are greater than 90%, but those for several paths in the lower ranks are remarkably small. Therefore, the data of $\overline{D}$ and N for these paths (represented by white marks in Fig. 3) must be shifted somewhat leftward (e.g., towards smaller characteristic numbers) if we subtract the travel-times for the continental part and make the dispersion curves for almost oceanic paths.

Before we discuss these results, it must be noticed that the observ-

Table 1.

No. of shocks	District	N	$\overline{D}$	%
30	Chile-Argentin border	1	4.56	100
18	Pacific Ocean	1	5.01	99
59	Northern California	1	4.78	98
27	Northern Chile	1	4.92	99
112-11		1	5.02	100
104	Galapagos Islands	1	4.28	99
124	Peru	1	4.54	100
105	Drake Passage	2	4.08	99
131	Chile	2	4.30	100
139	Eastern Islands	2	4.58	100
17	Samoa Islands	2	5.05	99
112	South Pacific Ocean	2	4.60	100
113-60		2	4.47	100
19	Marshall Islands	2	4.60	100
113	South Pacific Ocean	3	4.28	100
128	Fiji Islands	3	4.43	99
125	Helmahera Islands	3	4.19	96
116	Santa Cruz Islands	3	4.15	99
77	Mindanao Islands	3	4.45	92
13	Tonga Islands	3	4.25	97
10	Kermadec Islands	3	4.30	99
87-28		3	4.10	97
60	New Hebrides Islands	4	4.07	99
121	Solomon Islands	4	4.38	99
138	Norfolk Islands	4	3.47	99
134	South Island, New Zealand	4	3.39	97
111	〃	4	3.74	98
126	New Guinea	4	3.54	91
21	〃	4	3.31	95
114	Ceram Islands	4	3.77	94
34	Banda Sea	5	3.70	92
56	Molluca Passage	5	4.06	97
111-121		5	2.60	96
101	Celebes Island	5	3.61	85
90	Balleny Islands	6	2.29	78
33	Antarctic Ocean	6	1.85	63
29	Java Island	6	2.26	85
28	Sumatra Island	7	1.11	69

The last column means the percentage of the length of the oceanic paths.

ed variation of the dispersive characteristics indicated by numbers from 1 to 7 cannot be explained by the single effect of the variation of sea water depth. For, if the crustal structure beneath the water is the same and only the water depth varies, the dispersion curve must vary almost horizontally as is shown in Fig. 4. This is quite different from the observed one. As will be shown in the later section, the variation of the dispersion curves from 1 to 7 can be explained by changing the crustal properties beneath the water into more continental ones. Therefore, we may say from the results in Fig. 3 that, on the average, the crustal structure becomes oceanic with the increasing sea depth.

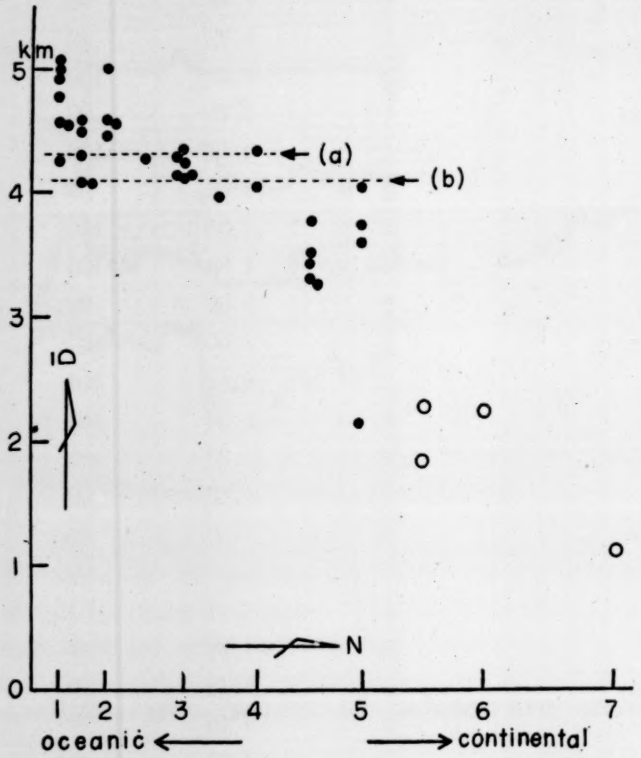

Fig. 3. The relation between $\bar{D}$ (the mean sea depth along the path) and N (the characteristic number of dispersive features). The white circles mean the data for which the path contains more than a 10% continental (geographical) part.

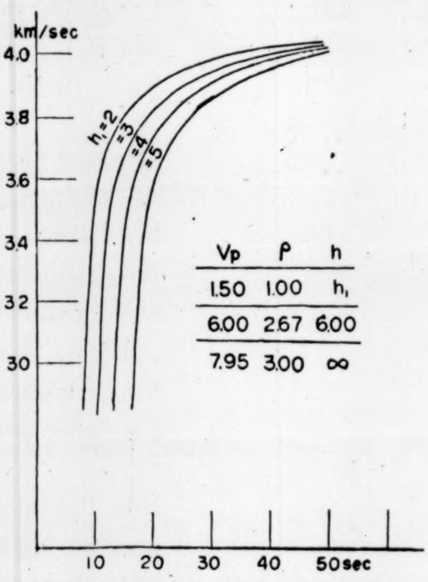

Fig. 4. Rayleigh wave dispersion curves for various depths of sea water over the same crustal structure.

There is another noticeable fact, that is, many points with values of $\bar{D}$ between 4.0 km and 4.3 km show especially large horizontal scattering. For instance, the characteristics numbers of the dispersion for several points around a dotted line (a) ($\bar{D}=4.30$ km) change from 1 to 4, and those around (b) ($\bar{D}=4.10$ km) from 2 to 5.

This fact means that there are peculiar regions in which the crustal structure differs remarkably in spite of an almost similar average water depth.

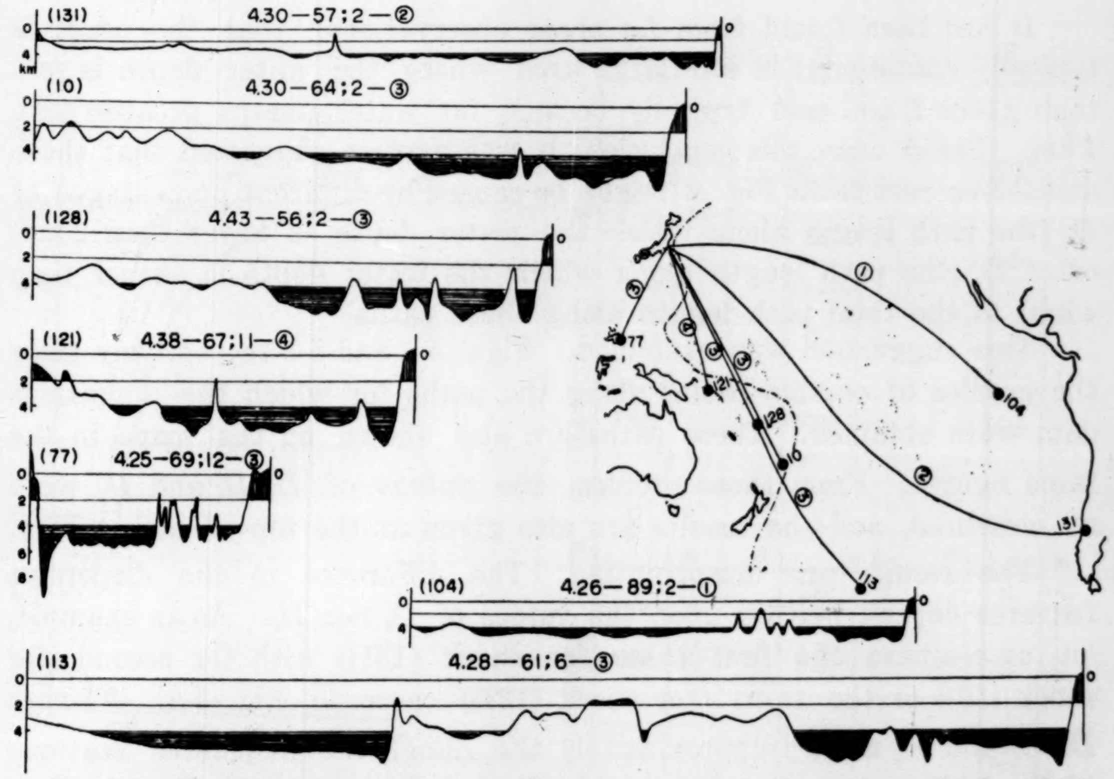
(131)
4.30—57;2—②
(10)
4.30—64;2—③
(128)
4.43—56;2—③
(121)
4.38—67;11—④
(77)
4.25—69;12—⑤
(104)
4.26—89;2—①
(113)
4.28—61;6—③
0
2
4
6
8
km
77
121
128
16
113
104
131

Fig. 5-a. Travelling paths and the profiles of the sea bed along the paths for which the data around (a) line in Fig. 3 were obtained. In each profile, the numbers in the brackets are the shock numbers. The values of $\overline{D}$, the percentage of D_4, D_2 and the characteristic number N are represented in this order above each profile. All the vertical scale of the profiles are exaggerated about 170 times as are the horizontal ones.

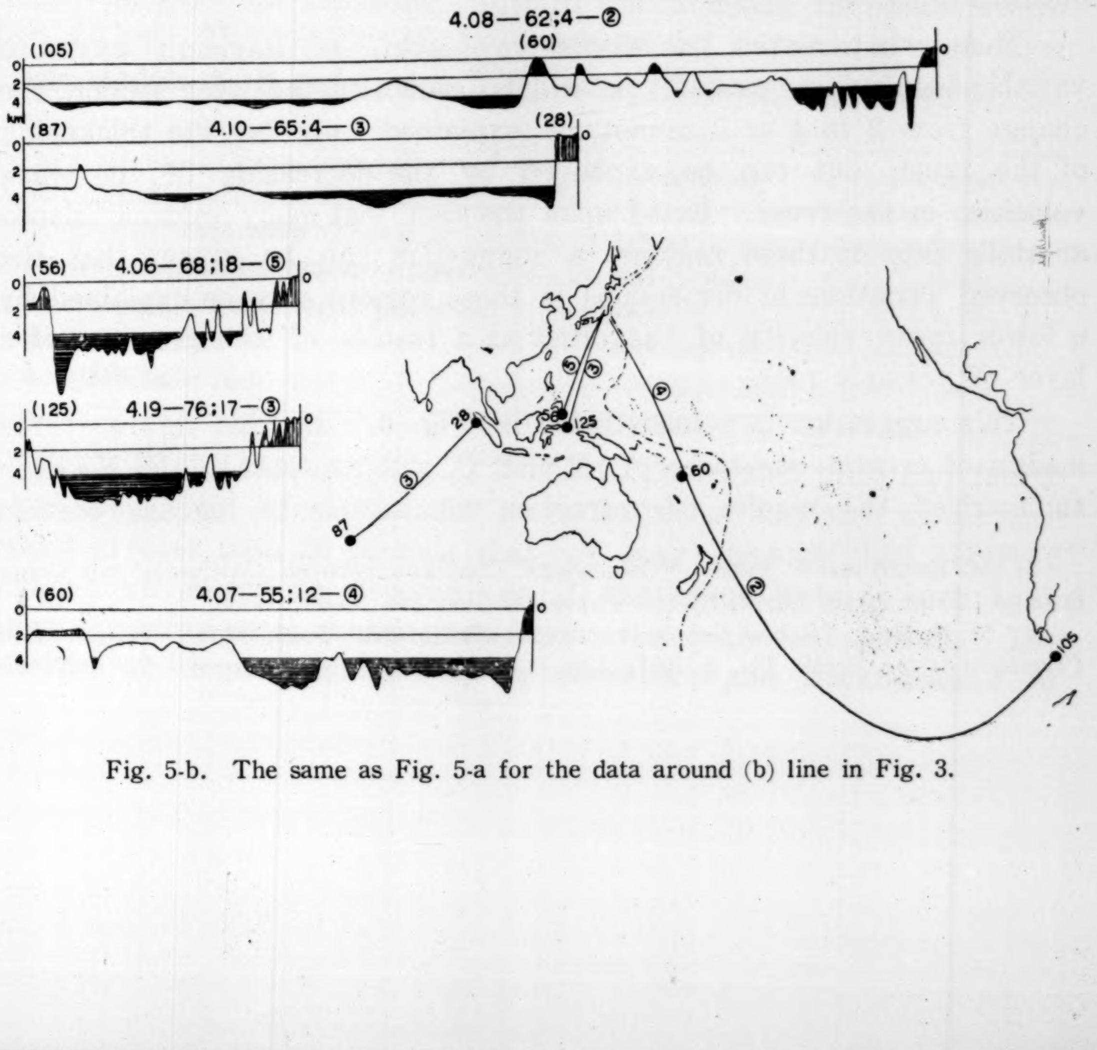
4.08—62;4—②
(105)
(60)
(87)
4.10—65;4—③
(28)
(56)
4.06—68;18—⑤
(125)
4.19—76;17—③
(60)
4.07—55;12—④
0
2
4
km
87
28
56
125
60
105

Fig. 5-b. The same as Fig. 5-a for the data around (b) line in Fig. 3.

It has been found from *Lg* phase observations[5] that the crust is typically continental in any large area where the water depth is less than about 2 km, and typically oceanic for water depths greater than 4 km. Based upon this conclusion, it was at first suggested that these anomalous results in Fig. 3 might be caused by different percentages of D_2 (the path length along which the water depth is lower than 2 km) or of D_4 (the path length along which the water depth is deeper than 4 km) to the total path length along these paths.

This suggestion was examined. Figs. 5-a and 5-b respectively show the profiles of oceanic basins along the paths for which the anomalous data were obtained. These paths are also shown on the maps in the same figures. From these profiles, the values of $\bar{D}$, D_4 and D_2 were all measured, and the results are also given at the top of each profile.

The results are disappointing. The difference in the dispersive features depend neither upon the values of D_4 nor D_2. As an example, let us compare the first case (for shock (131)) with the second (for shock (10)) or the third (for shock (128)) cases in Fig. 5-a. Though $\bar{D}$, D_4 and D_2 are all approximately the same, the dispersive features of Rayleigh waves along the path due to shock (131) (belonging to 2) differs from the two others (both belong to 3). The similar fact can be recognized by comparing the cases of shocks (121) and (77) in the same figure, and between (105) and (87), (56) and (125) in the next figure 5-b.

Then, what makes the dispersive feature of Rayleigh waves so variable along these paths? As will be shown in the later section, the change from 2 to 4 or 5 cannot be explained only be the thickening of the crust, but can be explained by the decreasing of the wave velocities in the crust. Based upon the fact that many volcanic islands or atolls exist in these regions, a suggestion can be given, that the observed variations of dispersions in these regions may be explained by a lower mean velocity of the crust as a results of the presence of a layer of volcanic rock.

This suggestion is demonstrated in Fig. 6. In this figure, three models of crustal structure A, B and C are presented. M. N. Hill[6] summarized the results of refraction measurements for the oceanic

---

5) M. EWING and F. PRESS, "Geophysical Contrasts between Continents and Ocean Basins," *Crust of the Earth. Special Paper 62, Geol. Soc. Amer.*, (1955), 1.

6) M. N. HILL, "Recent Geophysical Exploration of the Ocean Floor," *Physics and Chemistry of the Earth, Vol. 2* (1957), 129.

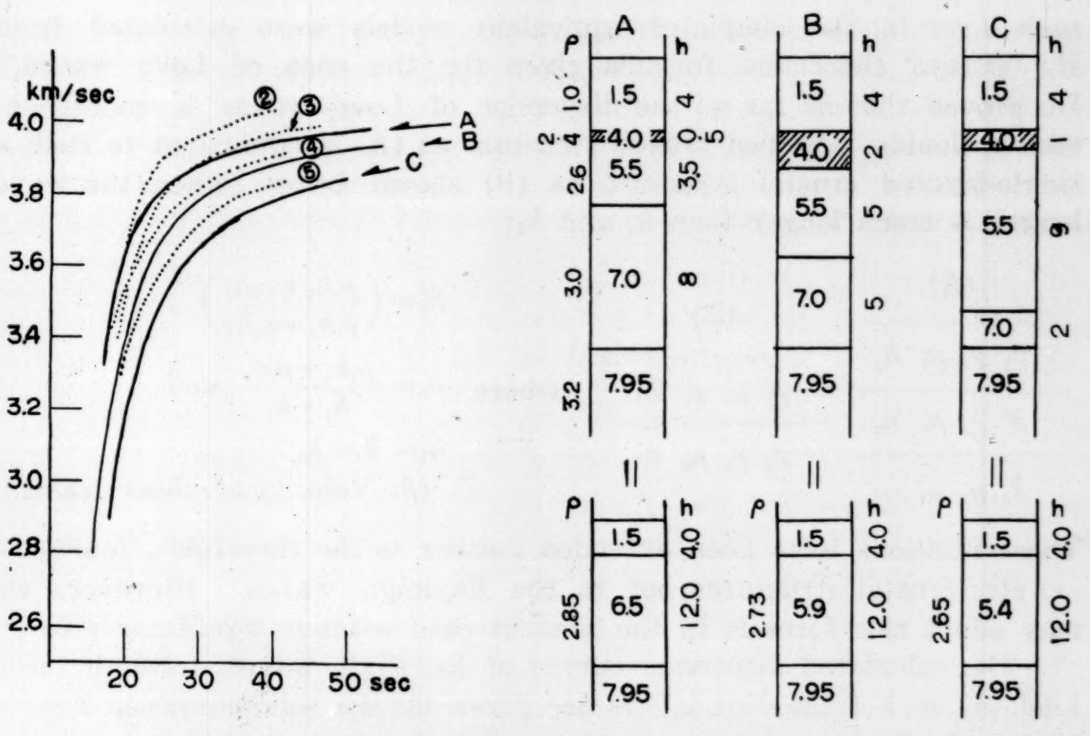

Fig. 6. This figure demonstrates that the dispersive character of Rayleigh waves greately varies with the presence of a layer of volcanic rock of varying thickness (hatched layer).

basins and gave the following standard crustal model for oceans deeper than 4.0 km. The velocity of the compressional waves α in each layer in our models A, B and C was based on a reference to his model.

Layer	α (km/sec)	h (km)
Sea water	1.5	4.5
1. Unconsolidated sedimentary layer	2 (1.5~2.5)	0.45
2. Volcanic or consolidated sediments	4~6	1.75
3. Basaltic rock	6.71 (6.4~7)	4.7
4. Ultra basic rock	7.09 (7.9~8.4)	∞

Since in our three models A, B and C, the second, third and fourth layers themselves are so thin for wave lengths of Rayleigh waves with periods greater than 20 seconds that we may suppose that observed Rayleigh waves will be dispersed as if the crust were of such equivalent structure as is shown just below the individual models. The velocities of compressional waves α, densities ρ and thicknesses h of each layer in the simplified equivalent models were calculated from H. Jeffreys' theoretical formula given for the case of Love waves.[7] He proved that as far as the dispersion of Love waves is concerned, such a doubly stratified crustal structure as (A) is equivalent to such a single-layered crustal structure as (B) shown below, when the wave length is much longer than h_1 and h_2:

$$\begin{array}{c} \text{(A)} \\ \hline \beta_1\ \rho_1\ \mu_1\ h_1 \\ \hline \beta\ \rho_2\ \mu_2\ h_2 \\ \hline \beta_3\ \rho_3\ \mu_3\ \infty \end{array} = \begin{array}{c} \text{(B)} \\ \hline \beta'_1\ \rho'_1\ \mu'_1\ h'_1 \\ \hline \beta_3\ \rho_3\ \mu_3\ \infty \end{array} \quad \text{where} \quad \begin{array}{l} \beta'_1 = \left(\dfrac{\mu_1 h_1 + \mu_2 h_2}{\rho_1 h_1 + \rho_2 h_2}\right)^{1/2}, \\ \rho'_1 = \dfrac{\rho_1 h_1 + \rho_2 h_2}{h_1 + h_2} \text{ and} \\ h'_1 = h_1 + h_2 \, . \end{array}$$

(β: Velocity of shear waves).

These relations have been extended neither to the threefold-, fourfold-, ⋯ etc. crustal structures nor to the Rayleigh waves. However, we may adopt this formula in the present case without significant error.

The calculated dispersion curves of Rayleigh waves through three kinds of such equivalent layers are given by the solid curves in Fig. 6. In this figure, we can recognize that the shifting of the theoretical dispersion curve caused by the addition of a sedimentary layer of varying thickness (marked by oblique lines) is quite similar to the ones actually observed (dotted curves). From these results, we may suggest that the observed variation of the dispersive character in such an anomalous region as was given in Fig. 5 may be caused by the decrease of the mean velocity of compressional waves in the crust due to the presence of a layer of volcanic rock in the oceanic islands region. This suggestion will further be affirmed in the next section.

3. Comparison of the observed dispersion curves with theoretical curves

It was suggested in the earlier part of this paper that the existence of "rashes" in some ocean floors may affect the dispersion of the Rayleigh waves which travel across it. Then, what kind of physical property in the crust at or around these rashes affects the dispersion of Rayleigh waves?

In order to answer this question, the observed dispersion curves

---

7) H. JEFFREYS, "The Effect on Love Waves of Heterogeneity in the Lower Layer," *Mon. Not. Roy. Ast. Soc., Geophys. Suppl.*, **2** (1928), 101.

numbered from 1 to 7 were compared with some theoretical dispersion curves. The results are given in Figs. 7-a, -b and -c, in which the wave paths are also shown in the lower maps. The models of the crust corresponding to the theoretical dispersion curves A, B, C, D and E are respectively as follows:

A

α	ρ	h
1.52	1.00	5.57
7.95	3.00	∞

B

α	ρ	h
1.50	1.00	5.30
6.90	2.57	5.30
8.10	3.00	∞

D

α	ρ	h
1.50	1.00	4.20
6.00	2.80	12.6
7.95	3.00	∞

D

α	ρ	h
1.50	1.00	3.70
6.00	2.80	15.0
7.95	3.00	∞

E

α	ρ	h
1.50	1.00	2.00
5.00	2.80	15.0
7.95	3.00	∞

The procedure usually adopted in determining the crustal structure along the travelling path of surface waves by the group velocity method is to find out the most suitable crustal model for which the theoretical dispersion curves best fit the observed data. But, this procedure will not be adopted here for the following two reasons: (1) The crustal structure cannot be uniquely determined without using two kinds of surface waves, Love and Rayleigh waves.8),9) (2) Even if we can observe the dispersions of both Love and Rayleigh waves, the determined crustal structure by the group velocity method is but an average one along the path. Therefore, the result is significant only when the surface waves travelled along an almost uniform crustal structure. Considering that the oceanic region in and around the Philippine basin and Melanesia is one of the most anomalous regions with rapid lateral variations in its structure, the usual method may lose its significance for these regions.

---

8) Y. SATÔ, "Study of Surface Waves IV. Equivalent Single Layer to Double Surficial Layer," *Bull. Earthq. Res. Inst.*, **29** (1951), 519.

9) T. AKIMA, "On Dispersion Curves of Surface Waves from the Great Assam Earthquake of August 15, 1950," *Bull. Earthq. Res. Inst*, **30** (1952), 237.

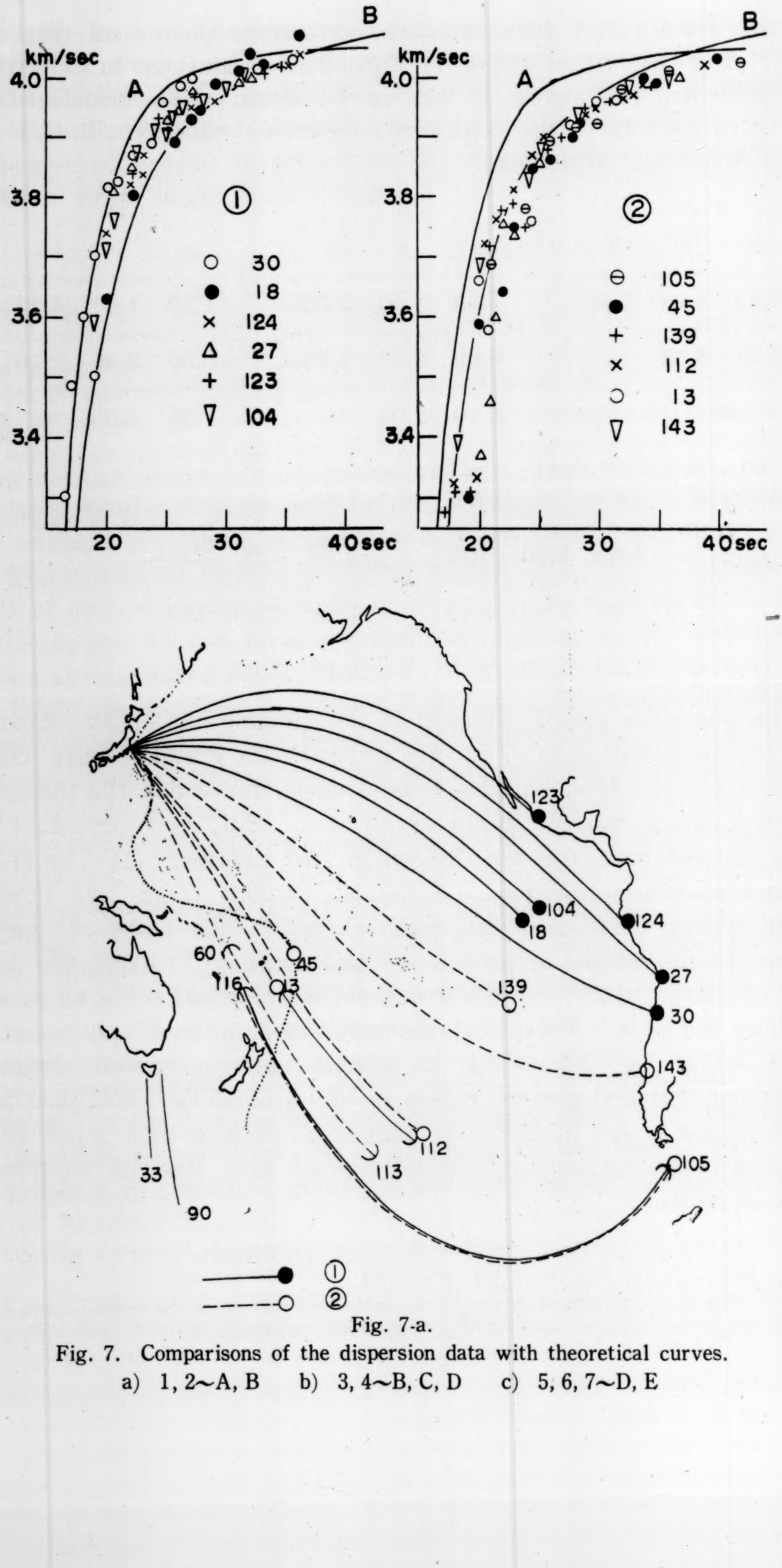

Fig. 7-a.

Fig. 7. Comparisons of the dispersion data with theoretical curves.
a) 1, 2∼A, B b) 3, 4∼B, C, D c) 5, 6, 7∼D, E

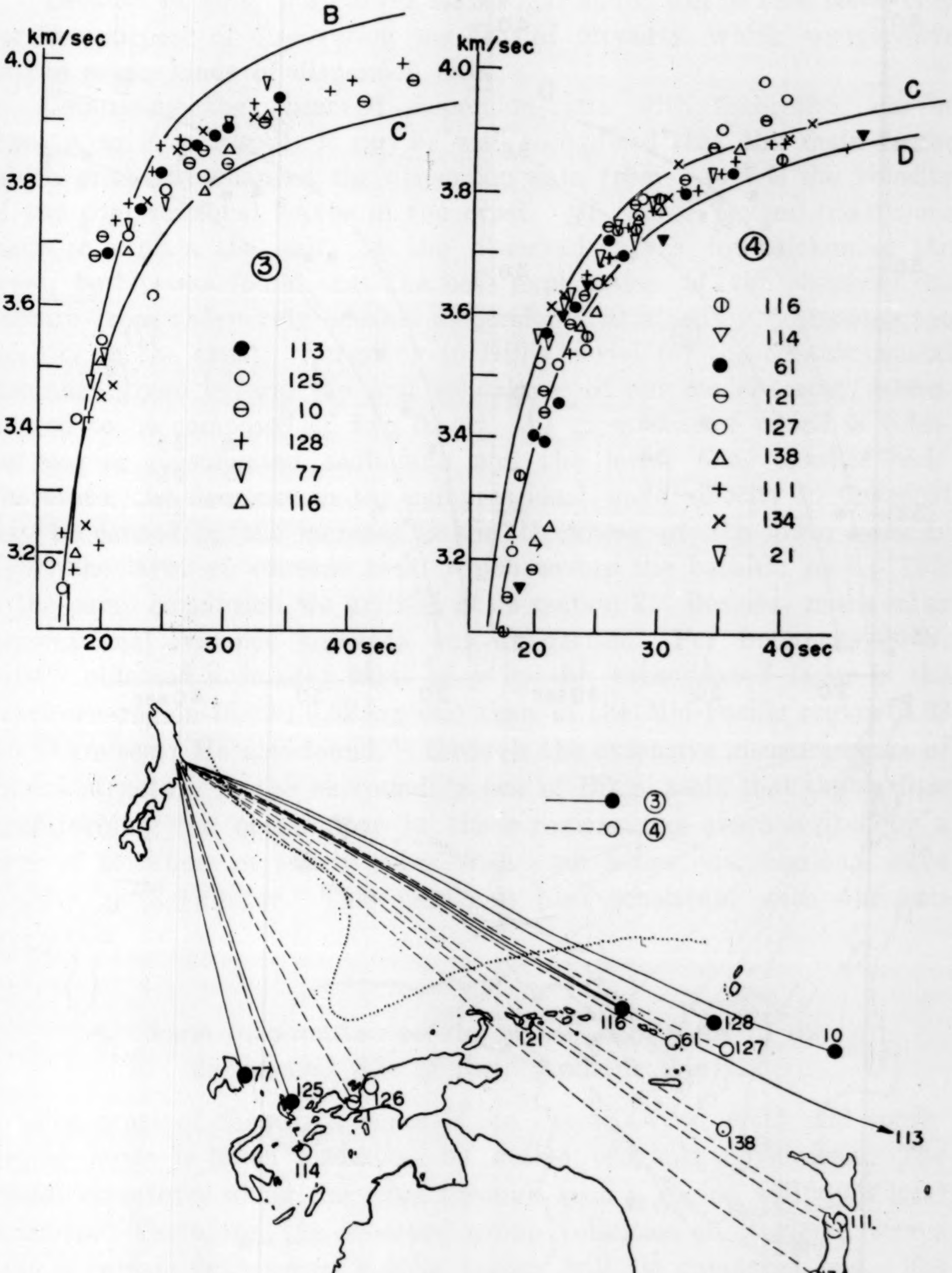
km/sec
4.0
3.8
3.6
3.4
3.2
20
30
40 sec
B
C
③
● 113
○ 125
⊖ 10
+ 128
▽ 77
△ 116
km/sec
4.0
3.8
3.6
3.4
3.2
20
30
40 sec
C
D
④
⦶ 116
▽ 114
● 61
⊖ 121
○ 127
△ 138
+ 111
× 134
▼ 21
● ③
○ ④
77
125
126
114
121
116
61
128
127
10
113
138
111
134

Fig. 7-b.

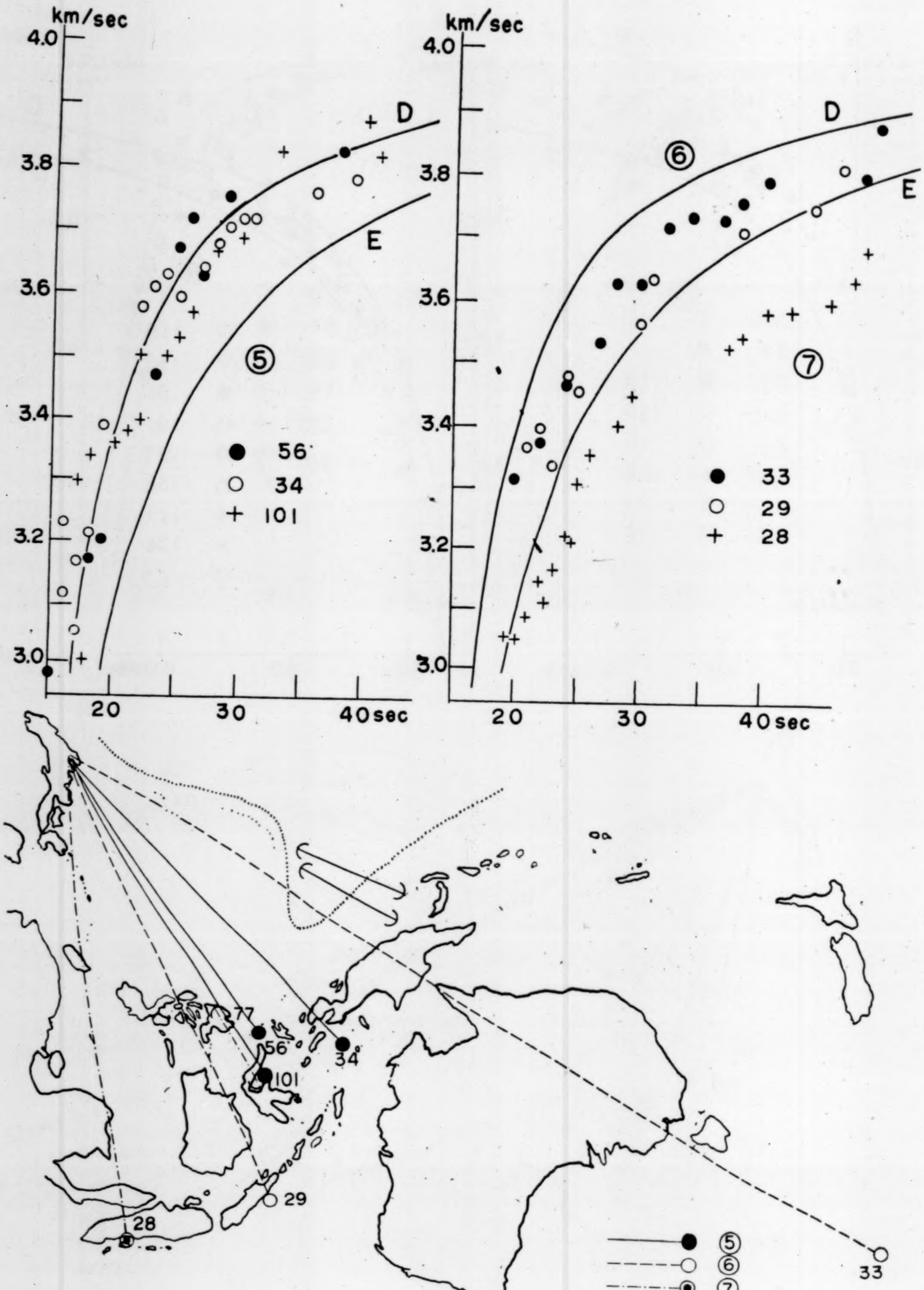
km/sec
4.0
3.8
3.6
3.4
3.2
3.0
20
30
40sec
D
E
⑤
● 56
○ 34
+ 101
km/sec
4.0
3.8
3.6
3.4
3.2
3.0
20
30
40sec
D
E
⑥
⑦
● 33
○ 29
+ 28
77
56
101
34
29
28
33
⑤
⑥
⑦

Fig. 7-c.

Because of this, the curves A, B, C, D and E will be used here only for the purpose of discovering the crustal property which corresponds to the seven kinds of dispersion data.

Comparing the observed dispersion data with theoretical curves from A to E in Fig. 7, it can be well recognized that the main factor which gradually changes the dispersion data from 1 to 7 is the velocity of the compressional waves in the crust. Of course, several trials were made to explain the shift in the observed curves by thickening the crust, but it was found that the best explanation of the observed departure from the purely oceanic dispersion is attained by decreasing the velocity in the crust. Referring to Hill's model for the oceanic crustal structure given before, the first solid layer of our model (crust) is considered to be composed of two layers, the uppermost of which is volcanic rock or consolidated sediments and the lower one, basaltic rock. Therefore, the decrease in the compressional wave velocity in the crust may be caused by the increase in the thickness of the lower velocity layer, the layer of volcanic rock, which covers the basaltic rock. This is the same conclusion we arrived at in section 2. Besides, much other observational evidence supports our suggestion. For instance, R. W. Raitt[10] obtained a smaller value of α in the consolidated layer in the Capricorn region (5.09 ± 0.52 km/sec) than in the Mid-Pacific region (5.38 ± 0.73 km/sec); He also found,[11] through the extensive measurements of crustal structure in the surrounding sea of Bikini atoll, that the surface layer forming the ocean floor in these regions was characterized by a layer of thickness of nearly 2 km, with such a low compressional wave velocity as 3.0 km/sec. This result is also consistent with our own suggestion.

4. Some information on the crustal conditions in the continental side of the "Andesite line"

The crust of the earth beneath the Pacific Ocean south and southeast of Japan is much disturbed by active orogenic movements. The crustal structures along the path through such a region will show local variation. Therefore, the observed group velocities of Rayleigh waves along a certain path across such a region will be composed one. For instance, when Rayleigh waves pass across two regions A and B with different crustal structures, the resultant group velocity V can be found by the following simple relation,

---

[10] R. W. RAITT, "Seismic Refraction Studies of the Pacific Ocean Basin. Part I: Crustal Thickness of the Central Equatorial Pacific," *Bull. Geol. Soc. Amer.*, **67** (1956), 1623.

[11] R. W. RAITT, "Seismic Refraction Studies of Bikini and Kawajalein Atolls," *Proc. Pap. U.S. Geol. Surv.*, **260** (1954), 507.

$$\frac{k\Delta}{V_A}+\frac{(1-k)\Delta}{V_B}=\frac{\Delta}{V}$$

in which, V_A and V_B are the group velocities of Rayleigh waves across A and B regions respectively and k is the ratio of the path length through the region A to the total one (Δ). Therefore, if we know two kinds of dispersion curves corresponding to these two regions, we can obtain the resultant group velocity V for each period as well as the resultant dispersion curves for various values of k. Some examples are shown in Fig. 8 by broken curves for $k=0.2$, 0.4, 0.6 and 0.8. For

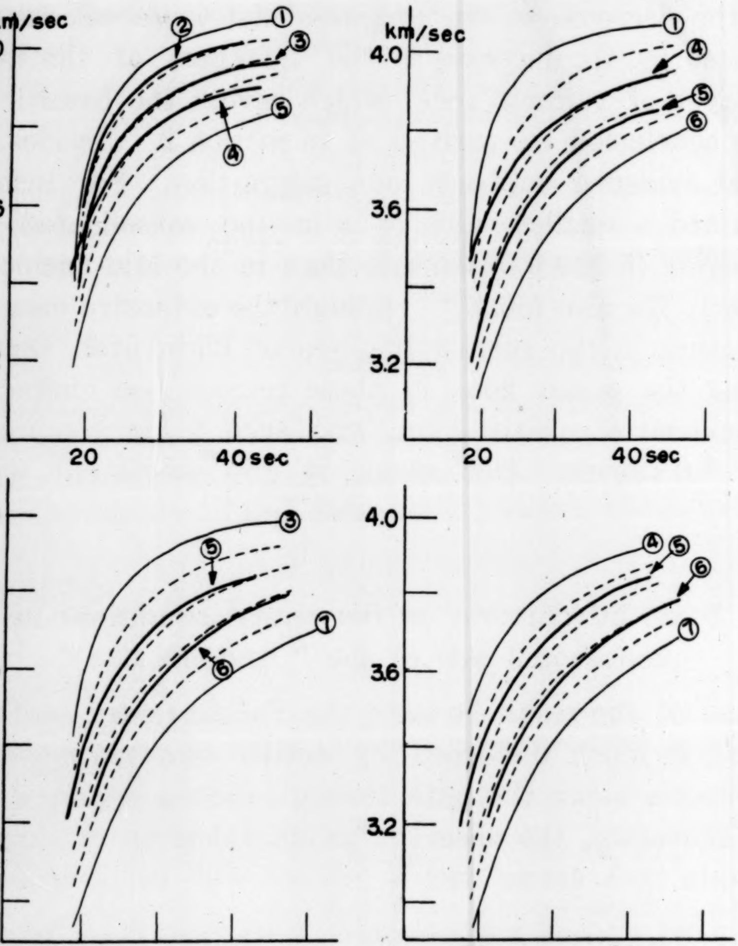

Fig. 8. Resultant dispersion curves (broken lines) calculated from two kinds of dispersion curves (the uppermost and lowermost ones).

instance in Fig. 8-a, the uppermost broken curve corresponds to the resultant one when Rayleigh waves travelled across the region "5" by 20% and the region "1" by 80%. (In order to prevent further trouble in terminology, we shall use, for instance, "the region "3"" instead of "the region across which Rayleigh waves show a dispersion characteristic of No. 3"). The thick solid curves mean other kinds of observed dispersion curves.

This results given in Fig. 8 support the previous consideration. For instance, in Fig. 8-a, curve 2 can be considered the resultant one when Rayleigh waves travelled through two different regions of crustal structure "1" and "5" with a path length ratio of 1:4. When this ratio becomes 2:3 or 3:2, the resultant curve will become "3" or "4" respectively.

This idea is schematically outlined in Fig. 9. In this figure, the region "1" and "7" represents the oceanic and continental crustal structure respectively, and the region "4" the intermediate one. Suppose now that the epicenters are distributed as shown in this figure, the resultant characteristic numbers of Rayleigh wave dispersions observed at a station (marked by a double circle) will become such as those shown beside each epicenter. When there is a good chance to obtain the dispersion data of a shock for which the travelling path occupies a part of the path of another shock, the dispersive characteristic number for the remaining part will also be

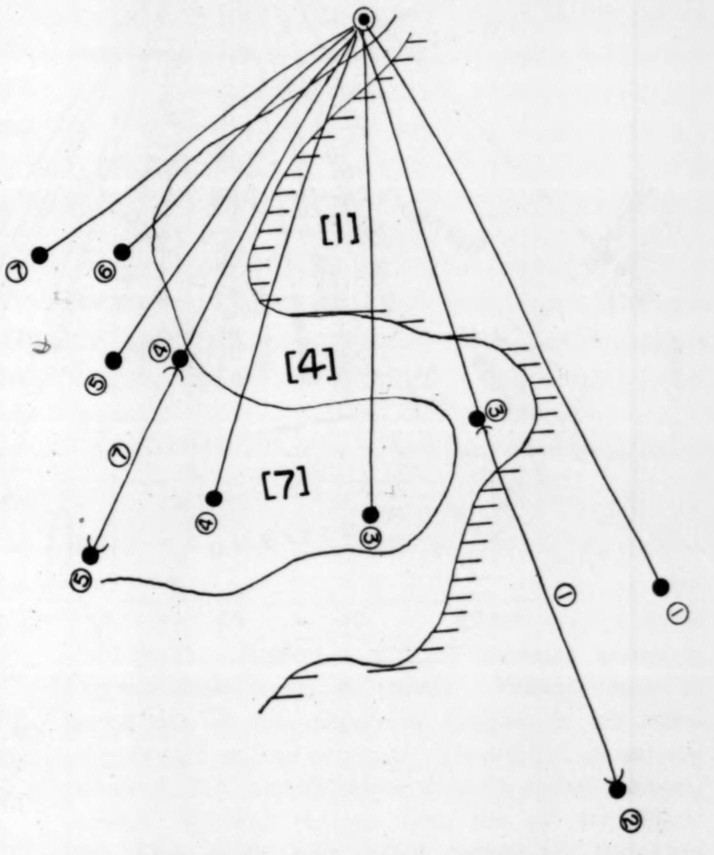

Fig. 9. Schematic figure which shows how the resultant dispersive character will become when the path runs through the different structured region with different ratio of path lengths.

calculated from the difference between the travel-times along these two paths. Such cases are also shown in brackets in this figure.

Our procedure is, however, entirely the reverse of the above. What we know are the locations of the epicenters and the characteristic numbers of the resultant dispersions. In some cases we may obtain the dispersion curves for a rather restricted region by subtracting the travel-times required along two suitable travelling paths. From these data we want to discover the boundary of such a region as "4" in

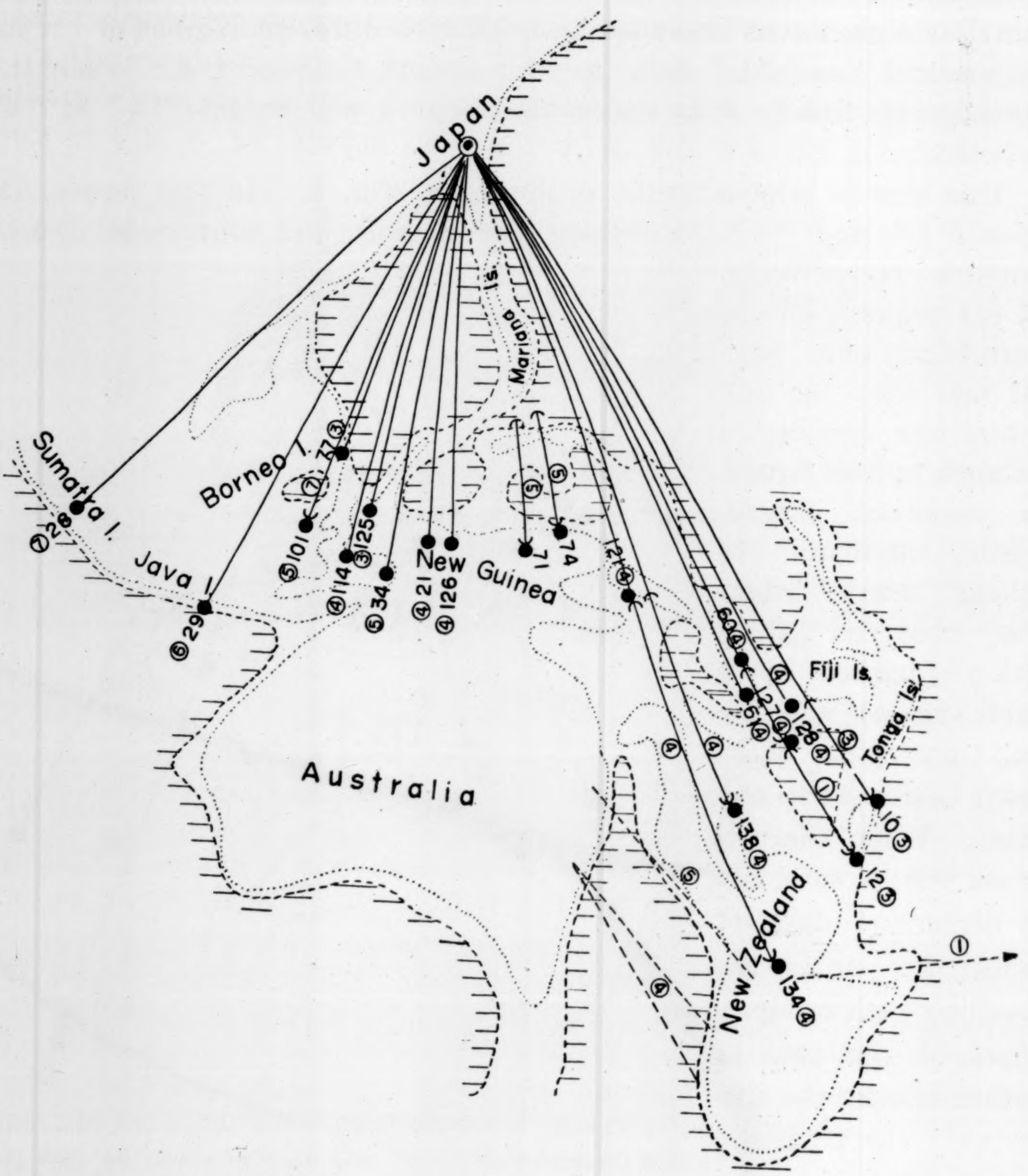
Japan
Mariana Is.
Sumatra I.
⑦28
Borneo I.
⑦77③
⑦
⑤101
④114
③125
⑤34
Java I.
⑥29
New Guinea
④21
④126
⑤
⑤
71
74
121④
60④
127④
61④
128④
①
④
④
④
④
Fiji Is.
Tonga Is.
10③
12③
138④
⑤
④
Australia
New Zealand
134④
①

Fig. 10. The characteristic numbers of dispersions for the paths across the southwestern Pacific Ocean.

Fig. 9. Of course, help from geographical and geological data is needed.

Our data are summarized in Fig. 10, in which the hatched regions indicate those parts where the sea depth is greater than 4 km and the dotted curves show the 2 km sea depth line. In order to avoid complications in the figure, all the coastal lines are omitted. The paths for several cases when the local dispersive character along the paths could be found by subtracting the travel-times are also shown by lines with brackets together with their characteristic numbers.

C. B. Officer[12] studied the Rayleigh wave dispersion across the Tasman Basin. The data were re-plotted in our group velocity versus period diagram in which the ratio of velocity scale to period scale is ten times larger than the original ones. The results are shown in Fig. 11. Comparing these dispersion data with those given in Fig. 7, we can recognize that the dispersive character of Rayleigh waves for the central and northern Basin (white circles and cross marks respectively) may be expressed as "4" and "5" respectively according to our notation. These available data are also added in Fig. 10. The data summarized in this figure is, however, not sufficient for the performance of our plan. In order to obtain reliable results, the writer will postpone the conclusion of this work for a future time. Beside the data at Tsukuba Station, those at another Station for which the travelling paths intersect the present ones

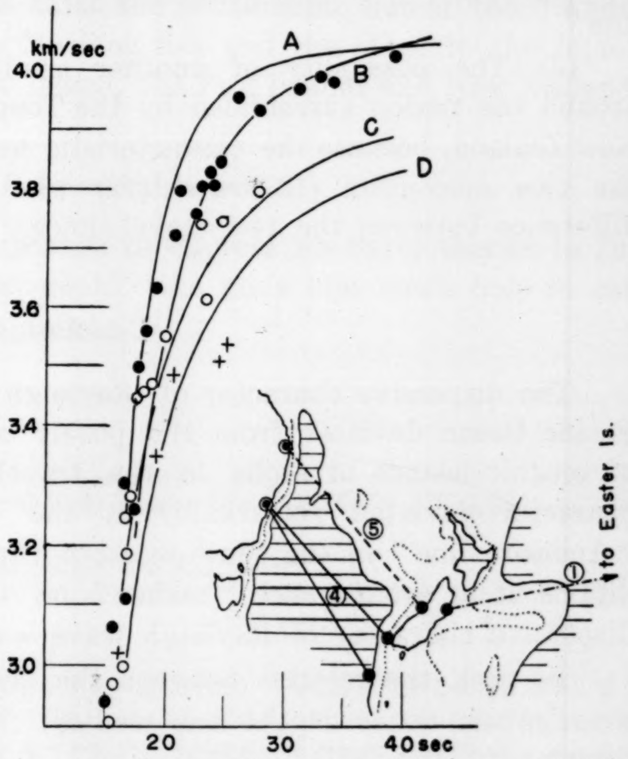

Fig. 11. Dispersion data of Rayleigh waves in Tasman Basin by C. B. Officer. Velocity scale to period one in the dispersion diagram is ten times exaggerated as the original. Theoretical dispersion curves A, B, C and D before used are shown for comparison. Hatched regions mean the sea with more than 4 km depth, and dotted curves are the 2 km depth contour line.

---

[12] C. B. OFFICER, "Southwest Pacific Crustal Structure," *Trans. Amer. Geophy. Union*, **38** (1955), 449.

will be quite useful.

However, the following two suggestions may be given here from the present data.

(1) The dispersive characteristic numbers for the shocks (114), (34), (21) and (126), the paths of which crossed the Mariana Sea, are nearly the same as those for the shocks (60), (61), (127) and (128) near the Fiji Islands. Considering here that approximately 60% of the travelling paths of the latter group are occupied by the oceanic region, off east of the Mariana Trench, we may suggest that some part of the Mariana Sea has an oceanic crustal structure, though it lies on the western side of the "Andesite line". In other words, there may be a "hole" of oceanic structure even on the continental side of "Andesite line".

(2) The possibility of another small "hole" may be suggested around the region surrounded by the Tongas, Fijis, New Caledonia and New Zealand, because the characteristic number for the region between the two epicenters (127) and (12) was found to be "1" from the difference between the two travel-times.

5. Conclusions

The dispersive character of Rayleigh waves in some parts of the Pacific Ocean deviates from the purely oceanic through the existence of oceanic islands or atolls in the travelling path. Particularly, the character deviated remarkably in the western side or around the "Andesite line" in the south-western Pacific Ocean. The physical conditions at or around such "rashes" on the sea-bed which affect the dispersive character of Rayleigh wave were investigated.

At first, the relation between the dispersive characteristics and the average sea water depths was studied. Synoptically, these two were correlated. But, this correlation was disturbed in the region around the "Andesite line"; that is, the dispersive character largely varied in spite of the almost equal water depths along the paths. This anomaly seems to occur owing to the presence of the volcanic rock layer which may cover the basaltic layer with various thicknesses.

Secondly, several theoretical dispersion curves for different crustal models were compared with seven kinds of observed dispersion curves which was obtained in the previous two papers. From these comparisons, the same conclusion was derived. That is, the shift in the dispersive character from a purely oceanic to rather the continental, is caused by the decrease in the body wave velocity in the crust owing to the presence of a layer of volcanic rocks in the oceanic islands region. The higher temperature in the crust owing to the possible magma reservoirs may also play a part in decreasing the body wave velocity in the crust around these region.

A plan to estimate the local crustal structures for the complicated regions by the group velocity method was also outlined. As the data we have obtained were still insufficient to complete this plan, the completion of this work was postponed to a future time. However, the following proposal was made.

Two small oceanic regions exist the continental side of the "Andesite line". One exists in the Mariana Sea and the other in the region surrounded by New Caledonia Island, the Fuji Islands and New Zealand.

6. Acknowledgments

In conclusion, the writer wishes to express his harty thanks to Dr. T. Kizawa and to Mr. R. Yamaguchi, who gave him much help in calculating theoretical dispersion curves.

---

1. 日本周辺の海洋底をつたわるレーリー波の分散 (第三報)

—東南太平洋の地殻構造—

地震研究所　三　東　哲　夫

太平洋の海底を伝わつて日本にやつてくるレーリー波の分散が7種に分類できることは,第1,第2報で詳しくのべてきた通りである. 筆者は, これらのうち, 従来から知られている純海洋的な分散と同一視される分散に対して番号1を, そして次第にそれが陸的なものに移るにつれて, それぞれ2, 3, 4 ･･･という番号をつけた. 7は最も陸的なもので, スマトラ島の地震でえられたレーリー波の分散がこれに属する.

同じ海洋底を伝わるにかかわらず, なぜ径路によつてこのように様々の分散傾向が現われるのか, これが残された重要な問題であつた.

M. N. Hill が, 屈折法による多くの資料をまとめてつくつた海洋底の地殻構造に関する代表的なモデルを参考にし, 今回観測されたレーリー波の波長も考慮して, 水—固体—半無限固体という二重層構造を仮定し, いくつかの分散曲線を計算し, それらと今回の7種の分散曲線とを相互に比較した結果 (第7図), 分散の傾向が, 2, 3, 4 ･･･ と徐々に純海洋的なものから外れてゆく原因は, むろん地殻の厚さが厚くなつてゆくためも多少はあるけれども, それだけでは解決できず, むしろ, 地殻内をつたわる実体波の平均速度がかなりおそくなつてゆくためだ, ということが分かつた. この速度減少は, それぞれの径路の地理的な条件を考え合せて見ると, Hill のモデルによる第二層,

つまり，火山の噴出物からなる層の厚みの増大によつて生じていると考えられる．つまり，太平洋上に点在するたくさんの海底火山の周辺では，場所によつていろいろの厚さで火山の噴出物が堆積していると思われるが，このことが，全体としての地殻内の実体波の速度に変化を生じ，従つて，そうした領域内を通るレーリー波の分散を変えている，と考えてよさそうである．あるいは，この速度の減少は，もし岩漿の溜りでもあると，その熱によつて引起されているかも知れない．径路にそつての平均的な海の深さと，レーリー波の分散の傾向との関係も調べてみた（第3図）が，全体としてみると，海が浅くなるにつれて，分散も陸的なものに移つてゆくようである．けれども，この大勢を著しく乱すいくつかの径路が発見された．こうした径路に関する限り，その平均的な海の深さも，更には深さの分布も殆んど同一であつても，分散の傾向だけは著しい相異を見せるのである（第5図）．この異常性もやはり，火山岩層の厚さの相異ということで説明することができた．

日本の南方および南東方海底は，地殻変動の最も活発な地域である．それでこのような複雑な変化の多い地殻内を伝わつてきたレーリー波の分散から，径路にそつての平均的な地殻構造をきめても余り意味がない．事実，観測された7種の分散のうちのいくつかは，それぞれ異なつた地殻構造を異なつた群速度で伝わつてきた結果生じたものと解釈できる（第8図）．筆者は，このような場合にも，これらの異なつた地殻構造をもつ領域自体の分散を推定し，従つてそれからそれぞれ構造を推定しうる一つの案を提出した．現段階では，未だ資料不足の感があるので，この方法を実際に適用するには至らなかつたが，この考え方に基づくと，今までの資料だけでも次のことはいえると思う．即ち，安山岩線の西側，つまり陸的構造と考えられている側にも，少なくとも2ヵ所，海的構造をしている「穴」が存在することである．1ヵ所は，マリアナ海の一部，もう1ヵ所はニューカレドニア島，フィージー諸島，それにニュージーランドで囲まれた海域である．

BULLETIN OF THE EARTHQUAKE
RESEARCH INSTITUTE
Vol. 39 (1961), pp. 23-75

2. *On Microseisms in Frequency Range from 1 c/s to 200 c/s.**

By Kei AKAMATU,

Geophysical Institute, Faculty of Science,
The University of Tokyo.

(Read March 22, 1960.—Received Dec. 28, 1960.)

§ 1. Introduction

In this paper microseisms in the frequency range of 1 c/s to 200 c/s are discussed.

Generally speaking, there are three kinds of ground unrests classified according to frequency range: the first kind in the frequency range of 1 c/s to 200 c/s, the second in the range of 1 c/s to 0.1 c/s, and the third in the range lower than 0.1 c/s. These microseisms vary in origin, wave character, mechanism and wave propagation. These items are investigated, each in its turn. Now, considering the origin of short period microseisms, various sources are enumerated; artificial noise sources, volcanoes, weather conditions, flows in rapids, etc.. These sources have various mechanisms of wave generation.

On the other hand, in the observation of small earthquake motions, explosion seismics, or in seismic exploration, ground noises create difficulties in picking out the initial motion in seismograms. Therefore it is also important to investigate the wave characteristics of short period microseisms.

There have been several investigations into short period microseisms. These investigations can be classified as (1) those concerned with sources, wave characteristics and wave attenuation, (2) those connected with ground structures, (3) those from the point of view of background noises in geophysical explorations, (4) those concerned with natural origins, such as volcanic tremors, microseisms accompanying cold fronts, etc..

As an example of category (1) dealing with artificial noise sources, L. Mintrop's[1] observations at distant points from the source of ground vibrations from a machine may be mentioned.

---

* Communicated by R. Takahasi.

[1] L. MINTROP, *Diss. Göttingen.*, (1911).

Many investigations along this line have been made especially in Germany[2]. In these investigations the attenuation of waves was measured, and attenuation coefficients were determined in each case.

Recently C. D. V. Wilson[3] investigated the origin and nature of short period microseisms. Wilson observed microseisms in the frequency range of 4 c/s to 100 c/s at several places, and determined noise levels during the day and at night. He pointed out traffic, aircraft, rain, wind, etc., as the sources of short period microseisms, but as for geophysical origins, he stated conjectures only.

In his paper on the vibration of machines[4], Wilson discussed the nature of waves, whether they are body waves or surface waves. From a spectrum analysis and from the decay in amplitudes depending on the distance he concluded that waves of frequency 9 c/s are surface waves and those of frequency higher than 9 c/s are body waves, and that from their phase velocities and orbits, it is supposed that waves lower than 9 c/s are also surface waves. In his case the sources of vibration were traffic.

K. Aki[5] believed microseisms to be Love type waves from his statistical method of auto-correlation analysis. This method is effective at places where wave sources are very complex.

It is often stated that there arises a "dominant frequency" of the ground from short period microseisms in a way similar to the excitation of the "dominant frequency" of the ground by the passage of earthquake waves[6]. D. S. Carder and M. H. Gilmore[7] have observed "dominant frequencies" in short period microseisms near Los Angeles. Kanai[8],[9] is trying to determine the architectural quality of the ground from the frequency distributions of short period microseisms. In these investigations as the "dominant frequency" is thought to result from multiple reflections in the ground layers, this amounts to considering short period microseisms as body waves.

Also there is an idea that the various phases in seismograms between P and S waves are surface waves which have been converted from body waves by topography[10]. Such an idea assumes secondary origins of waves.

---

[2] for example, O. FÖRTSCH, *Zeit. für Geophys.*, **16** (1940), 57.

[3] C. D. V. WILSON, *Proc. Roy. Soc.*, **A**, **217** (1953), 176.

[4] C. D. V. WILSON, *Proc. Roy. Soc.*, **A**, **217** (1953), 188.

[5] K. AKI, *Bull. Earthq. Res. Inst.*, **35** (1957), 416.

[6] M. ISHIMOTO, *Bull. Earthq. Res. Inst.*, **15** (1937), 697.

[7] D. S. CARDER and M. H. GILMORE, *Bull. Seis. Soc. Amer.*, **35** (1945), 13.

[8] K. KANAI, T. TANAKA and K. OSADA, *Bull. Earthq. Res. Inst.*, **32** (1954), 199.

[9] K. KANAI, T. TANAKA and K. OSADA, *Bull. Earthq. Res. Inst.*, **35** (1957), 109-191.

In seismic exploration the problem of the background noise is handled by filtering and by group setting to increase the signal to noise ratio[11]. In explosion seismology besides these precausions, the proper selection of location of the seismometers is also necessary.

Concerning microseisms of natural origin, detailed research has been carried out in particular cases for those arising from volcanic activity[12],[13],[14],[15],[16]. Volcanic tremors may be the most significant among short period microseisms of natural origin. As for the effects of local topographic conditions, for example, an increase in water volume in rivers gives rise to an increase in the local noise level[17]. In setting up sensitive seismometers near a seashore or on an island the influence of the sea waves must be taken into consideration.

In this paper, the characteristics of waves of short period microseisms are investigated. The frequency spectrum is derived and its occurrence and diurnal variations are discussed. Also the characteristics of the waves are investigated for direction of wave propagation, phase velocity, wave length and orbital motion. From the result thus obtained the author discusses the problem of "dominant frequency". The individual origin of particular short period microseisms is not discussed except for a few examples, for, the author thinks that minute analyses of individual waves at the observation point and statistical investigations of them are more useful for an interpretation of the nature of waves, as they are the results of superpositions of waves from many origins.

§ 2. Equipment

The instruments are electro-magnetic seismometers of the moving coil type. They are horizontal seismometers with a natural frequency of 1 c/s and vertical seismometers with natural frequencies of 1 c/s, 3 c/s

---

10) H. E. TATEL and M. A. TUVE, *Journ. Geophys. Res.*, **59** (1954), 287.

11) for example, T. KANEKO, *Report No. 182, Geological Survey of Japan*, (1957).

12) K. SASSA, *Memoirs of the College of Science, Kyoto Univ.*, Ser. **A**, **18** (1935), 255.

13) R. TAKAHASI, T. NAGATA and K. HIRANO, *Bull. Earthq. Res. Inst.*, **16** (1938), 87.

14) S. SAKUMA, *Zisin*, [ii], **9** (1956), 1.

15) D. SHIMOZURU, K. GOTO, O. NAKAMUTA and H. NODA, *Kazan*, [ii], **3** (1958), 35.

16) S. YOSHIKAWA and C. KITSUNEZAKI, *Kazan*, [ii], **3** (1959), 147.

17) K. SASSA, *ibid.*

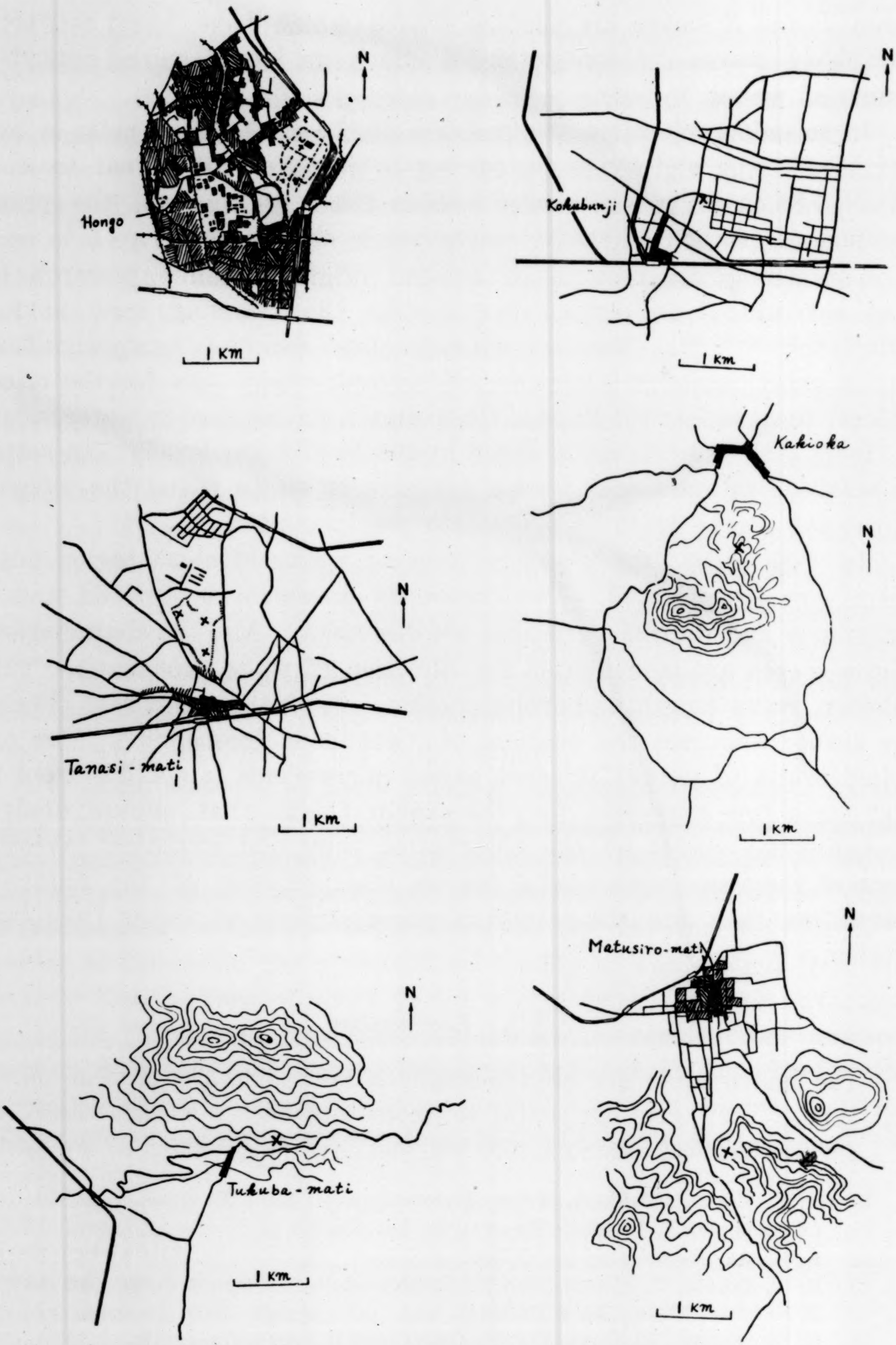
Hongo
N
1 km
Kokubunji
N
1 km
Kakioka
N
1 km
Tanasi-mati
N
1 km
Matusiro-mati
N
1 km
Tukuba-mati
N
1 km

Fig. 1. Topographical maps of observation point.
X Observation point.

and 10 c/s respectively. As for amplifiers, several channels of the C–R coupling type with a frequency range from 1 c/s to 30 c/s used in explosion seismology, and some with a frequency range from 1 c/s to 200 c/s used in micro-earthquake observations were used. In the observations one or two step integrating circuits with only C–R coupling were used. Values of C and R were selected in ranges of $C=1$–$2\ \mu$fd. and $R=200$–500 kΩ according to the condition of each observation point. The recording system was an electro-magnetic oscillograph, and time marks were put in at every 1/50 second. Paper speeds were ordinarily 3 cm/s and 10 cm/s. Galvanometers with natural frequencies of 100 c/s and 300 c/s were used. The sensitibity of the seismometers was 3.7 volt/cm/s for the 1 c/s horizontal seismometer, 4 volt/cm/s for the 3 c/s vertical seismometer, and 5 volt/cm/s for the 10 c/s vertical seismometer.

The frequency response of the seismometer combined with the amplifier, with an integrating circuit was almost flat from 1 c/s to 10 c/s, and in this range it was used as a displacement seismometer. A magnification of between 20,000 times and 10^7 times was adopted.

The observation points were at Hongo, Kokubunzi (Kokubunji), and Tanasi-mati in Tokyo, Kakioka and Mt. Tukuba in Ibaraki prefecture, and Matusiro in Nagano prefecture. Topographical maps of each observation point are shown in Fig. 1.

§ 3. The spectra of short period microseisms and their diurnal variations

1) Method of investigation.

For observations, amplifiers with integrating circuits as described in section 2 were used. The time constant ranged from one to four seconds. In places where waves shorter than 10 c/s were outstanding and the noise level was rather low, amplifiers without an integrating circuit were used.

The seismometers were set on a concrete block in a room or directly on the ground outdoors.

For the analysis, 6–8 seconds intervals were taken from a certain time selected in a record and amplitudes at every 1/50 second or 1/100 second were read. Hence, the sample size is about 300 or 400. Amplitudes were rounded out as $+1$ or -1, according to whether they were above or below the zero line, and following Tomoda's method[18] correlation coefficients and correlograms were calculated. In a product of amplitudes $f(t)f(t+\tau)$, where $\tau=k\tau_0$, the values $\tau_0=1/50$ second or 1/100 second and $k=1, 2, \cdots, 20$ or 30 were used. Tomoda's method can be safely applied to an analysis of short period microseisms if the sample size is larger than 300[19]. Examples of correlograms are shown in Fig. 2. In Fig. 2 two classes, regular or periodic and rather irregular, are found. As seen in some cases at Tanasi-mati or at Kakioka there were cases where the correlogram was periodic without decrement. Records from the same observation point at different times were a little variant, that is to say, the microseisms were not always stochastically stationary

---

[18] Y. TOMODA, *Journ. of Physics of the Earth*, **4** (1956), 67.

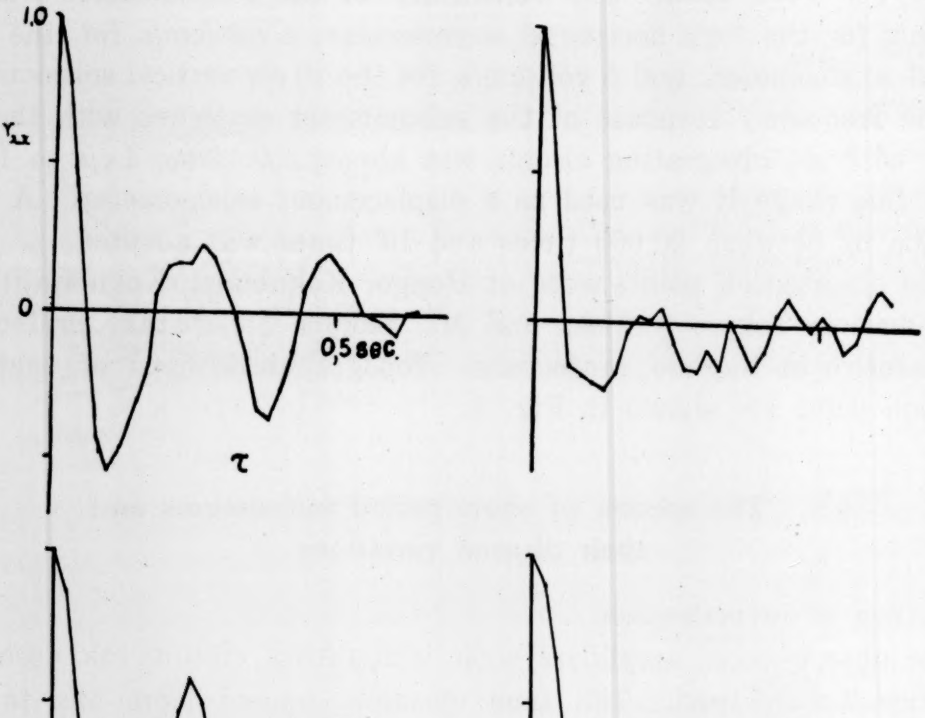

Fig. 2 I. Correlograms from records with 1 c/s horizontal seismometer at Hongo.

---

[19] K. AKAMATU, *Journ. of the Physics of the Earth,* **4** (1956), 81.

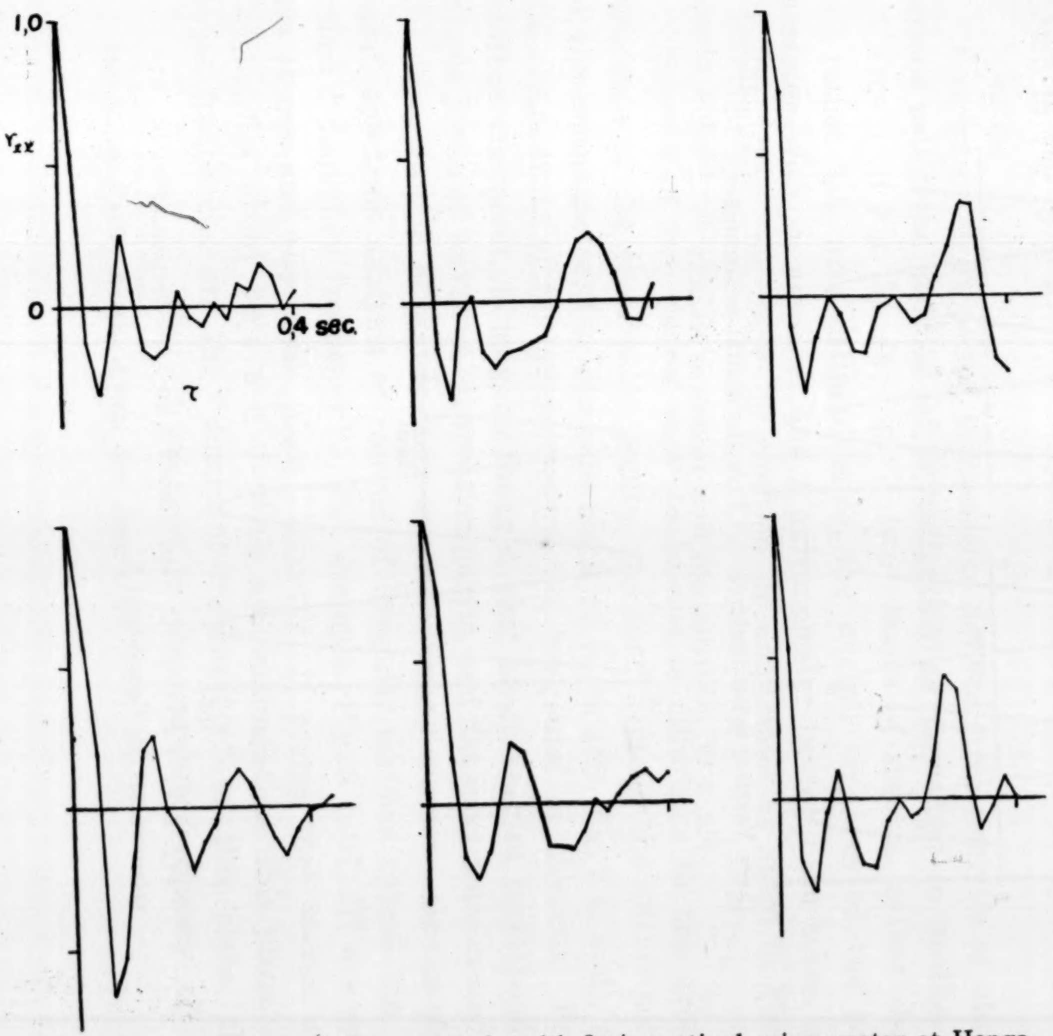

Fig. 2 II. Correlograms from records with 3 c/s vertical seismometer at Hongo.

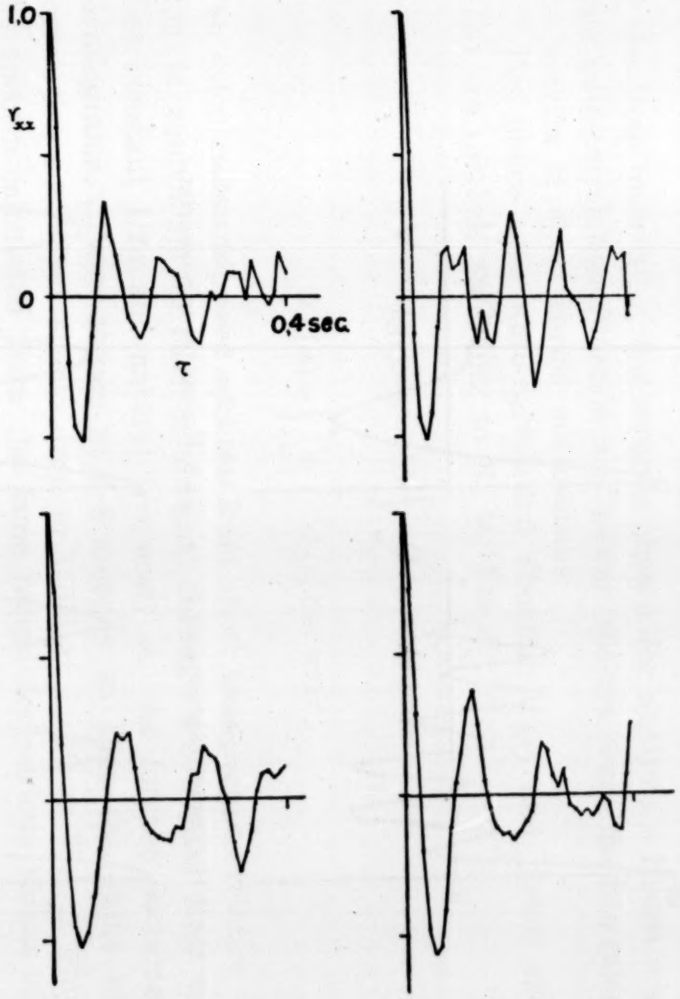

Fig. 2 III. Correlograms from records with 10 c/s vertical seismometer at Hongo.

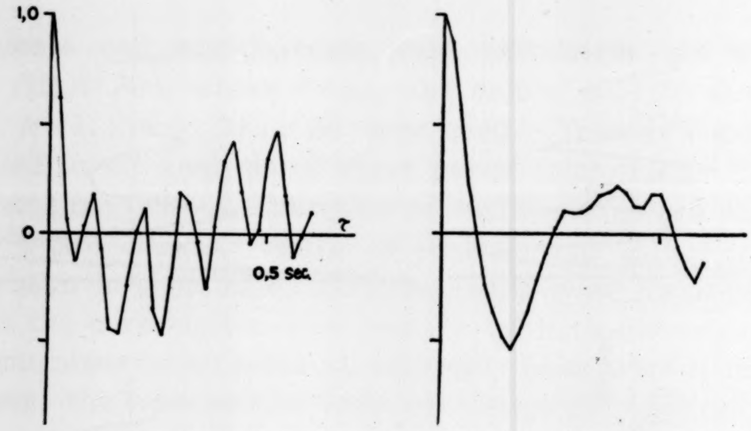

On the ground. In a hole 2.5 m below the surface.
(1 c/s Horizontal seismometer.) (1 c/s Horizontal seismometer.)

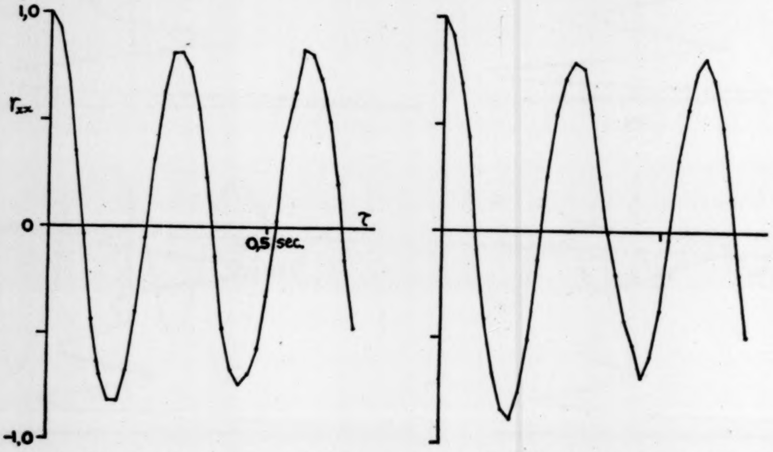

(1 c/s Vertical seismometer.) (1 c/s Horizontal seismometer.)

Fig. 2 IV. Correlograms from records at Kakioka

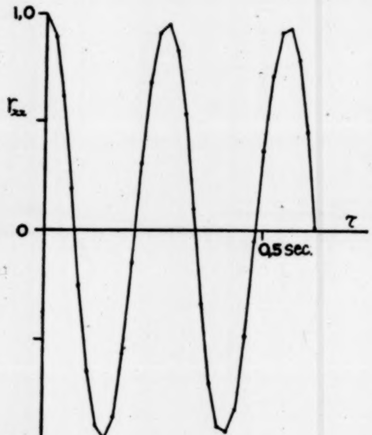

Fig. 2 V. Correlogram from record with 1 c/s horizontal seismometer at Tanasi-mati C.

in the time interval of 6–8 seconds chosen for analysis. Hence a short time auto-correlation function and power spectra were used to calculate the spectra of short period microseisms.

The short time auto-correlation function $\phi_t(\tau)$ and power spectra $G_t(\omega)$ are related, according to R. M. Fano[20] by

$$\phi_t(\tau)=e^{\alpha|\tau|}/2\pi\int_{-\infty}^{\infty}G_t(\omega)\cos\omega\tau d\omega$$

$$G_t(\omega)=\int_{-\infty}^{\infty}e^{-\alpha|\tau|}\phi_t(\tau)\cos\omega\tau d\tau\ .$$

The calculation of power spectra from short time auto-correlation function is equivalent to passing a signal through a low pass filter with a time constant $1/2\alpha$ and natural frequency ω. As for the decrement of correlograms, α was chosen at 4–8 seconds so that the value of the correlation coefficient should drop to 1/100 at $k=20$ or 30. A graph of the spectra calculated from the same record for various values of α is shown in Fig. 3 II a.

2) Spectra.

Spectra of short period microseisms derived from analysis of observations using the method of investigation as described in section 1) are shown in Fig. 3. In Fig. 3 two classes of spectra, rather sharp and rather flat, are distinguishable, the overall response of the seismometer with an amplifier and a galvanometer having been taken into account. The frequency distribution of amplitudes as given in Fig. 4 seems almost Gaussian.

Spectra of two classes seem to be due to difference in the ground structure of the observation points, and conditions for the setting points of the seismometer, i.e. concrete block or earth (cf. Fig. 3 II a, d), and the components of the seismometers, i.e. horizontal or vertical. From another viewpoint, it may be thought that sharp spectra correspond to simple forms of waves at observation points, and flat spectra are caused by the superposition of waves from several or many sources. On the other hand, spectrum analysis of records of irregular motions reveal the so-called "dominant frequency". For example, Fig. 3 I, II, III are spectra at one and the same place; however, it seems that waves with frequencies about 3 c/s and 7–10 c/s are dominant at this place. As these frequencies are the "dominant frequencies" of this place, they always appear in spite of changes in the natural frequency of the seismometer and in the frequency range of the amplifier. As seen in Fig. 3 III, although the recording utilizing a 10 c/s vertical seismometer was done through coupling to an amplifier with a range extending to higher frequency bands, a sharp peak appears near 10 c/s frequency.

---

[20] R. M. FANO, *Journ. Acous. Soc. Amer.*, **22** (1950), 546.

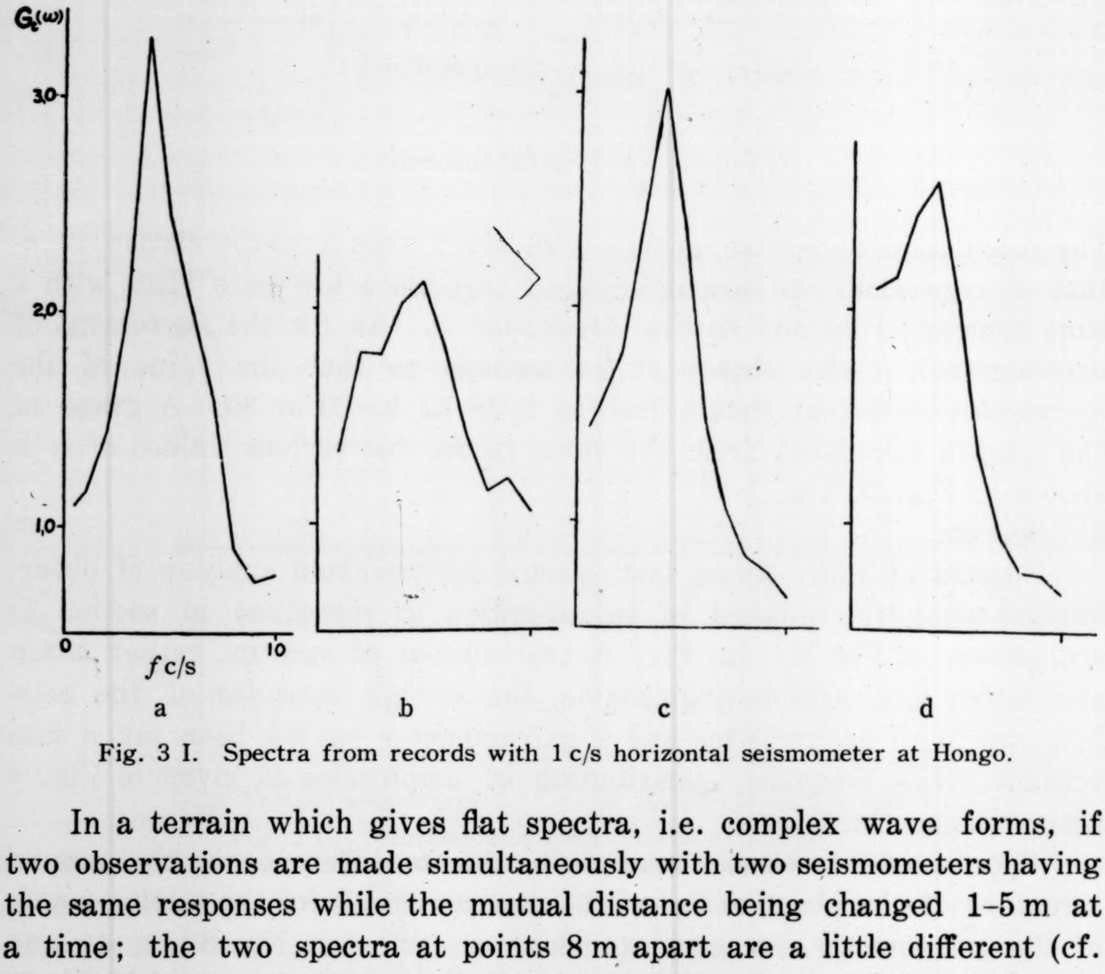

a b c d

Fig. 3 I. Spectra from records with 1 c/s horizontal seismometer at Hongo.

In a terrain which gives flat spectra, i.e. complex wave forms, if two observations are made simultaneously with two seismometers having the same responses while the mutual distance being changed 1–5 m at a time; the two spectra at points 8 m apart are a little different (cf. Fig. 3 II b, f) and the spectra for consecutive 6 second intervals extended from an appointed time are also different (cf. Fig. 3 II a, c).

Another difference which appears in the spectra of microseisms is between the spectra of horizontal and vertical motions. For microseisms of several seconds period, it was reported that there was almost no difference between the horizontal and vertical motions[21]. For short period microseisms on the other hand, it has been reported that there were remarkable differences[22].

In observations at Kakioka there was a case where the horizontal

---

[21] J. DARBYSHIRE, *Proc. Roy. Soc.*, **A**, **223** (1954), 96.

[22] D. S. CARDER and M. H. GILMORE, *ibid.*

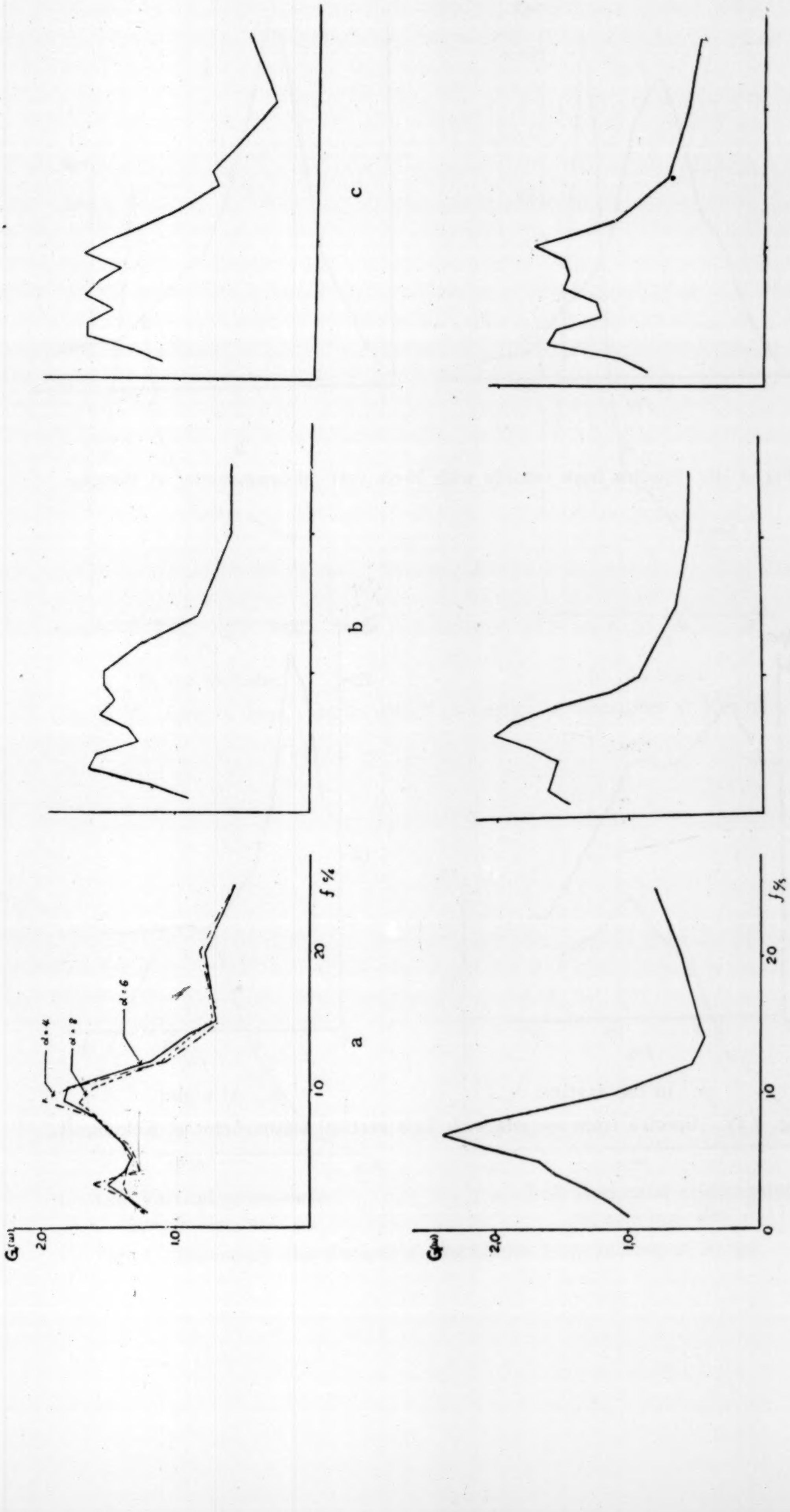

Fig. 3 II. Spectra from records with 3 c/s vertical seismometer at Hongo.

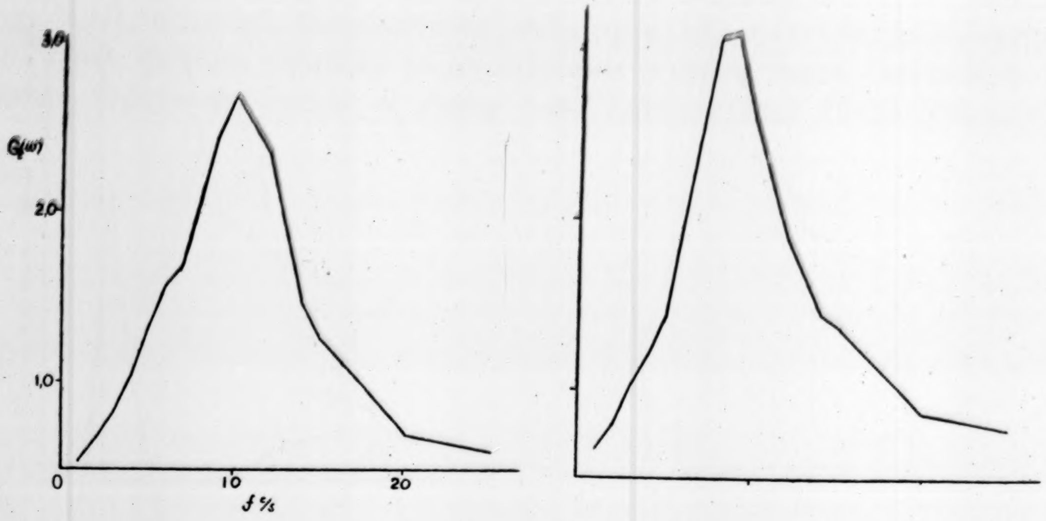

a b

Fig. 3 III. Spectra from records with 10 c/s vertical seismometer at Hongo.

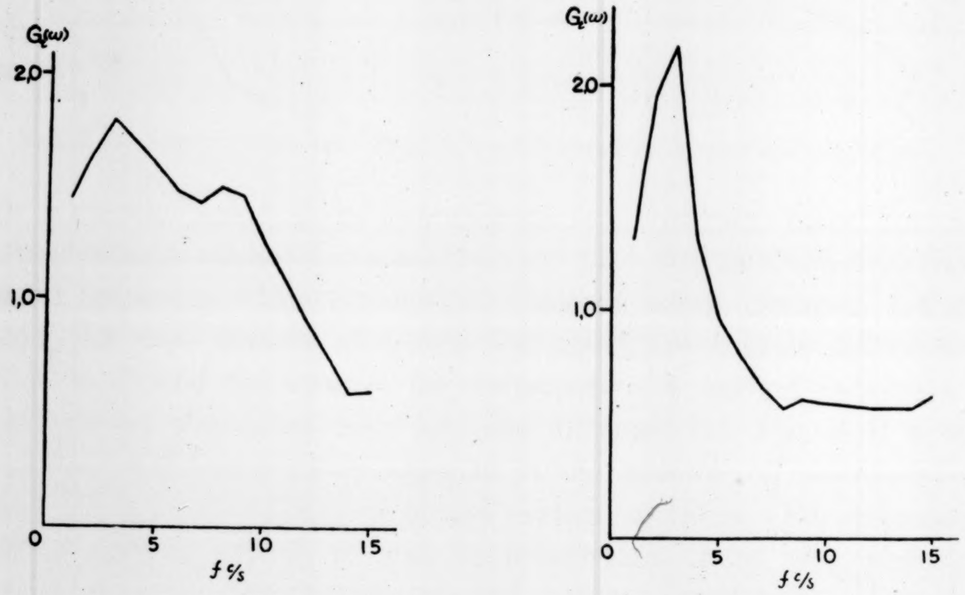

a. In the daytime. b. At night.

Fig. 3 IV. Spectra from records with 3 c/s vertical seismometer at Kokubunzi.

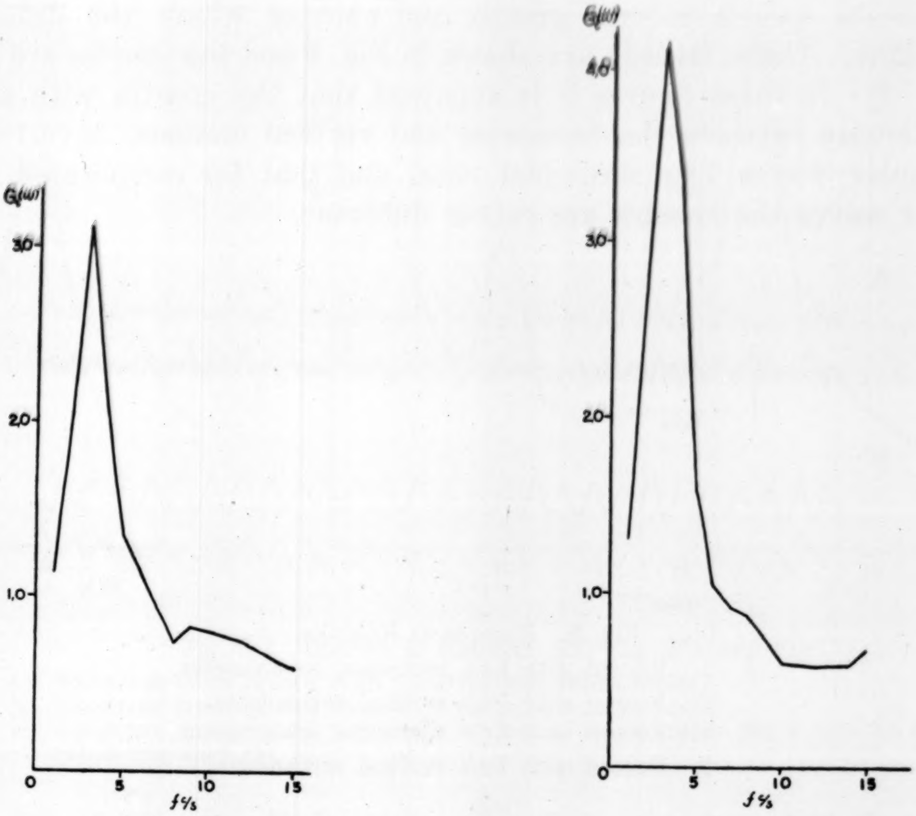

a. In the daytime. b. At night.

Fig. 3 V. Spectra from records with 3 c/s vertical seismometer at Kakioka.

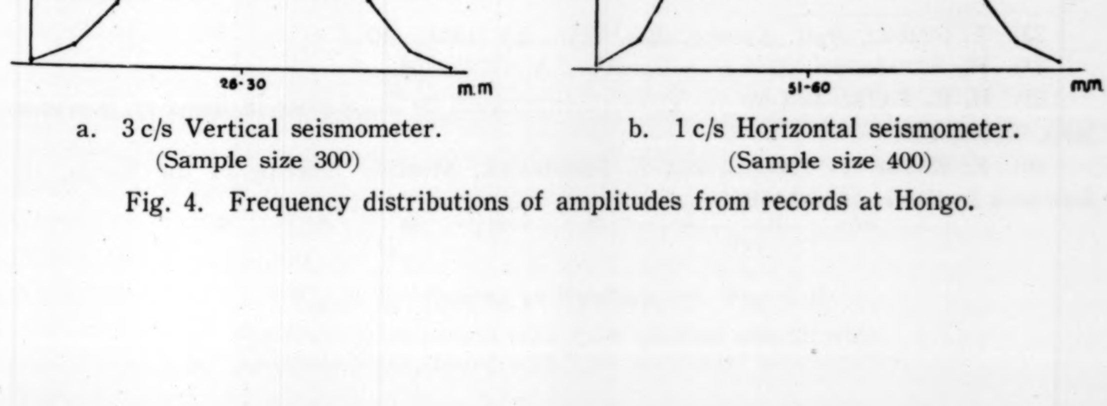

a. 3 c/s Vertical seismometer. (Sample size 300)

b. 1 c/s Horizontal seismometer. (Sample size 400)

Fig. 4. Frequency distributions of amplitudes from records at Hongo.

and vertical spectra differed greatly and another where the difference was slight. These records are shown in Fig. 5 and the spectra are given in Fig. 6. In these figures it is apparent that the spectra with almost no difference between the horizontal and vertical motions, have records of regular waves like sinusoidal ones, and that for complicated or irregular waves the spectra are rather different.

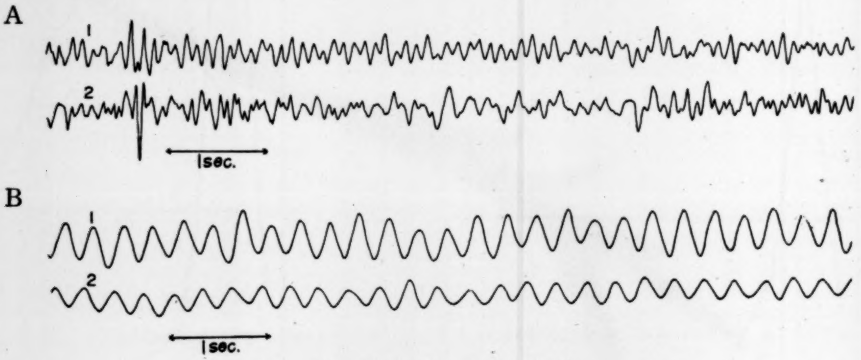

Fig. 5. Records at Kakioka.
A 1. Record with 1 c/s horizontal seismometer.
2. Record with 1 c/s vertical seismometer.
B 1. Record with 1 c/s horizontal seismometer.
2. Record with 1 c/s vertical seismometer.

At Kakioka, the vertical component of the amplitudes of short period microseisms of a frequency about 10 c/s were somewhat larger than the horizontal, and in microseisms of frequency 3–4 c/s, the amplitudes of the vertical motions were about half the horizontal motions. The variation of the ratio of the horizontal motion to the vertical one with frequency can be explained by the theory of surface waves in layered ground[23)].

Spectra in Fig. 6 and records in Fig. 7 are those which were observed simultaneously on the ground and in a hole 2.5 m below the surface. In the hole, waves of a frequency higher than 9 c/s decreased rapidly. The phase velocity of those waves is associated with the uppermost surface of the ground. Simultaneous observations on the ground surface and under it are found in literature[24),25),26)]. For example H. E. Tatel and M. A. Tuve have observed that on the subject a

---

23) T. SUZUKI, *Bull. Earthq. Res. Inst.*, **11** (1933), 187.

24) W. SCHNEIDER, *Zeit. für Geophys.*, **4** (1928), 103.

25) H. E. TATEL and M. A. TUVE, *Contribution in Geophysics in honor of B. Gutenberg*, (1958), 152.

26) K. KANAI, T. TANAKA and S. YOSHIZAWA, Monthly Meeting of the Earthquake Research Institute, (April, 1959).

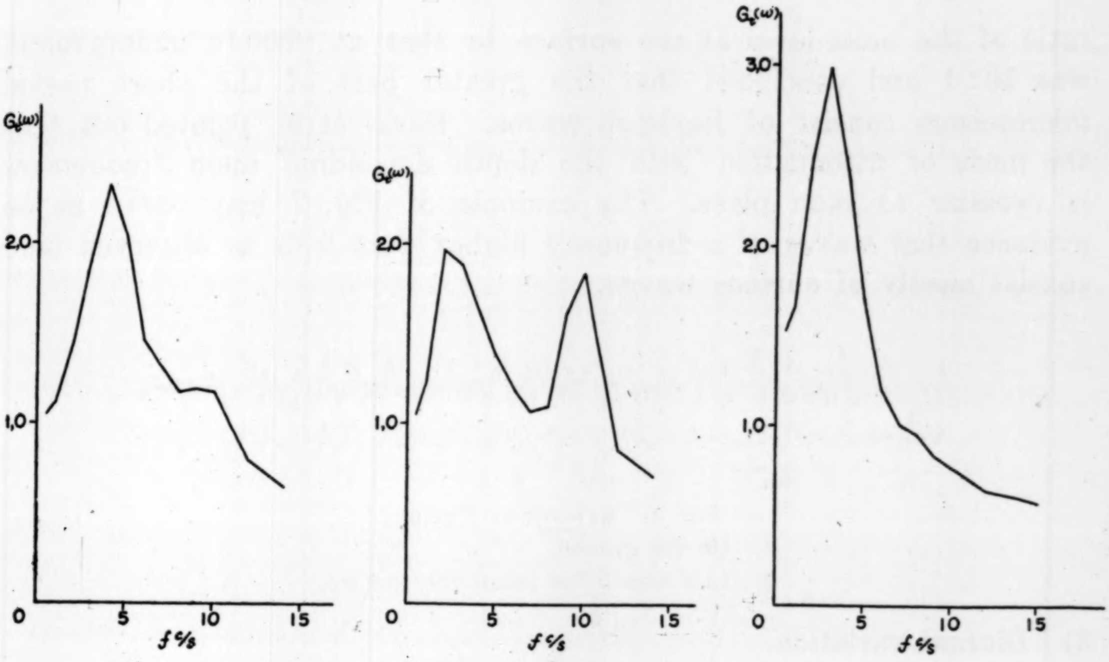

a b c

Fig. 6 I. Spectra at Kakioka. (cf. Fig. 5 A and Fig. 7)

a. Spectrum from record with 1 c/s vertical seismometer.
b. Spectrum from record with 1 c/s horizontal seismometer.
c. Spectrum from record with 1 c/s horizontal seismometer (in a hole 2.5 m below the surface).

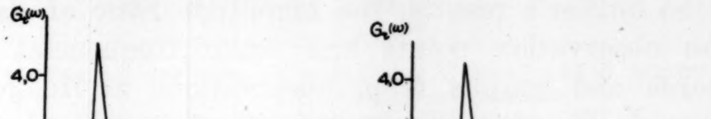

a b

Fig. 6 II. Spectra at Kakioka. (cf. Fig. 5 B)

a. Spectrum from record with 1 c/s vertical seismometer.
b. Spectrum from record with 1 c/s horizontal seismometer.

ratio of the noise level at the surface to that at 3000 ft underground was 10 : 1 and concluded that the greater part of the short period microseisms consist of Rayleigh waves. Kanai et al. pointed out that the mode of attenuation with the depth depending upon frequencies is peculiar to each place. The example of Fig. 7 may serve as an evidence that waves of a frequency higher than 9 c/s as observed here consist mostly of surface waves.

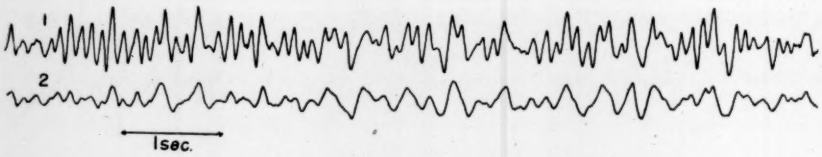

Fig. 7. Records at Kakioka.
1. On the ground.
2. In a hole 2.5 m below the surface.

3) Diurnal variation.

There have been some observations about the diurnal variation of the amplitude of short period microseisms and the amplitude ratios of day to night have been given[27),28)]. It has also been pointed out that in large towns the amplitude ratio of day to night is related to traffic[29)]. According to the author's results, the amplitude ratio of day to night depended upon observation points and wave frequencies in varying degrees. Records and graphs from observations at Hongo in uptown Tokyo are shown in Fig. 8. Observations have been made hourly and a day was taken as a cycle. Double amplitudes were read on record at various points and the amplitude was derived from their mean value. (At Hongo, the sensitivity of the instrument is about 20,000 times the ground displacement for the horizontal seismometer with an amplifier.) As shown in Fig. 8, in simultaneous observations with seismometers with different natural frequencies, that is with 1 c/s horizontal, and 3 c/s and 10 c/s vertical seismometers, the amplitude ratio of day to night was different for each seismometer. For example, the amplitude ratio of day to night was 17 : 1 with the vertical seismometer, 4 : 1 and 6 : 1 with the 1 c/s horizontal and 10 c/s vertical seismometer respectively. Waves recorded by the 3 c/s vertical seismometer contained waves with frequencies 7–10 c/s. It is possible that the wave sources of these frequency ranges may be more dense here than at other places.

---

27) C. D. V. WILSON, *ibid.* 3).

28) K. KANAI, T. TANAKA and K. OSADA, *ibid.*

29) Y. TOMODA and K. AKI, *Zisin*, [ii] **5** (1952), 85.

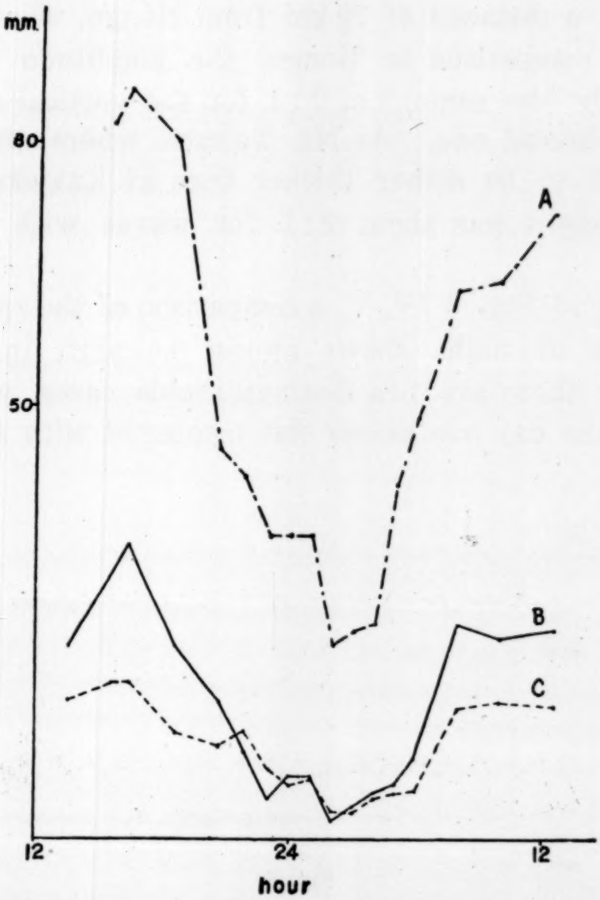

I. Diurnal variation of amplitudes of short period microseisms.
A 1 c/s Horizontal seismometer.
B 3 c/s Vertical seismometer.
C 10 c/s Vertical seismometer.

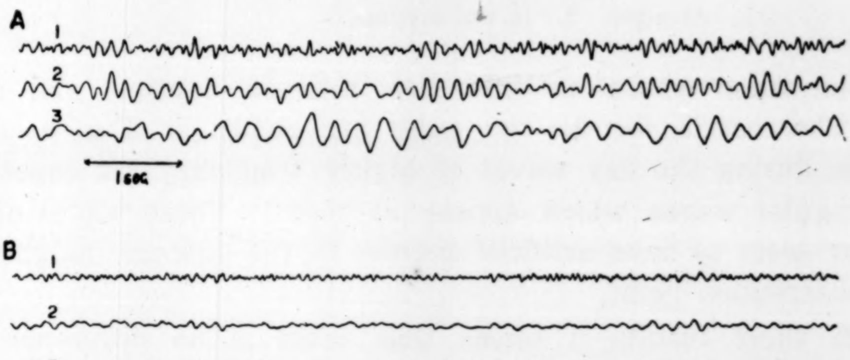

II. A Day (12 h) B Night (02 h)
1. 10 c/s Vertical seismometer.
2. 3 c/s Vertical seismometer.
3. 1 c/s Horizontal seismometer.
(The ratio of sensitibity of amplifier in the daytime to that in the night was 1 : 2 for 1 c/s and 10 c/s seismometers and 1 : 5 for 3 c/s seismometer.)

Fig. 8. Diurnal variation at Hongo.

At Kakioka, a distance of 70 km from Hongo, where the noise level is about 1/60 in comparison to Hongo, the amplitude ratio of day to night was nearly the same, i.e. 7 : 1 for the vertical seismometer and 8 : 1 for the horizontal one. At Mt. Tukuba where the wave sources may be thought to be rather thicker than at Kakioka, the amplitude ratio of day to night was about 2 : 1 for waves with a frequency of 20 c/s.

As apparent in Fig. 3 IV, V, a comparison of the spectra in the daytime with those at night shows almost no shift in the "dominant frequency", but there are two distinguishable cases, where in one the spectra during the day are rather flat compared with spectra at night, and in the other where no difference between daytime and night is found. The records for the two cases are shown in Fig. 9. As seen in Fig. 9, during the day waves of higher frequency are superimposed on the regular waves which appear at night. These waves of higher frequency seem to have artificial sources in the extreme neighbourhood of the observation point.

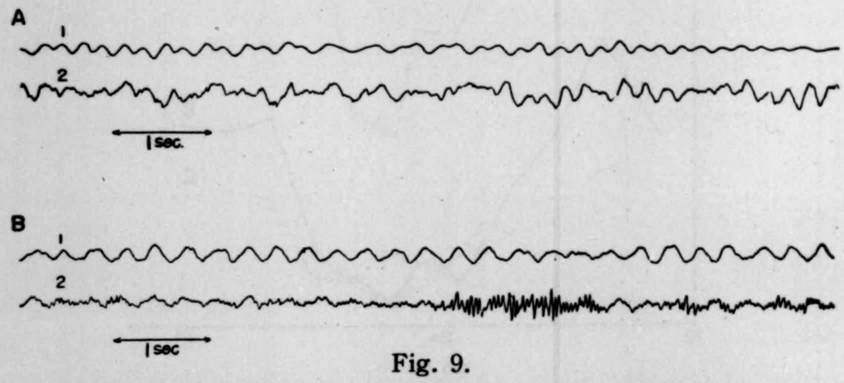

Fig. 9.

A Records with 1 c/s horizontal seismometers at Kokubunzi.
1. At night. 2. In the daytime (The ratio of sensitibity of amplifier in the daytime to that in the night 1 : 3).

B Records with 3 c/s vertical seismometers at Kakioka.
1. At night. 2. In the daytime.

From these results it seems that there is no difference in the "dominant frequency" of the spectra between day and night for a given location. The "dominant frequency" proper to the location persist day and night. During the day the wave sources of short period microseisms are more dence; and artificially generated waves near the observation point are superimposed on waves that already were there.

§ 4. The characteristics of short period microseisms

1) Method of observation and analysis.

In section 3, a macroscopic view has been taken in the study of short period microseisms; however, in this section characteristics of the individual wave are investigated from the microscopic point of view. As the method of investigation, tripartite observations with three components were adopted. The tripartite observation has been used frequently for the study of microseisms and C. D. V. Wilson[30] also used this method for calculating the direction of wave propagation caused by vehicles.

In this investigation for the net of observation right angled triangles were chosen in most cases to facilitate calculations. The length of a side of a triangle was taken about 1/4 of the wave length observed, i.e. 10–50 m as a rule. Sometimes seismometers were set at three fixed vertices of a triangle; at other times the vertex at the right angle was fixed and the other two points were shifted along each side by 2–5 m in order. The result from these methods is used for the calculation of the cross-correlation coefficients of waves at two points. For the study of wave orbits a tripartite observation was combined with a three component observation. For the observation sites terrains flat enough and rather large in area compared with a triangle were chosen. The seismometers were usually set on the ground surface; occasionally however, they were set in a shallow hole about 50 cm deep to protect them from the direct influence of wind. Observations were made in most cases at night, because the waves with high frequencies (above 10 c/s) decreases in amplitude and the correspondence from wave to wave is facilitated at night. The microseisms we are concerned with here are those with frequencies 1–10 c/s. These waves could be easily observed at any observation point and for waves with a frequency above 10 c/s the correspondence from wave to wave becomes difficult with the increase in the distance between two or three observation points. For example, for waves with a frequency above 10 c/s the cross-correlation coefficient between two observation points decreases rapidly.

For the determination of the direction of wave propagation and phase velocity as seen in Fig. 10, the crests and troughs of waves with good correspondences at three points were chosen on record and the differences in their arrival times, i.e. phase differences, were read.

---

[30] C. D. V. Wilson, *ibid.* 4).

Even for waves with frequencies 1–10 c/s there were places at which the correspondence from wave to wave was poor. For example, in a triangle with one side 14 m long, there was a good correspondence at two corners, but at the third corner the wave form was deformed (Fig. 11). It seems that at such a place the sources of the short period microseisms are distributed comparatively densely; waves propagated from each source interfere with one another; and the resultant waves are observed. Although analysis by a method of tripartite observation only is not sufficient where the wave formation seems complex, however, this analysis was applied to seismograms obtained from places where the wave formations seemed simple. Records of tripartite observations are shown in Fig. 12. Fig. 12 VI A, B, C are examples which illustrate very good correspondences of waves at each vertex of a triangle.

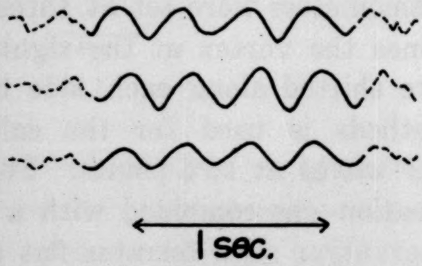

Fig. 10. Wave to wave correspondence.

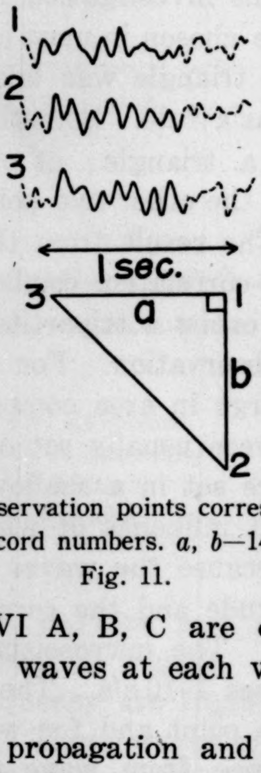

(Observation points corresponding to record numbers. a, b—14 m.)

Fig. 11.

Probable errors in the direction of wave propagation and velocity due to the reading error of the crest and trough of a wave is respectively about ±10%.

Even in a predominant wave packet series, as small waves are superimposed on this wave packet, the positions of crest and trough apparently fluctuate. Therefore, it would be impossible in such a case to obtain the true direction of the wave propagation and velocity without the aid of statistical methods, that is, the method of obtaining the position of the maximum value of their respective frequencies of appearance, calculated from the crests and troughs of individual waves

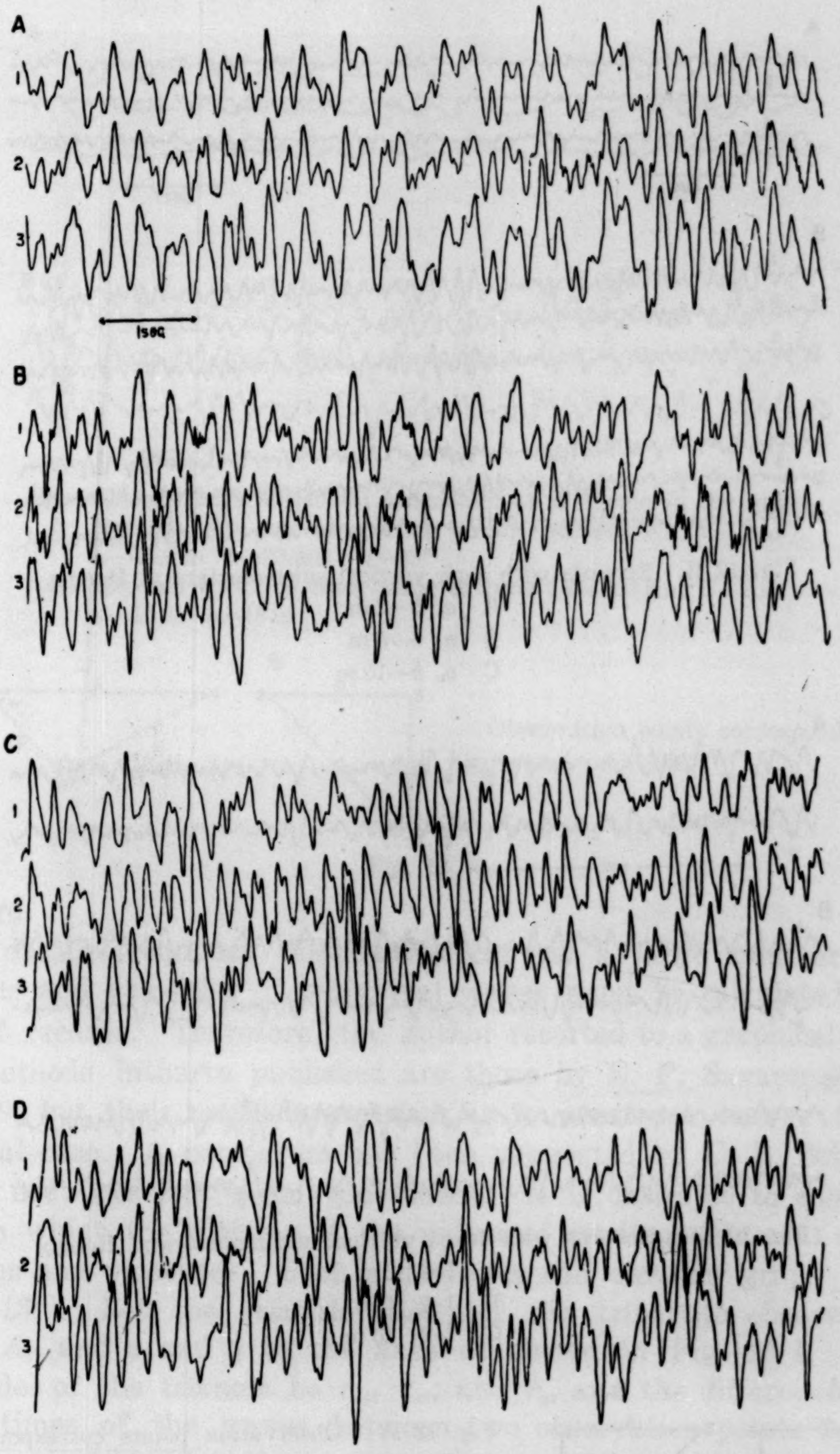

Fig. 12 I. Records with 1 c/s horizontal seismometers at Hongo.
A a, b—2 m B a, b—6 m
C a, b—10 m D a—12 m b—18 m
(a, b—cf. Fig. 12 IV.)

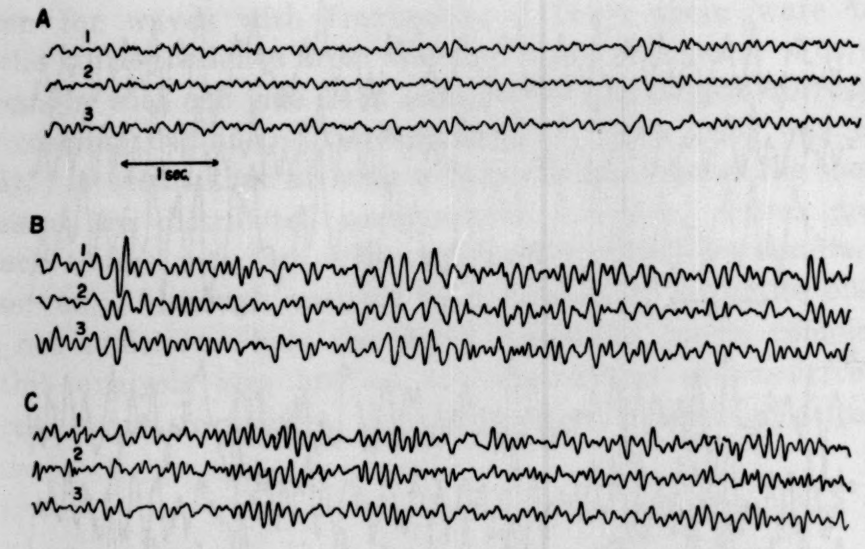

Fig. 12 II. Records with 3 c/s vertical seismometers at Hongo.

A *a*, *b*—2 m
B *a*, *b*—6 m
C *a*, *b*—10 m

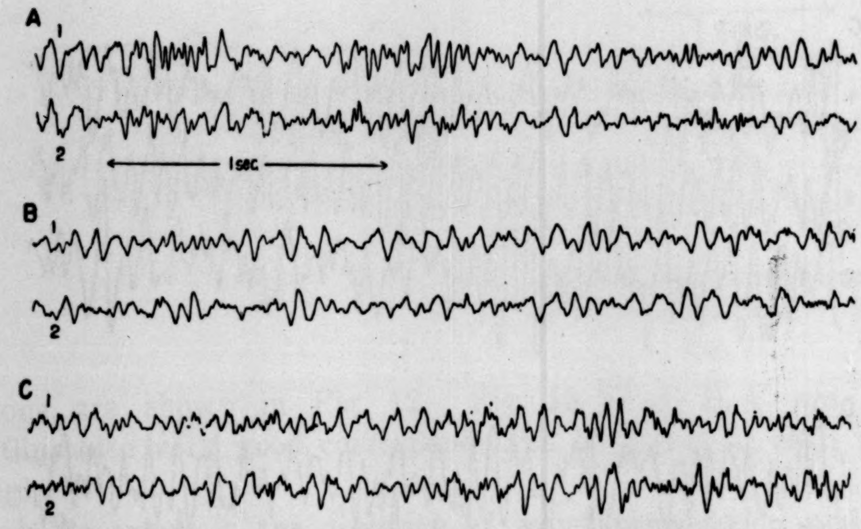

Fig. 12 III. Records with 10 c/s vertical seismometers at Hongo.

A 1-2 2 m
B 1-2 6 m
C 1-2 10 m

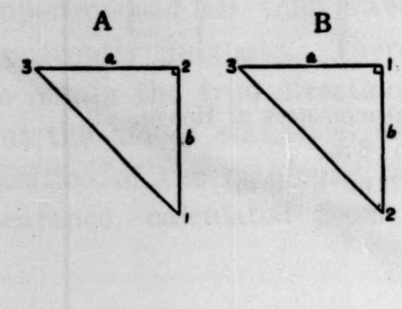

Fig. 12 IV. Observation points corresponding to record numbers.

A—Fig. 12 I.
B—Fig. 12 II.

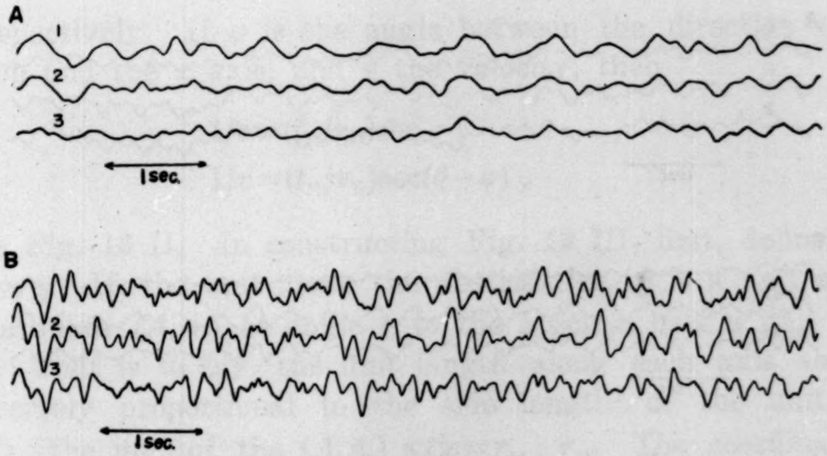

Records with 1 c/s horizontal seismometers at Hongo in the night.
A Records with two integrating circuits ($R=200$ KΩ, $C=2\,\mu$F).
a—46.8 m b—23.4 m α—45°
B Records with one integrating circuits ($R=200$ KΩ, $C=2\,\mu$F).
a—15 m b—18 m

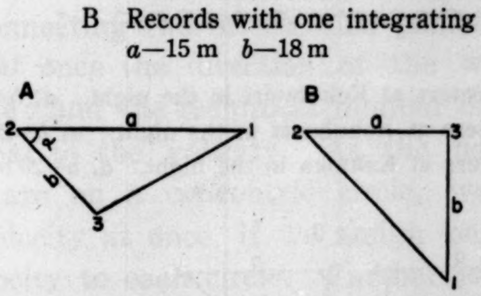

Observation points corresponding to record numbers.

Fig. 12 V.

on record.

To obtain frequency distribution curves, a large number of the directions and velocities of individual waves must be calculated from a series of records. Therefore, the author resorted to a graphical method. Such methods hitherto published are those by E. F. Savarensky[31)] and K. Aki[32)], but their methods are such as to construct curves for each individual case. A nomogram has been suggested by C. L. Schuyler[33)], but its use does not seem convenient. It is desirable to construct a graph in which the plotting of the values of readings gives at once the directions and velocities. Such a device is the circular graph as seen in Fig. 13[34)]. Let the triangle used for the tripartite observation be A_1, A_2, A_3, and x and y be the axes as shown in Fig. 13 I. Let the three sides of the triangle be r_{12}, r_{13}, and r_{23} and the differences in the arrival times of the waves between two observation points be t_{12}, t_{13},

---

31) E. F. SAVARENSKY, i D P. KIRNOS, *Elementi Seismologii i Seismometrii,* (1955), 188.

32) K. AKI, *ibid.*

33) G. L. SCHUYLER, *Bull. Seism. Soc. Amer.,* **45** (1955), 285.

34) K. AKAMATU, The meeting of the Seismological Society of Japan, (Dec. 1958).

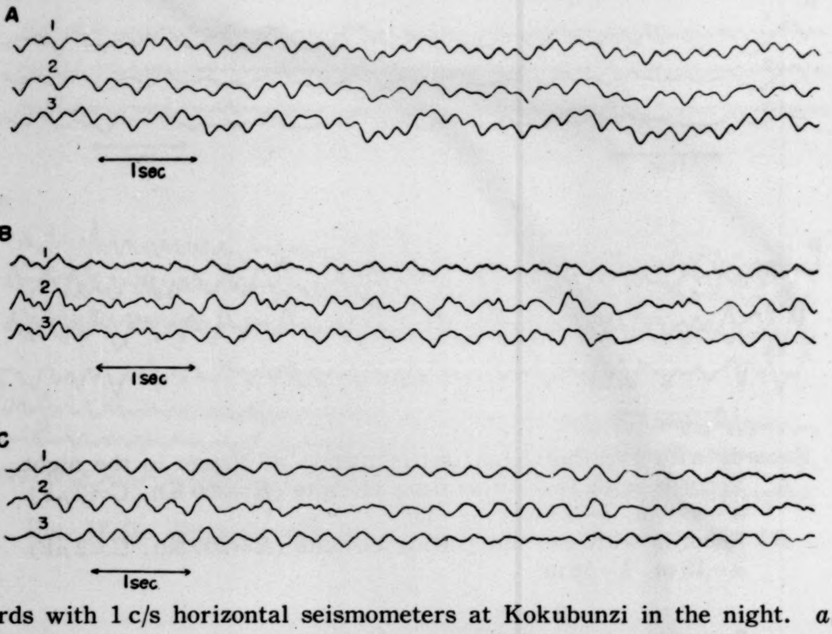

A Records with 1 c/s horizontal seismometers at Kokubunzi in the night. *a*, *b*—20 m
B Records with 3 c/s vertical seismometers at Kokubunzi in the night. *a*, *b*—20 m
C Records with 3 c/s vertical seismometers at Kakioka in the night. *a*, *b*—20 m

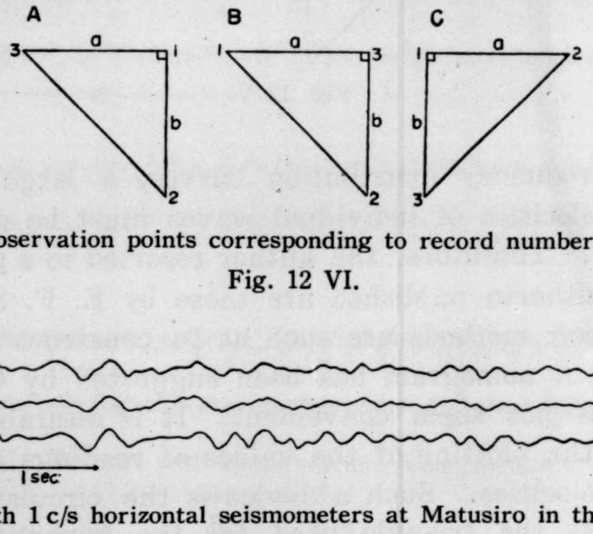

Observation points corresponding to record numbers.

Fig. 12 VI.

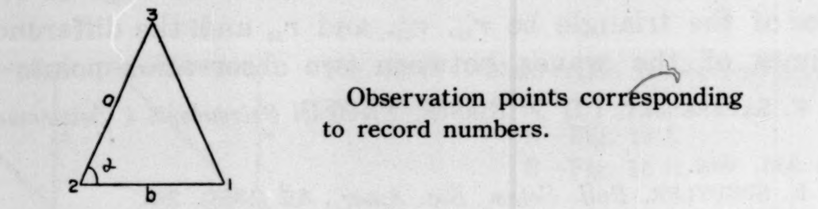

Records with 1 c/s horizontal seismometers at Matusiro in the daytime.
a—183 m *b*—147 m *α*—67°

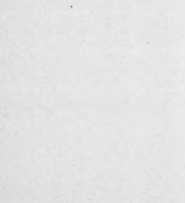

Observation points corresponding to record numbers.

Fig. 12 VII.

and t_{23} respectively. If φ is the angle between the direction of wave propagation and the x axis, and v the velocity, then

$$1/v=(t_{12}/r_{12})\sec\varphi\ ,$$
$$1/v=(t_{13}/r_{13})\sec(\theta-\varphi)\ ,$$

as seen in Fig. 13 II. In constructing Fig. 13 III, first, define a such that $ar_{13}=r_{12}$. If the unit along the abscissa (A_1A_3) is a unit of t, the inclined ordinate (A_1A_2) at angle θ to the abscissa uses a unit a times that of t. That is to say, the unit length along each axis should be taken inversely proportional to the side length; or the unit of the (A_1A_3) axis : the unit of the (A_1A_2) axis$=r_{12} : r_{13}$. The coordinate point in this system is represented by the intersection of two straight lines, each of which is perpendicular to each respective axis. The straight line connecting the intersection point with the origin of the coordinates gives at once the direction of the wave propagation, relative to the triangle; and the reciprocal number of the length of this vector is proportional to the velocity. As the points at which the velocities are equal are on a concentric circle, we can read the values of direction and velocity at once, if we assign beforehand the corresponding value of velocity to each circle. Furthermore, the advantage of this representation is that the range of errors in the direction of wave propagation and velocity can easily be found. On the seismograms the values of t_{12} and t_{13} are read with a uniform unit of scale, but the corresponding φ and v are not proportional to t_{12} or t_{13}. Thus, although the absolute error of the t reading is uniform throughout, corresponding errors in φ and v have no uniform distributions. This circumstance is clear on the graph. This method in which the length of the vector is a inversely proportional to the velocity is more convenient for a graphical representation than the other method in which the vector is proportional to the velocity, because in practical cases, large apparent values of v appear more frequently as compared with small values of v.

Graphs of the frequency distributions of the direction of wave propagation and velocity are drawn with the overlapping mean value by $(f_{i-1}+2f_i+f_{i+1})/4$. In constructing wave orbits, two corresponding components are read on the records at every 1/50 second and combined with each other. As for orbits in the vertical plane, first, an orbit in the horizontal plane is drawn, and then, the horizontal component in the vertical plane containing the direction of wave propagation obtained from tripartite observation is combined with the vertical component.

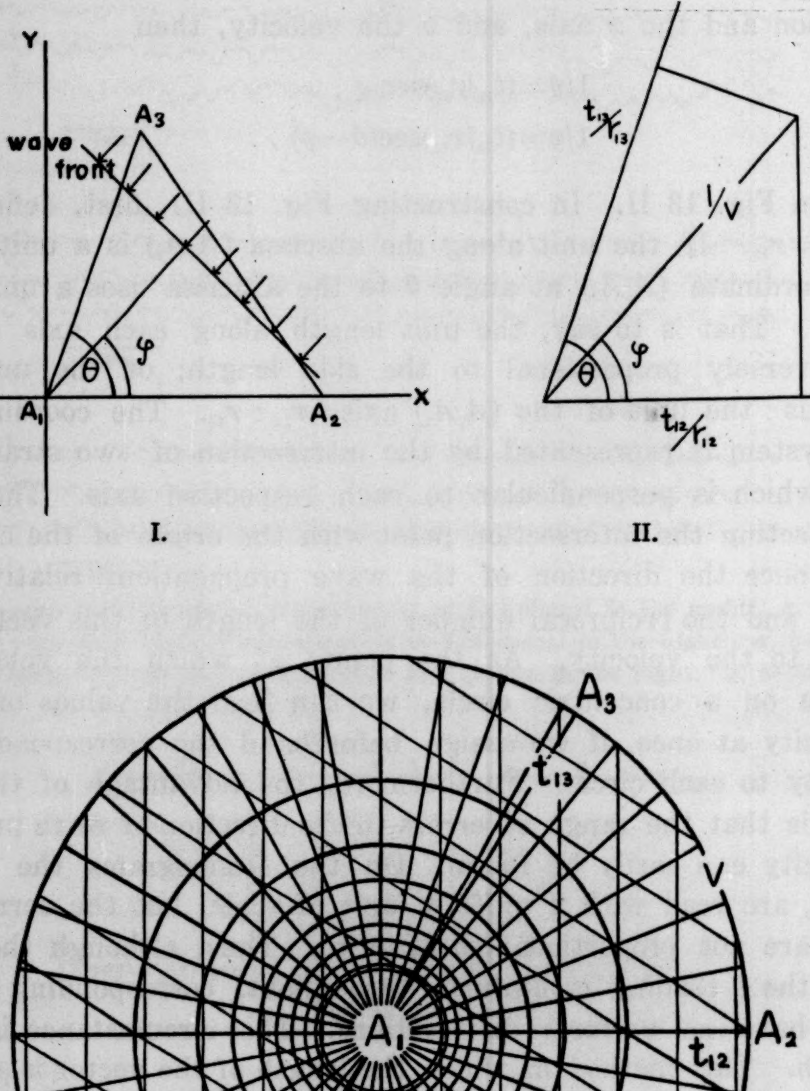
Y
wave front
A3
φ
θ
A1
A2
X
t13/r13
1/V
φ
θ
t12/r12
A3
t13
V
A1
A2
t12

I. II.

III.

Fig. 13. Circular graph.

In drawing vertical orbits, the direction of wave propagation is taken as the standard of reference, because the existance of Rayleigh and Love type waves is theoretically presumed.

2) Wave lengths, direction of wave propagation and velocity.

Frequency distributions of the direction of wave propagation and those of velocity obtained by the method stated in section 1) are shown in Figs. 14 and 15. As seen in the figures, curves are sharper at night than in the daytime. The reason may be that the chances of interference with the waves might be smaller at night.

From records which have rather sharp frequency distributions of velocity regular waves appear for the most part as seen in Fig. 12 IV A, and the correspondence of wave forms at three points is good. On the contrary, records which have flat frequency distributions of velocity are more complex than the former and it seems that they are composed of waves with a different frequency and velocity.

In frequency distributions of the directions of wave propagation, even for rather regular waves there are two cases where the directions seems sharply concentrated and cases where the directions are evenly distributed.

The velocity of short period microseisms is different from place to place but the range of values is from 200 m/s to 600 m/s in most cases. These values are also different for every predominant frequency, for example, about 600 m/s for the horizontal motion with a frequency of 2.6 c/s and 300 m/s for the vertical motion with a frequency of 3.6 c/s at Kakioka, 350 m/s for the horizontal motion with a frequency of 4 c/s at Tanasi-mati B, and 200 m/s for the vertical motion with a frequency of 10 c/s at Hongo. Places which have wave velocities over 1 km/s are rare, and the wave frequency with such velocity is rather low, i.e. from 1 c/s to 1.5 c/s. Wave lengths calculated from the frequency and velocity are between 20 m and 230 m. Waves of such wave lengths are well observed at every observation point. For frequencies from 1 c/s to 10 c/s, wave lengths over 300 m are rare. At every observation point the values obtained are mutually independent and depend upon the ground structure.

Graphs of the cross-correlation of waves simultaneously observed at two points and calculated by the method of section 3, 1) are shown in Fig. 16. If the ground is vibrating uniformly, the cross-correlation is always high at two points some distance apart, but in the result obtained, the correlation decreased gradually with the distance as seen in Fig. 16. In Fig. 16, waves with a higher frequency decrease more rapidly than those with a lower frequency. From records it was also found that for waves over 10 c/s no correspondence is found even at places only a few meters apart.

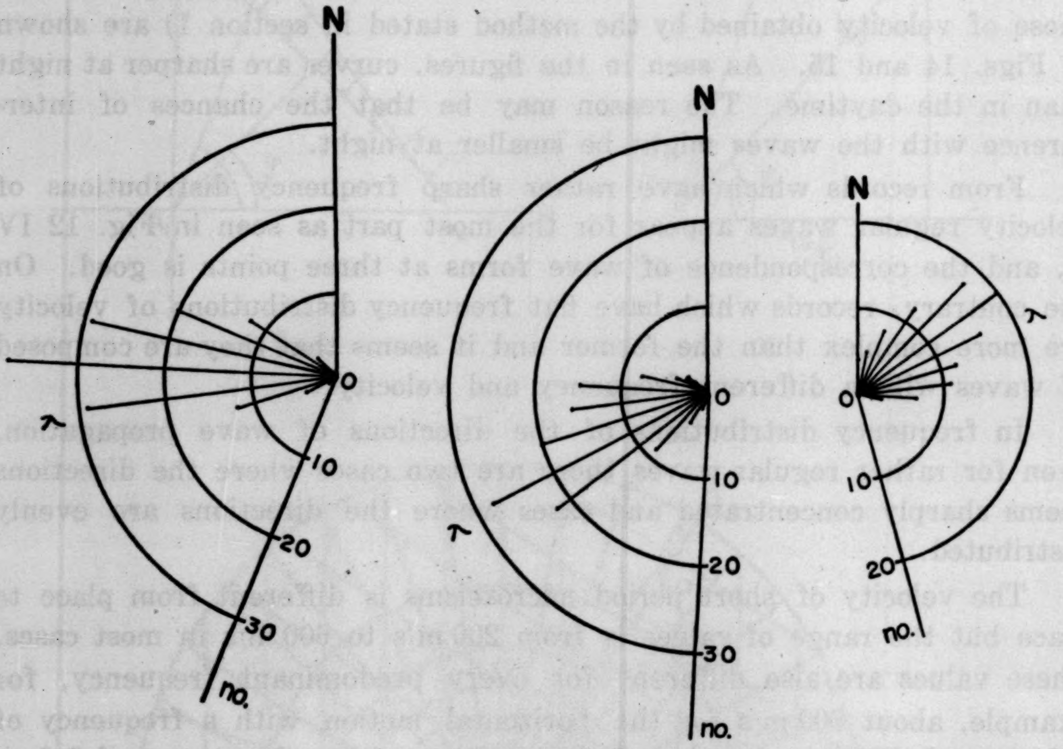

I. (1 c/s Horizontal seismometer.) II. (3 c/s Vertical seismometer.) III. (3 c/s Vertical seismometer.)

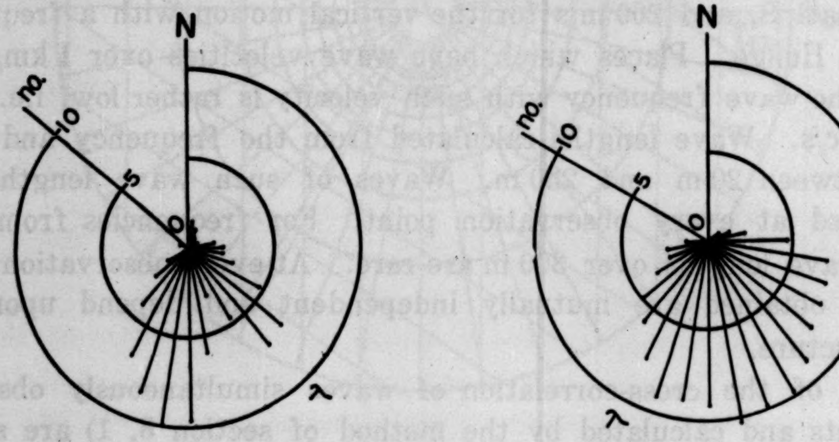

IV. (3 c/s Vertical seismometer.) V. (1 c/s Horizontal seismometer.)

Fig. 14.

I, II. Frequency distributions of the direction of wave propagation at Kokubunzi.
III, IV, V. Frequency distributions of the direction of wave propagation at Kakioka.

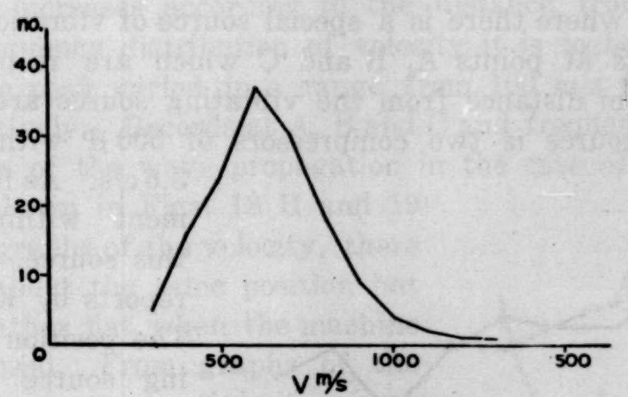

I. (1 c/s Horizontal seismometer.)

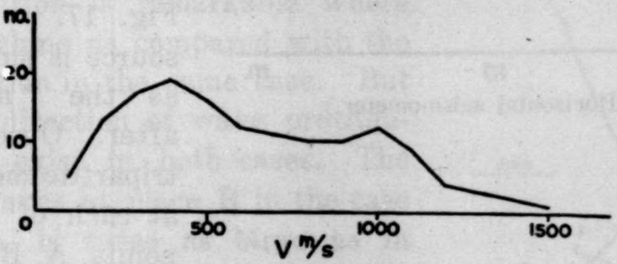

II. (3 c/s Vertical seismometer.)

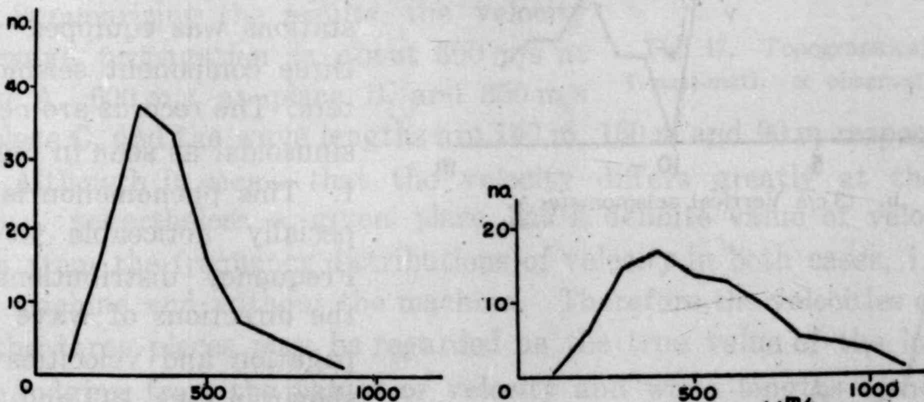

III. (3 c/s Vertical seismometer.) IV. (3 c/s Vertical seismometer.)

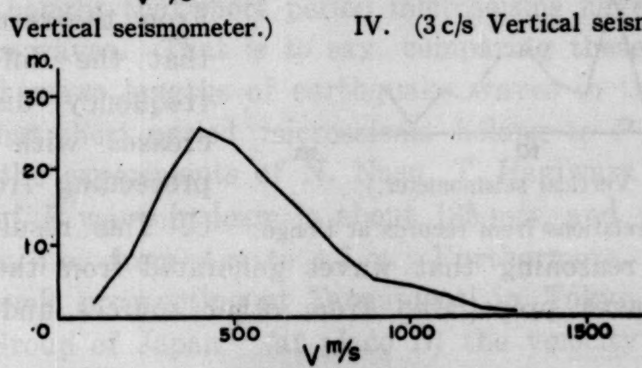

V. (1 c/s Horizontal seismometer.)

Fig. 15.

I, II. Frequency distributions of the phase velocity at Kokubunzi.

III, IV, V. Frequency distributions of the phase velocity at Kakioka.

In the case where there is a special source of vibrations, the results of measurements at points A, B and C which are respectively 610 m, 730 m and 1190 m distance from the vibrating source are shown below. The vibrating source is two compressors of 500 HP with the frequency 3.6 c/s. As for the measurement within 600 m from this source, there are some reports by K. Kanai et al[35]. The position of the vibrating source and the topographical map are given in Fig. 17. The vibrating source is simply referred to as the "machine" hereafter. Observations of the tripartite method were made at each of the observation points, A, B and C. In each tripartite set, one of three stations was equipped with three component seismometers. The records are nearly sinusoidal as seen in Fig. 18 I. This phenomenon is especially noticeable at A. Frequency distributions of the directions of wave propagation and velocities are shown in Figs. 19 I and 20 I. From the result it is found that the diffusion of the frequency distribution increases with the distance proceeding from A to B to C. This result can be explained by the reasoning that waves generated from the machine are interfered by waves propagated from other sources and the ratio of

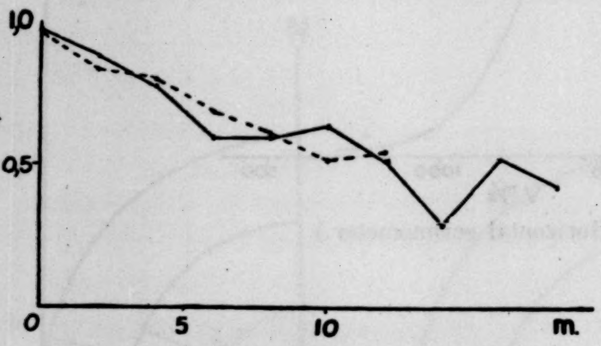

a. (1 c/s Horizontal seismometer.)

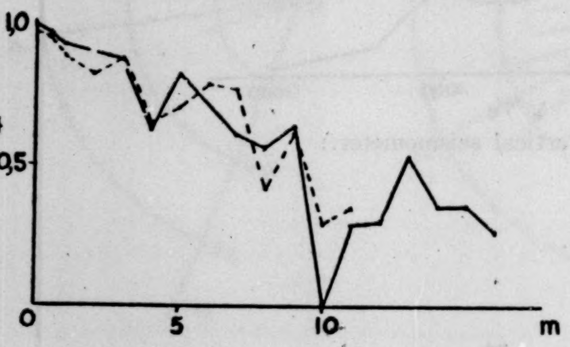

b. (3 c/s Vertical seismometer.)

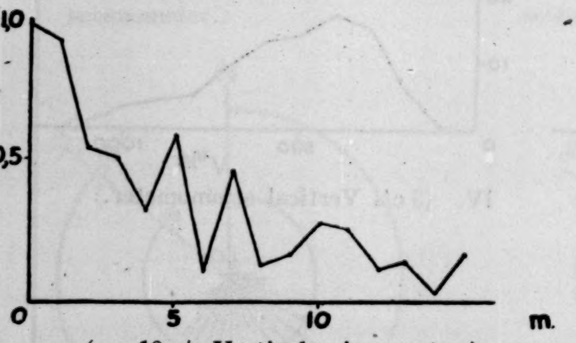

(c. 10 c/s Vertical seismometer.)

Fig. 16. Space correlations from records at Hongo.

---

[35] K. KANAI, T. TANAKA and K. OSADA, Monthly Meeting of the Earthquake research Institute, (March, 1959).

noise to signal increases according to the distance from the machine. As for the frequency distribution of velocity it is to be noted that the positions of the peak varied in a range from 100 m/s to 200 m/s at A, B and C respectively. Records at A, B and C and frequency distributions of the direction of the wave propagation in the case of there being no machine are shown in Figs. 18 II and 19 II. Comparing graphs of the velocity, there is a peak at about the same position but the curve is rather flat when the machine has not been used. From graphs of the direction of wave propagation it is seen that its fluctuation is remarkable where there is no machine as compared with the velocity fluctuation in the same case. But a predominant direction of wave propagation seems to exist in both cases. The amplitude of waves at place B in the case of the machine, is twice as large as in the case without the machine.

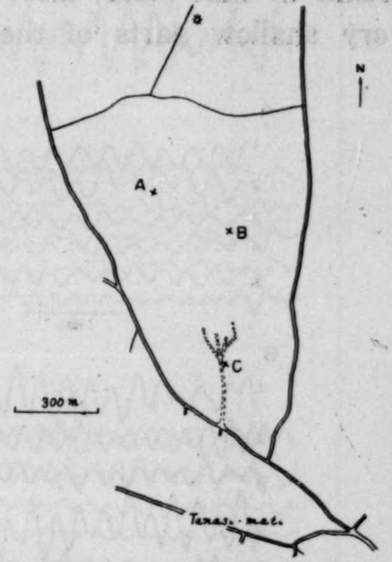

Fig. 17. Topographical map of Tanasi-mati. × observation point.

Summarizing the results, the velocity of wave propagation is about 500 m/s at place A, 600 m/s at place B, and 350 m/s at place C, and the wave lengths are 140 m, 160 m and 90 m respectively.

Although it seems that the velocity differs greatly at the three points, nevertheless a given place has a definite value of velocity, as seen from the frequency distributions of velocity in both cases, i.e. with the machine and without the machine. Therefore the velocities obtained at the three places may be regarded as the true value of the locations.

Judging from the values of velocity and wave lengths hitherto obtained, it is thought that short period microseisms have the characteristics of surface waves. That is to say, comparing these values with the velocities and wave lengths of earthquake waves in the soil, it cannot be thought that short period microseisms belong to *P* waves. For example, from the experiments of N. Nasu, T. Hagiwara and S. Omote36), the velocity of *P* wave in loam is about 135 m/s, and its wave length is very short, i.e. from 4 m to 4.5 m. Furthermore, according to the results of seismic prospecting at Tanasi-mati in Tokyo by the Seismic Exploration Group of Japan37) (at place B) the velocity of *P* wave to a

---

36) N, NASU, T. HAGIWARA and S. OMOTE, *Bull. Earthq. Res. Inst.*, **14** (1936), 561.
37) T. KAMETANI, Zisin Tankô Zitkken Gurûp Kaihô, (1954), 13.

depth of 2 m below the surface is about 200 m/s, to a depth of 10 m is 1210 m/s, and farther down to 20–30 m is 1780 m/s, and 2280 m/s at an ever greater depth (Fig. 21). The velocity of short period microseisms observed at this place is from 500 m/s to 600 m/s and the wave length about 150 m. Judging from the wave lengths of short period microseisms at that place, most of the waves are not connected with the very shallow parts of the ground, but with the deeper parts. There-

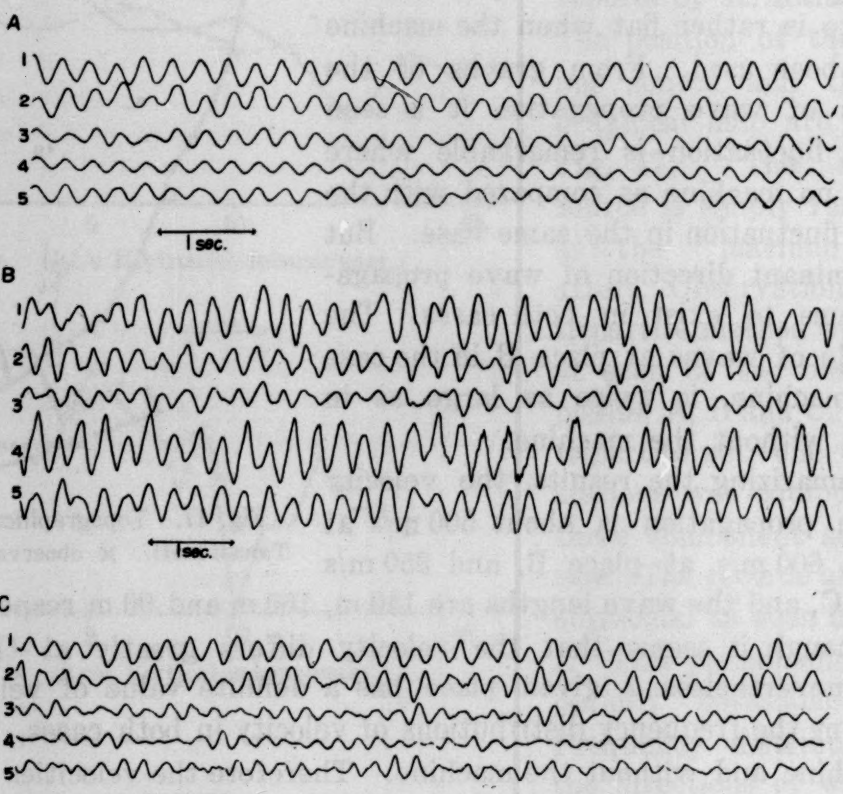

A 1, 2, 3—Horizontal seismometer with the same direction.
4—Horizontal seismometer with the direction 90° different from 1, 2, 3.
5—Vertical seismometer.
a, b—30 m
B 1, 2, 5—Horizontal seismometer with the same direction.
4—Horizontal seismometer with the direction 90° different from 1, 2, 5.
3—Vertical seismometer.
a, b—50 m
C 3, 4, 5—Horizontal seismometer with the same direction.
2—Horizontal seismometer with the direction 90° different from 3, 4, 5.
1—Vertical seismometer.
a, b—30 m

(a, b—cf. Fig. 18 III.)

Fig. 18 I. Records at Tanasi-mati A, B, C with the machine.

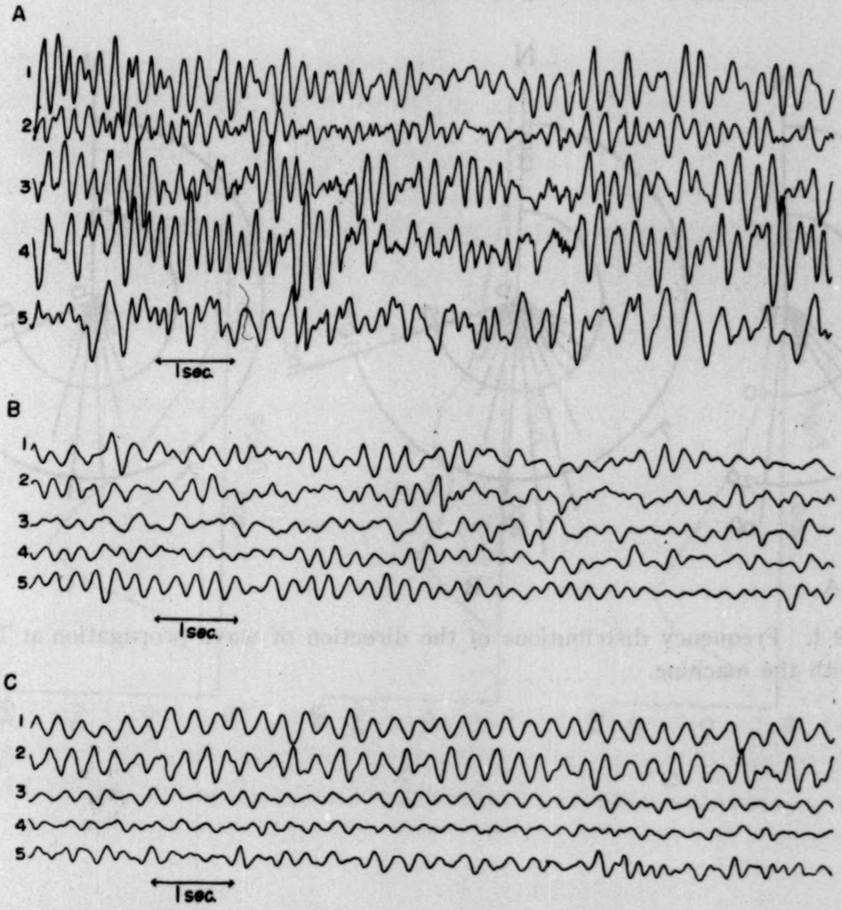

A 1, 2, 3—Horizontal seismometer with the same direction.
4—Horizontal seismometer with the direction 90° different from 1, 2, 3.
5—Vertical seismometer.
a, b—30 m

B 1, 2, 4—Horizontal seismometer with the same direction.
5—Horizontal seismometer with the direction 90° different from 1, 2, 4.
3—Vertical seismometer.
a, b—50 m

C 3, 4, 5—Horizontal seismometer with the same direction.
2—Horizontal seismometer with the direction 90° different from 3, 4, 5.
1—Vertical seismometer.
a, b—30 m

(a, b—cf. Fig. 18 III.)

Fig. 18 II. Record at Tanasi-mati A, B, C without the machine

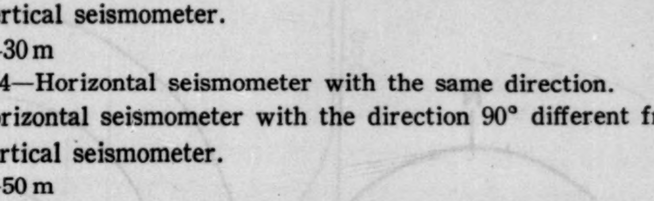

Fig. 18 III. Observation points corresponding to record numbers.

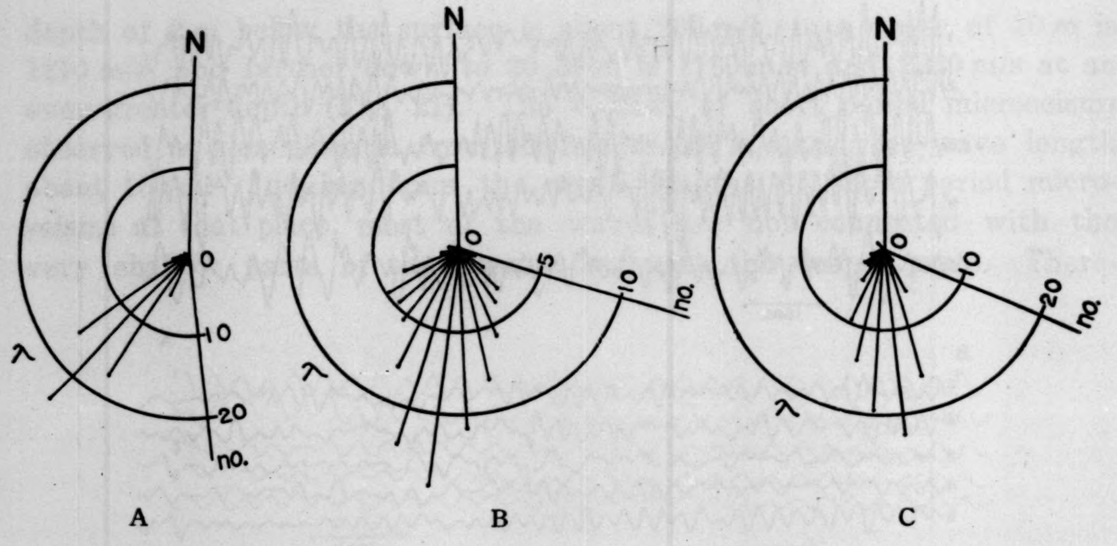

Fig. 19 I. Frequency distributions of the direction of wave propagation at Tanasi-mati A, B, C with the machine.

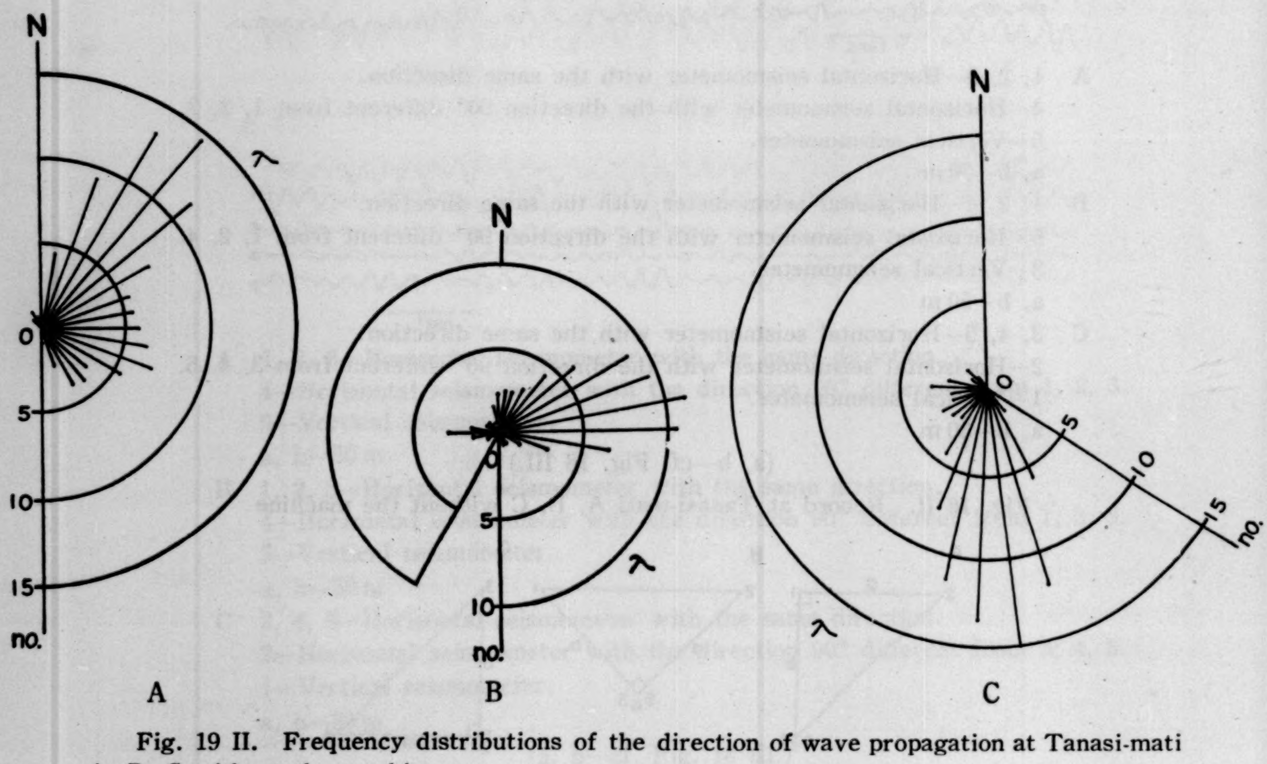

Fig. 19 II. Frequency distributions of the direction of wave propagation at Tanasi-mati A, B, C without the machine.

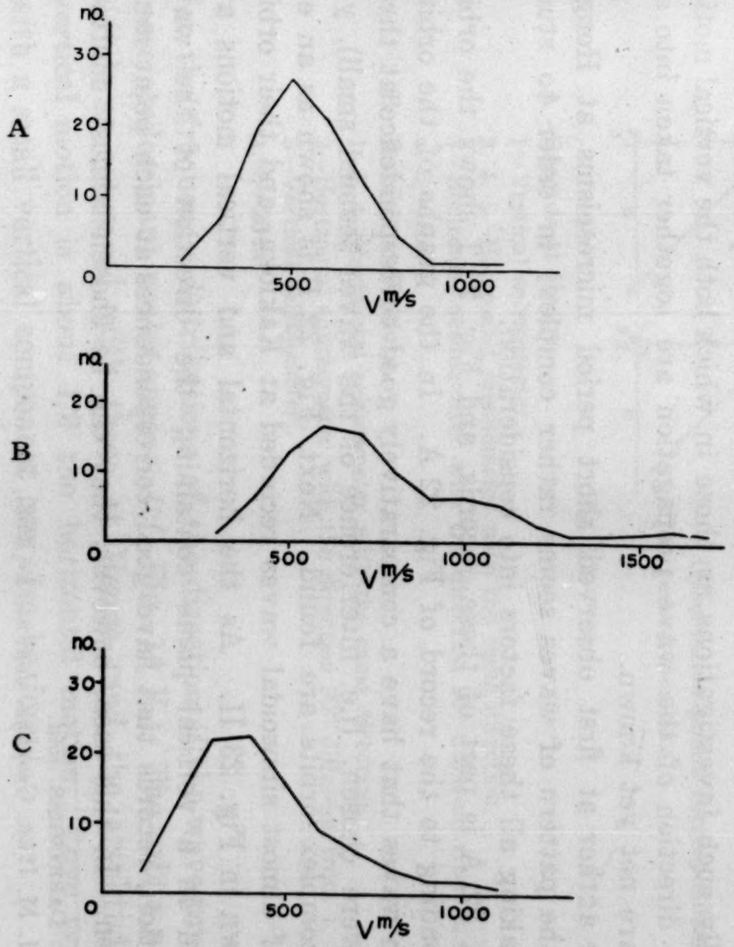

Fig. 20 I. Frequency distributions of the phase velocity at Tanasi-mati A, B, C with the machine.

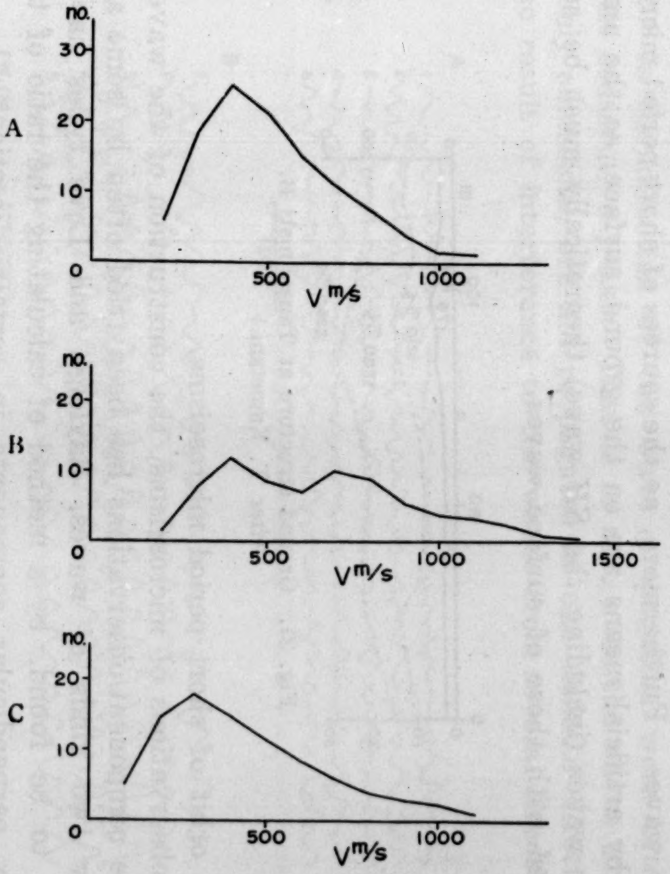

Fig. 20 II. Frequency distributions of the phase velocity at Tanasi-mati A, B, C without the machine.

fore, it is difficult to think that the velocities obtained above are those of body waves. Furthermore, as the sources of short period microseisms caused by artificial means are on the ground surface, so the amplitude of body waves (including the *SH* wave) theoretically must be small as compared with those of surface waves.

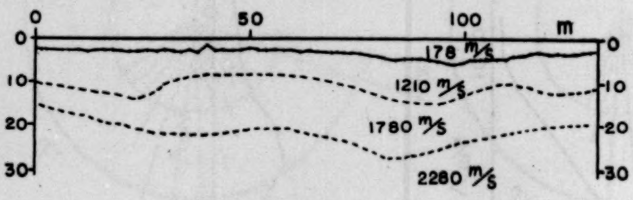

Fig. 21. Ground structure at Tanasi-mati B. (After T. Kametani.)

3) The orbit of short period microseisms.

In observations of microseisms, the construction of the wave orbits by three component observations has been tried often by some authors. Recently two kinds of waves, Rayleigh and Love types have been claimed to be found, by a method of calculating the ratio of the two mutually perpendicular components in certain direction[38),39)]. But in these cases, the assumption of the definite direction of the wave propagation was their common weak point.

Research of this kind has been limited for short period microseisms. Especially such investigations as those in which both the vertical motion and the direction of the wave propagation are together taken into account, are not yet known.

The author at first observed short period microseisms at Hongo, where the pattern of waves seems rather complex, in order to study orbits taking all these factors into consideration.

Fig. 22 A is part of these records, and Fig. 23 I shows the orbits corresponding to the record of Fig. 22 A. In the graphs of the orbits, although waves that have a comparatively good correspondence at three points were chosen, (i.e. interference of the waves seemed small), yet rather complex orbits are found. Next, Fig. 22 B is shown as an example of almost sinusoidal waves recorded at Kakioka, and their orbits are shown in Fig. 23 II. As the horizontal and vertical motions are combined in a vertical plane containing the direction of the wave propagation, records that have good correspondences at each point must be chosen. In this case, however, they can be chosen almost continu-

---

38) J. DARBYSHIRE, *ibid.*

39) H. M. IYER, *Geophys. Journ.*, **1** (1958), 32.

ously in a long series. Even in a record which seems simple, differences of ±20° in the direction of the wave propagation were often found between consecutive peaks. That is to say, even the waves which seem uniformly sinusoidal, are not propagated in one definite direction, but are the result of interference to the waves from several directions. As

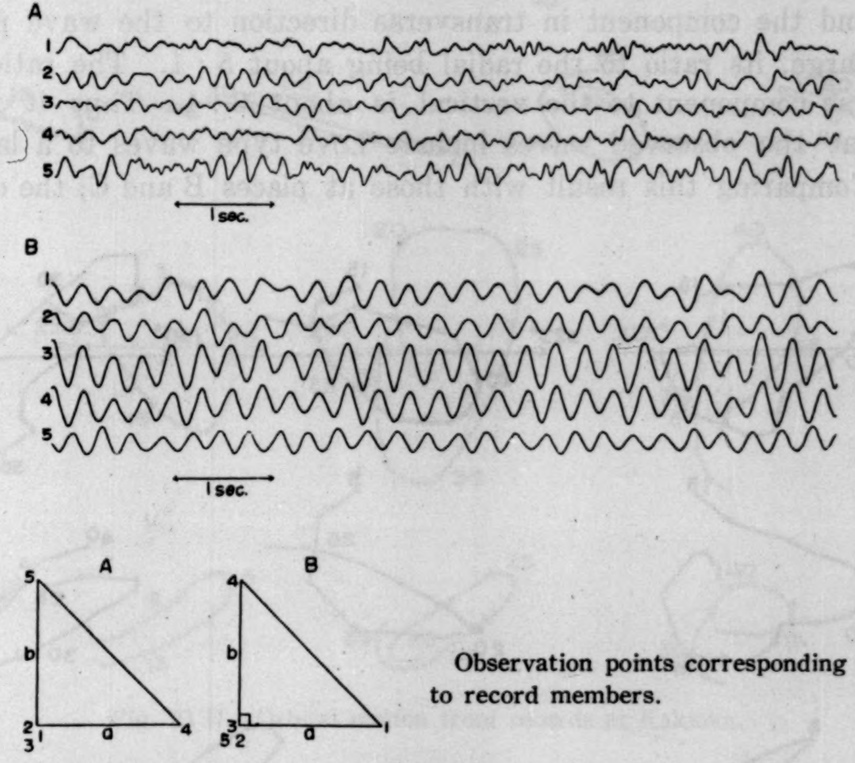

Observation points corresponding to record members.

Fig. 22.

A Records at Hongo.
1—Vertical seismometer..
2, 4, 5—Horizontal seismometer with the same direction.
3—Horizontal seismometer with the direction 90° different from 2, 4, 5.
a, b—15 m
B Records at Kakioka.
1, 3, 4—Horizontal seismometer with the same direction.
2—Horizontal seismometer with the direction 90° different from 1, 3, 4.
5—Vertical seismometer.
a, b—20 m

for the frequency distributions of the direction of the wave propagation, some predominant peaks appear. (cf. Fig. 14 V.) The orbits are rather simple as compared with those at Hongo, and the amplitude of the vertical motion is about 1/2 the horizontal motion. Love type waves with a small vertical component can also be found.

The wave orbit derived from seismograms in accordance with the machine observed at places A, B and C, A, 610 m, B, 730 m, and C, 1190 m distant from the source respectively mentioned in section 2), are shown in Fig. 24 A, B and C. The results from place A are simple and uniform compared with those places B and C. That is to say, the fluctuations of wave propagation are within ±10° in the horizontal plane, and the component in transverse direction to the wave propagation is large, its ratio to the radial being about 5 : 1. The ratio of the transverse component to the vertical is about 3 : 1. Thus it may be seen that the observed waves include Love type waves to a large extent. Comparing this result with those at places B and C, the orbits at

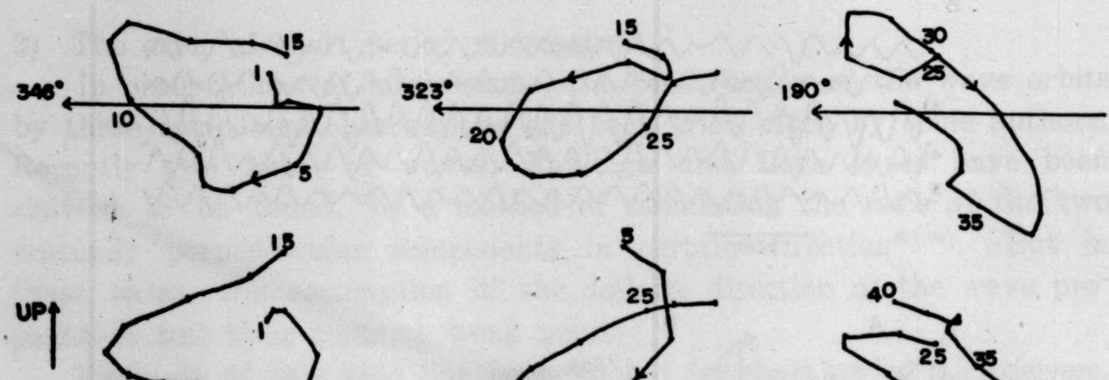

Fig. 23 I. Orbital motions from records at Hongo.
1–5, 5–10, etc. show the time intervals of each 1/10 sec.

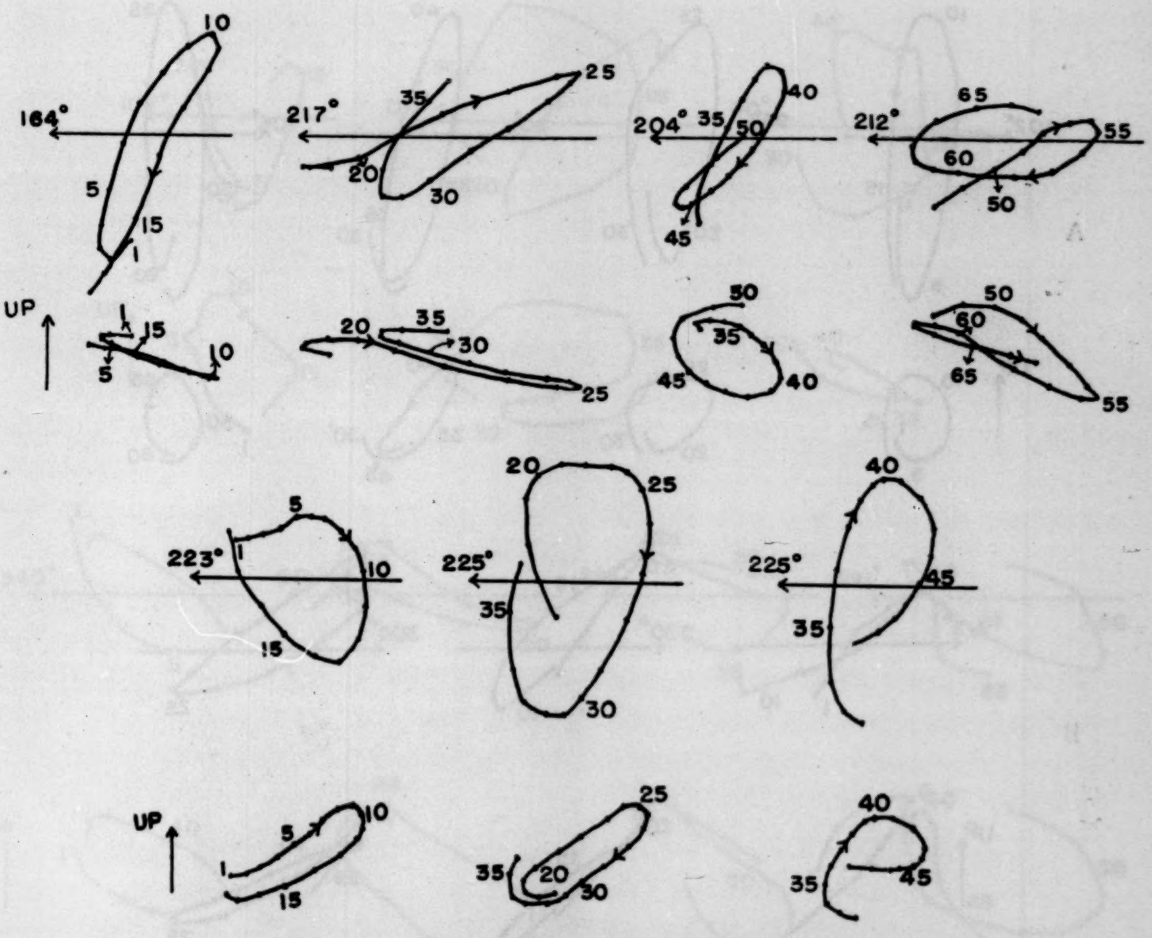
10
164°
5
15
1
35
25
217°
20
30
204°
35
50
40
45
212°
65
55
60
50
UP
1
15
10
5
20
35
30
25
50
35
45
40
50
60
65
55
5
223°
1
10
15
20
25
225°
35
30
40
225°
45
35
UP
5
10
1
15
25
35
20
30
40
35
45

Fig. 23 II. Orbital motion from records at Kakioka.

B and C are complex. This fact can be explained by the interference of other waves with those from the machine, which are more attenuated at B and C than at A. Even at these observation points, vibration due to the machine is not as predominant as at A. There is no special direction of wave polarization relative to the direction of wave propagation and the amplitudes are almost equal in both the vertical and horizontal motions. Examples of waves at place A observed with the machine and without the machine are shown in Fig. 24 A and A′.

The above stated orbits were drawn directly from records and they are at once obvious from a glance at the figures; however, mathematical expressions for some typical cases shall be given.

Let mutually perpendicular components, say the x and y components of waves, be recorded on seismograms. If a conspicuous packet of a wave or waves is picked out, it consists of a part or a whole of a sinusoidal wave or waves, and generally the period is equal in both com-

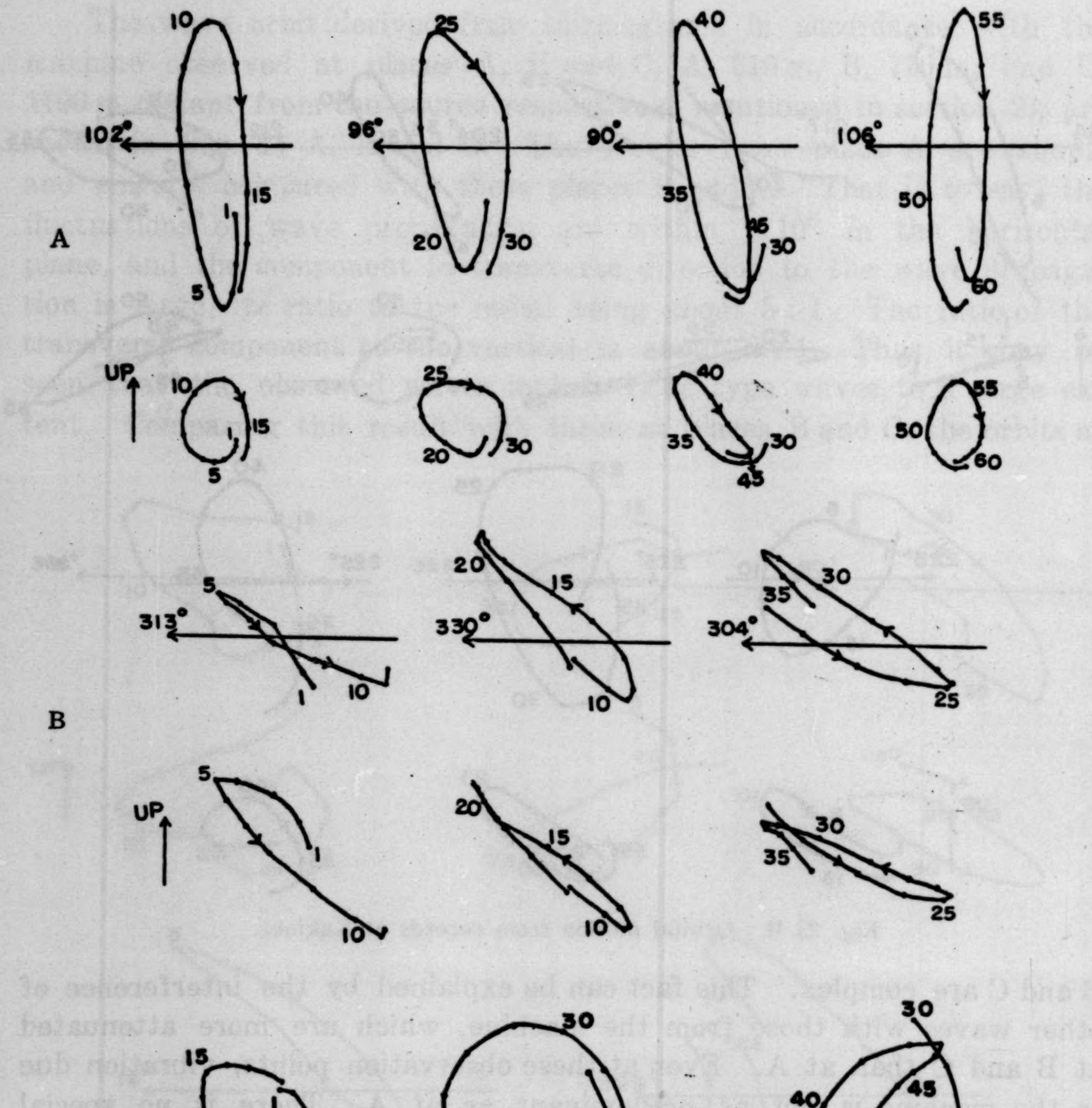

Fig. 24 A, B, C. Orbital motions from records at Tanasi-mati A, B, C with the machine.

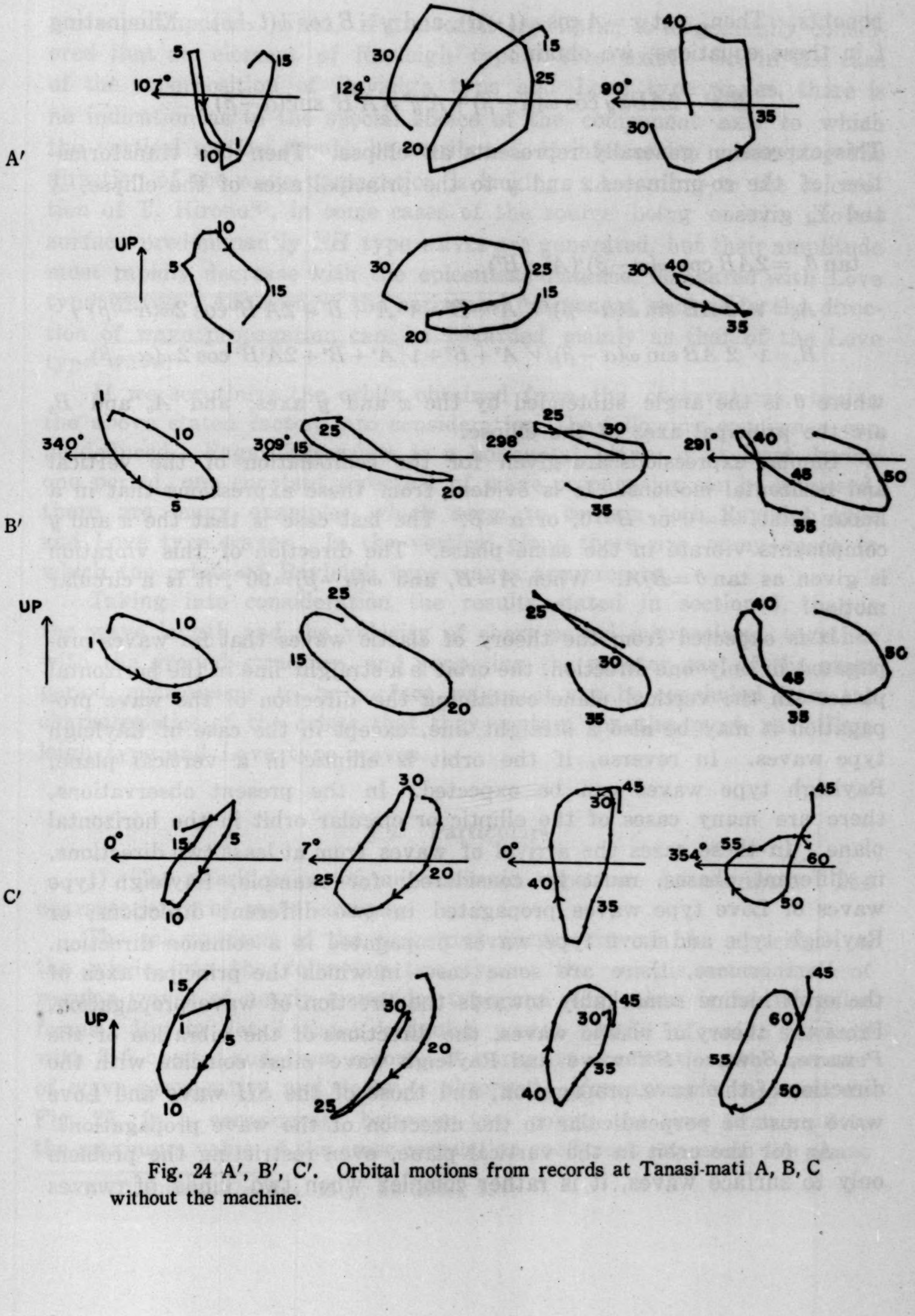

Fig. 24 A′, B′, C′. Orbital motions from records at Tanasi-mati A, B, C without the machine.

ponents. Then, put $x=A\cos\omega(t-\alpha)$, and $y=B\cos\omega(t-\beta)$. Eliminating t in these equations, we obtain:

$$B^2x^2-2ABxy\cos\omega(\alpha-\beta)+A^2y^2=A^2B^2\sin^2(\alpha-\beta)\ .$$

This expression generally represents an ellipse. Then the transformation of the co-ordinates x and y to the principal axes of the ellipse, X and Y, gives

$$\tan\theta\ =2AB\cos\omega(\alpha-\beta)/(A^2-B^2)\ ,$$

$$A_0=\sqrt{2}\,AB\sin\omega(\alpha-\beta)/\sqrt{A^2+B^2-\sqrt{A^4+B^4+2A^2B^2\cos 2\omega(\alpha-\beta)}}\ ,$$

$$B_0=\sqrt{2}\,AB\sin\omega(\alpha-\beta)/\sqrt{A^2+B^2+\sqrt{A^4+B^4+2A^2B^2\cos 2\omega(\alpha-\beta)}}\ ,$$

where θ is the angle subtended by the x and y axes, and A_0 and B_0 are the principal axes of the ellipse.

Similar expressions are given for the combination of the vertical and horizontal motions. It is evident from these expressions that in a linear orbit, $A=0$ or $B=0$, or $\alpha=\beta$. The last case is that the x and y components vibrate in the same phase. The direction of this vibration is given as $\tan\theta=B/A$. When $A=B$, and $\omega(\alpha-\beta)=90°$, it is a circular motion.

It is expected from the theory of elastic waves that for waves propagated in only one direction, the orbit is a straight line in the horizontal plane. In the vertical plane containing the direction of the wave propagation it may be also a straight line, except in the case of Rayleigh type waves. In reverse, if the orbit is elliptic in a vertical plane, Rayleigh type waves can be expected. In the present observations, there are many cases of the elliptic or circular orbit in the horizontal plane. In these cases the arrival of waves from at least two directions, in different phases, must be considered; for example, Rayleigh type waves or Love type waves propagated in two different directions, or Rayleigh type and Love type waves propagated in a common direction.

Farthermore, there are some cases in which the principal axes of the orbit incline remarkably towards the direction of wave propagation. From the theory of elastic waves, the directions of the vibration of the P wave, S wave, SV wave and Rayleigh wave must coincide with the direction of the wave propagation, and those of the SH wave and Love wave must be perpendicular to the direction of the wave propagation.

As for the orbit in the vertical plane, even restricting the problem only to surface waves, it is rather complex when two kinds of waves are superimposed. First, if the orbit is elliptic, it is generally considered that an element of Rayleigh type waves exist. Or, in the case of the superposition of Rayleigh type and Love type waves, there is no indication as to the special choice of the component axis to which the vertical motion should be attributed, if information concerning the direction of the wave propagation is lacking. According to the calculation of T. Hirono[40], in some cases of the source being on the ground surface predominantly *SH* type waves are generated, but their amplitude must rapidly decrease with the epicentral distance, compared with Love type waves. Accordingly the horizontal component normal to the direction of wave propagation can be regarded mainly as that of the Love type wave.

If we scrutinize the orbits obtained from the observations, taking the above stated factors into consideration, the following conclusion can be deduced. Ragarding orbits in a horizontal plane, if at least during one period, one constant direction of wave propagation can be supposed, there are many examples which seem to contain both Rayleigh type and Love type waves. In the vertical plane there are many cases in which the orbits of Rayleigh type waves are present.

Taking into consideration the results stated in section 3, that is the wave length and the velocity of short period microseisms, together with the ground structure, and supposing the greater part of the short period microseisms to be surface waves, it can be concluded from the characteristics of the orbits that they contain for the most part Rayleigh type and Lave type waves.

§ 5. Particulars

1) The classification of microseismic types on seismograms. The characteristics of wave sources.

The seismograms of the concerned microseims can be classified on the whole into the following two types: the one is set of train of regular waves of nearly sinusoidal type and the other is of irregular forms. But in detail these irregular waves consist of wave packets with 3-5 crests, and from records of tripartite observation, the manner of wave propagation and decay is observed. For example, as seen in Fig. 25, in a correlogram between two points the time from $\tau=0$ to the maximum value of the cross-correlation coefficient expresses the phase difference between two points. Waves which seem to vibrate in the same phase at three points, that is, waves with apparently infinite velocity can be generated as a result of the interference of waves propagated in opposite directions, and such waves are actually observed but their recorded frequency of appearance is only 1% or 2%.

---

[40] T. Hirono, *Geophys. Mag.*, **18** (1948), 1.

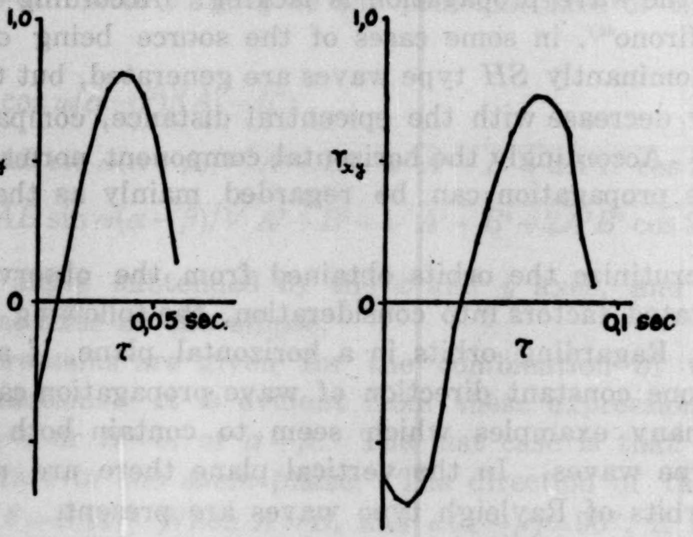

1-3 2-3

Fig. 25. Cross-correlation functions. (cf. Fig. 11)

In our tripartite observations the wave sources we are concerned with in this paper seem to exist in places at tens of times distant from the linear dimensions of the triangle chosen for observation, because flat terrain with rather large dimensions as compared with the triangle has been chosen and no special vibration sources were existent near the triangle. Wave lengths observed are from 30 m to 250 m. It seems that the vibration sources are located at for greater distances than the wave length. The vibration sources we are concerned with are those of stationary short period microseisms, that is, those which determine the noise level of the place.

Considering the individual wave sources, as stated in section 4, waves can be observed at a place 730 m distant from the machine (in this case the wave length obtained was about 160 m). On the other hand, in some special kinds of wave sources, there are cases when the waves decay rapidly at a place only 20 m from the source. Fig. 26 A shows an example where a large automobile passed 4-5 m distant from the seismometers. A seismometer set near the source (record A 2) recorded very sensibly, but at a place 30 m distant from that seismometer the waves decayed completely (record A 1). Ground motions caused by vehicles which move at a uniform speed over the ground should be referred to the ground motion caused by a heavy load moving uniformly over the ground at a speed far less than those of *P* and *S* waves which was calculated by T. Inui, M. Kotani and Z. Sakadi[41]. According to their calculations, the displacement of the ground surface caused nearly statically by the load moves uniformly with the load, and no other waves connected with the moving load are generated.

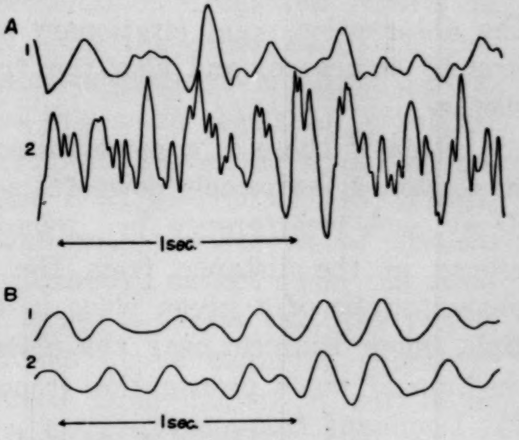

Fig. 26. Records at Tanasi-mati C.
A Where there is a large automobile.
B In the case of stationary noise level.
(A, B The same observation point.)

For the wave generation in our example, variations in velocity or shocks are neccessary. A modified mathematical calculation related to this case can be obtained from the calculations by T. Hirono[42].

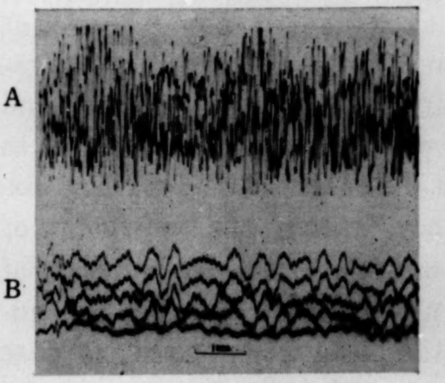

Fig. 27. Records at Kakioka.
A Where there is moving wooden cart.
B In the case stationary noise level.
(A, B The same observation point.)

An example of waves caused by a moving wooden cart is shown in Fig. 27 A. In this case velocity variations and remarkable shocks are naturally expected.

Comparing this with the case when there is no wave source from traffic (Fig. 27 B) at the same observation point, it is seen that waves with a higher frequency appear abundantly in A. In case A, it can be thought that the wave source generates various types of waves when it makes an impact on the ground, but as waves with a high frequency decrease greatly with the distance from the source, so the waves observed as stationary noises at the observation point should not be body waves.

---

[41] T. INUI, M. KOTANI and Z. SAKADI, *Proc. Physiko-Math. Soc. Jap.* [iii] **13** (1923), 223.

[42] T. HIRONO, *ibid.*

Summarizing the above stated considerations, the manner of appearance of short period microseisms caused by a special vibrating source near the observation point is different according to the noise level at the observation point (stationary short period microseisms), topography, ground structure, and also the frequency characteristics of the instruments.

Even if there is a powerful source such as the machine described in section 4, extremely powerful sources excepted, since there is energy decay and interference by microseisms from other sources with increase in the distance from the source, in general the microseismic characteristic of a given place is determined by the distribution of multiple wave sources near the place together with the properties of the medium of wave propagation (topography, ground structure, etc.).

2) Dominant frequency.

While short period microseisms seem to consist of random waves generated from various wave sources, on the other hand, as described in section 3, a " dominant frequency " characteristic to a station exists. The " dominant frequency " we are concerned with here is the frequency which corresponds to the maximum intensity of the spectra of short period microseisms. These frequency spectra are remarkably sharp at some places, and rather flat at other places.

It is natural that the reason for the existence of the " dominant frequency " should be sought in the ground structure[43),44),45)]. As frequently stated hitherto, judging from their wave length, velocity, and wave orbit etc., the greater part of short period microseisms seems to have the characteristics of surface waves. Therefore, the author discussed the problem of " dominant frequency " from the viewpoint of surface waves. C. D. V. Wilson[46)] points out that the frequencies of short period microseisms already observed are constant and not dependent upon the distance from the source to the observation point, (a case of existence of a special source of vibration), and this phenomenon depends upon the local geological structure. On the other hand, there is the so called quarter wave length law asserted by K. Tazime[47)], i.e. $H=1/4\, V_pT$ (V_p: velocity of the P wave, H: thickness of the surface layer, T: period of the observed surface wave). Let us apply this law

---

43) C. D. V. WILSON, *ibid.* 4).

44) K. KANAI and S. YOSHIZAWA, *Bull. Earthq. Res. Inst.*, **34** (1956), 167.

45) K. TAZIME, *Journ. of Physics of the Earth*, **5** (1957), 43.

46) C. D. V. WILSON, *ibid.* 4).

47) K. TAZIME, *ibid.*

to the result of the author's observation, that is, to the example from Tanasi-mati in Tokyo shown in section 4. The outline of the ground structure at this observation point, as obtained from the results of seismic prospecting, is shown in Fig. 21. On the other hand, the frequency of the short period microseisms observed here is about 3.8 c/s. As the wave length is about 160 m, so this wave seems to be related to the second and third layers of the ground. For example, if 1780 m/s is taken as the velocity of P wave, then $H=1/4\times 1780\times 1/3.8 \fallingdotseq 117$(m), and this value of H is too thick compared with the results of seismic exploration. As this law does not apply exactly, except when the ratio of the elastic constants, μ_3/μ_2, is rather large, it seems that the condition of a large μ_3/μ_2 is not satisfied in the above example. Further, Tazime's semi-empirical formula is deduced from dispersion curves in the case of Poisson's ratio $\sigma=1/4$, but it is to be expected that $\sigma=1/4$ does not necessarily apply to ground near the surface.

However, the "dominant frequency" exists, as Tazime also pointed out, and the frequency corresponding to the minimum group velocity of the dispersion curve, characteristic to the ground structure, is apt to appear. This circumstance would be explained as follows.

In order to explain the matter as clearly as possible, the author will assume an idealized dispersion curve which should distinctly represent the salient features of the ordinary real dispersion curve, as shown in Fig. 28. Namely,

$$\begin{aligned}
&c=c_1 \qquad \text{for} \quad 0<\xi<\xi_1\,,\\
&c=(c_2\xi_2-c_1\xi_1)/(\xi_2-\xi_1)+(c_1-c_2)\xi_1\xi_2/(\xi_2-\xi_1)\xi \qquad \text{for} \quad \xi_1<\xi<\xi_2\,,\\
&c=c_2 \qquad \text{for} \quad \xi>\xi_2\,,
\end{aligned}$$

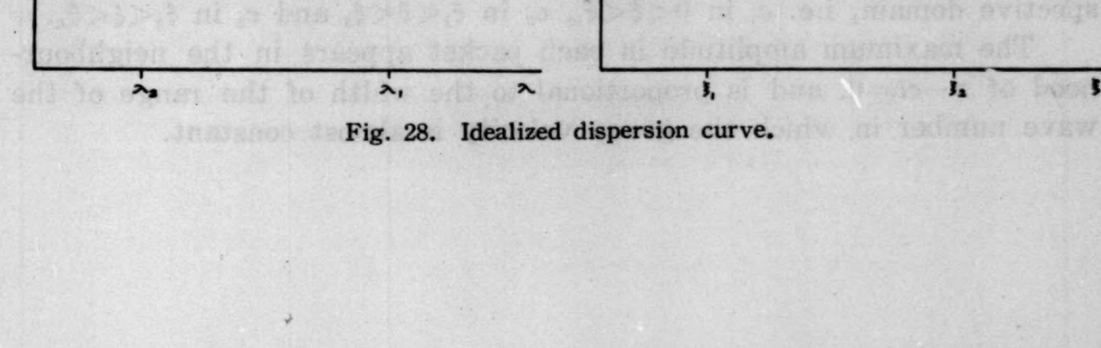

Fig. 28. Idealized dispersion curve.

where

$$\xi=2\pi/\lambda\,, \qquad \lambda\text{: wave length}\,.$$

Considering that in an area with such a dispersion curve waves which have such a displacement as $u(x)=A\sin\xi_k x/x$ at $t=0$ are propagated. Fourier transform of $u(x)$ is

$$g(\xi)=1/\sqrt{2\pi}\int_{-\infty}^{\infty} u(x)\cos\xi x dx=\sqrt{\pi/2}\,A \qquad \text{for} \quad 0<\xi<\xi_k\,,$$
$$=0 \qquad \text{for} \quad \xi_k<\xi\,.$$

This expression corresponds to a random noise which has a flat spectrum between 0 and ξ_k.

When this wave begins to move with the initial velocity of displacement $v_0=0$, and considering that waves are advancing only in the positive direction of x,

$$u(x)=1/2\sqrt{2\pi}\int_{-\infty}^{\infty} g(\xi)\cos\xi(x-ct)d\xi = 1/\sqrt{2\pi}\int_{0}^{\infty} g(\xi)\cos\xi(x-ct)d\xi\,.$$

This integral is expressed by the following three parts, i.e.,

$$u_1(x)=(A/2)\sin\xi_1(x-c_1t)/(x-c_1t)$$
$$=A\sin(\xi_1/2)(x-c_1t)\cos(\xi_1/2)(x-c_1t)/(x-c_1t)\,,$$

$$u_2(x)=A\sin\{(\xi_2-\xi_1)/2\}(x-c_gt)\cos\{(\xi_1+\xi_2)/2\}$$
$$\times\{x-(\xi_2c_2+\xi_1c_1)t/(\xi_1+\xi_2)\}/(x-c_gt)\,,$$

$$u_3(x)=A\sin\{(\xi_k-\xi_2)/2\}(x-c_2t)\cos\{(\xi_2-\xi_k)/2\}(x-c_2t)/(x-c_2t)\,,$$

where

$$c_g=(c_2\xi_2-c_1\xi_1)/(\xi_2-\xi_1)\,,$$

$(c_2\xi_2+c_1\xi_1)/(\xi_1+\xi_2)$ is the phase velocity at $\xi=(\xi_1+\xi_2)/2$. The amplitude is expressed by the addition of these three parts, i.e. these three wave packets.

Considering such a factor as $\sin\{(\xi_i-\xi_j)/2\}(x-ct)/(x-ct)$ in each packet, c_1, c_g, and c_2 can be regarded as group velocities in each respective domain, i.e. c_1 in $0<\xi<\xi_1$, c_g in $\xi_1<\xi<\xi_2$ and c_2 in $\xi_2<\xi<\xi_k$.

The maximum amplitude in each packet appears in the neighbourhood of $x-ct=0$, and is proportional to the width of the range of the wave number in which the group velocity is almost constant.

Such a range corresponds to the neighbourhood of the maximum or minimum value of group velocity. This is explained simply as follows. As $dc_g/d\lambda = -d^2c/d\lambda^2$ from $c_g = c - \lambda(dc/d\lambda)$, the said range of the wave number is in the neighbourhood of the inflection point of the $c-\lambda$ curve, that is, the linear range, or the width of the range in which the group velocity c_g is practically constant. The phase velocity, wave length, and frequency in each packet correspond to those values in the middle of the said range, as can easily be seen in the factor $\cos\{(\xi_i + \xi_j)/2\}(x - ct)$.

This is the reason why wave packets correspoding to the minimum value (or maximum value) of the group velocity predominate, and for other parts $\int g(\xi)\cos\xi(x-ct)d\xi$ does not become large because of the rapid change in c against ξ.

In the case in which the spectrum $g(\xi)$ of the initial wave has a sharp peak, waves with the wave number ξ around the peak predominate. For example, when $u(x) = A\cos\xi_0 x$ in the range $-L < x < L$, $g(\xi) = 1/\sqrt{2\pi}\{\sin L(\xi-\xi_0)/(\xi-\xi_0) + \sin L(\xi+\xi_0)/(\xi+\xi_0)\}$. Then, when L becomes very large, the spectrum becomes a line spectrum such as the type of Dirac's δ-function in the neighbourhoods of $\xi = \xi_0$ and $\xi = -\xi_0$. In such a case, trains with a wave length and frequency at ξ_0 appear. This phenomenon corresponds to the case when waves generated by powerful vibrations from a source such as in our case a compressor are contained at an observation point.

3) The influences of rain and wind.

Rain and wind are examples of natural phenomena which have direct influences on short peoiod microseisms. Rain and wind are factors

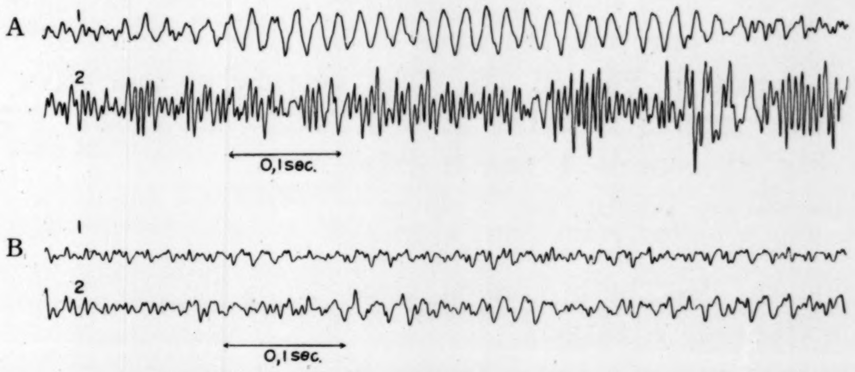

Fig. 29. Example of influence of rain and wind. Records at Mt. Tukuba.
A In the case of rain and wind.
B In the case of stationary noise level.
(A, B The same observation point.)

which, temporarily, rapidly increase the noise level on the ground and ordinarily waves with a frequency higher than 10 c/s dominate through the influences of these factors. For example, as seen in Fig. 29, waves with frequencies about 60 c/s and 200 c/s dominate remarkably at Mt. Tukuba where comparatively hard rocks are exposed. Correlograms of this example are shown in Fig. 30.

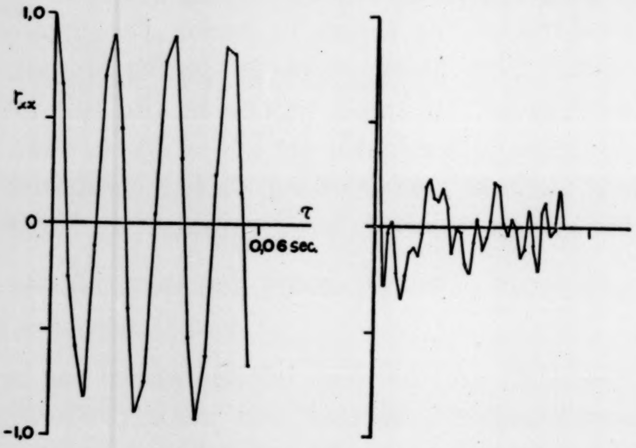

a b

Fig. 30. Correlograms from records at Mt. Tukuba in the case of rain and wind. (cf. a—Fig. 29 A 1. b—Fig. 29 A 2.)

4) Microseisms with a frequency about 1 c/s.

From urban examples when waves with a high frequeney were eliminated by equipping an amplifier with two step low-pass filters, the waves observed were those with a low frequency of about 1.5 c/s. As seen in Fig. 12 V A, these lower frequency waves seem to have good correspondence even at two points 47 m apart. That is to say, the cross-correlation coefficient between two points is about 0.7.

On the other hand, in cases when waves were observed at Mt. Tukuba and Matusiro, by the same instruments as described in section 2 waves with frequency range from 1.5 c/s to 0.6 c/s were observed. At Matusiro, the three sides of a triangle were taken as 183 m, 180 m and 147 m respectively, but the wave to wave correspondence was satisfactory as shown in Fig. 12 VII. The velocity of this wave is over 1 km/s. Next, records obtained at Mt. Tukuba are shown in Fig. 31, 1, 2. In Fig. 31 records 1 and 2 differ in the observation points, i.e. 1 is in a horizontal tunnel and the other is on the ground surface, but both records show almost simultaneous vibrations.

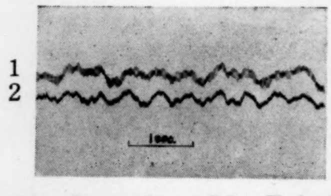

Fig. 31. Records at Mt. Tukuba.
1. In a horizontal tunnel.
2. On the ground surface.

Waves with rather a lower frequency and higher velocity than those with a frequency over 3 c/s as described above, would be classified in another group of microseisms. These waves seem to have the characteristics of microseisms because of their artificial noise sources at a very long distance, the influences of sea wave or of weather conditions, etc. It was experienced that such waves were observed when the seismometers were set at places near the seashore or on islands.

§ 6. Summary

As for spectra of short period microseisms, a "dominant frequency" particular to every observation point exists. But there are two different types of place where they appear: one type is where the "dominant frequency" appears remarkably sharp and the other is where the spectra are flat. These two differences also exist according to the conditions of the setting place of the seismometers even in the same area, for example, on a concrete block or on soil ground. As for amplitudes of short period microseisms, the amplitude ratio in the daytime and at night are from 2 : 1 to 10 : 1 and over. This result is the same as results obtained previously. At the places at which the observations outlined in this paper have been made, the spectra do not differ in the daytime and at night. This result shows that a "dominant frequency" prticular to each locality exists through the day and night.

Judging from the wave length, velocity, and orbit together with the direction of the wave propagation obtained by the method of tripartite observation, short period microseisms seem to have the characteristics of surface waves. First, if they were body waves, for the wave length and the ground structure at the observation point the waves should have a higher velocity than those observed. Secondly, from investigations of the relation between the orbit and the direction of wave propagation, show that short period microseisms seem to contain surface waves, i.e. Rayleigh and Love type waves or combinations of both waves.

Of "dominant frequency" of the ground, various explanations have been proposed ever since A. Imamura, and most opinions are that the "dominant frequency" could be attributed to multiple reflections of waves in the ground. This idea presumes that incident waves would be body waves.

If short period microseisms have for the most part the characteristics of surface waves, the frequency corresponding to the minimum group velocity for the ground is apt to predominate. In this case, the ground layer is equivalent to some kind of filter, and the dispersion curve inherent to the ground structure may be regarded as a characteristic frequency curve of the filter.

Acknowledgement

The author wishes to express her deep gratitude to Prof. T. Matuzawa for his various valuable suggestions and encouragement. Her cordial thanks are also due to Dr. T. Asada who has rendered the most pertinent directives and encouragement throughout the course of this study. She gratefully thanks Dr. R. Satô for his kind advice and Messrs. Y. Oguchi, H. Kurimoto and T. Terashima for their helpful assistance.

The Director of the Radio Research Laboratories, and Prof. K. Kawatei, Faculty of Agriculture, the University of Tokyo permitted her to carry out her experiments at the Radio Research Laboratories, Kokubunzi, and at the University of Tokyo Agricultual Farm, Tanasimati.

Personnel at the Tukuba Observatory of the Earthquake Research Institute of the University of Tokyo, and at the Matusiro Observatory of Japan Meteorological Agency rendered kind help to her.

The author wishes to express her thanks to these people also.

2. 微動について

東京大学理学部
地球物理学教室 赤松 敬

研究の対象となる微動はその周波数帯域が 1-200 c/s のいわゆる短周期脈動である．

この論文では微動の波の性質として微動のスペクトラム，周波数および日変化を論ずる．また，波の伝播方向，伝播速度，波長を求め，波の軌道と合わせて，波の性質を調べる．以上の結果から卓越周波数の問題を論ずる．

スペクトラムを求めるには，短時間自己相関函数を用いて，**Power Spectrum** を求める．波の微視的な性質を調べる一手段としては，いわゆる3点観測と，3成分観測を合わせて行ない，波の伝播方向，伝播速度，波長を求め，さらに，伝播方向と組合わせて波の軌道がえがかれる．

微動のスペクトラムを求めると，観測場所ごとに卓越周波数が存在する．そのあらわれ方は，ある周波数が著しく卓越する場所と，スペクトラムのグラフにたいらにあらわれる場所がある．一つの場所での昼夜のスペクトラムについては殆んど差がないようである．これはその土地の卓越周波数が昼夜とも存在することを示す．

伝播速度，伝播方向，および軌道から考えて，微動はその大部分が表面波の性質をもつようである．そのひとつは実体波と考えるには，観測点の地下構造を考え合わせると，波長に較べて伝播速度が遅すぎる．その二は波の伝播方向と振動の軌道をいろいろな場合について調べると，微動は主として表面波，すなわち **Rayleigh** 型の波，あるいは **Love** 型の波，ないしはその合併したものとみられるからである．

土地の卓越周波数の問題については，これまで種々議論されてきているが，大部分はその原因が地層の重複反射にあるとするものである．これは入射してくる波を実体波的に考えるわけである．

観測される微動の大部分を表面波であるとすると，観測点の地下構造に対する分散曲線の群速度の極少に対応する周波数があらわれ易いことになる．この場合，地層は一種の沪波器と同じで，地下構造に対する分散曲線を一種の沪波器の周波数特性とみることができる．

3

BULLETIN OF THE EARTHQUAKE
RESEARCH INSTITUTE
Vol. 39 (1961), pp. 77-84

3. *Further Studies of Microseisms by Observation.*

By Fuyuhiko KISHINOUYE,

Earthquake Research Institute.

(Read Oct. 29, 1956 and Feb. 24, 1959.—Received Dec. 28, 1960.)

Observation of microseisms was commenced in Japan by J. Milne early in 1885, however, the nature of microseisms are not clear even now. And now exact observations are required for the study of microseisms at many places on many occasions. The aim of this paper is to publish data on microseisms observed different places.

Tripartite Observations at Shinkawa, Mitaka, Tokyo

Three horizontal seismographs were set in the grounds of the Mitaka Branch of the Transportation Technical Research Institute, which is situated in Shinkawa, Mitaka. Positions of temporary stations in the grounds are shown in Fig. 1. The instruments used for the observations were mechano-optical horizontal pendulum seismographs[1] which were employed in many observations carried out by the writer and others in studies of microseisms. Constants of the seismographs were $T=10$ sec., $V=2000$ and critical damping.

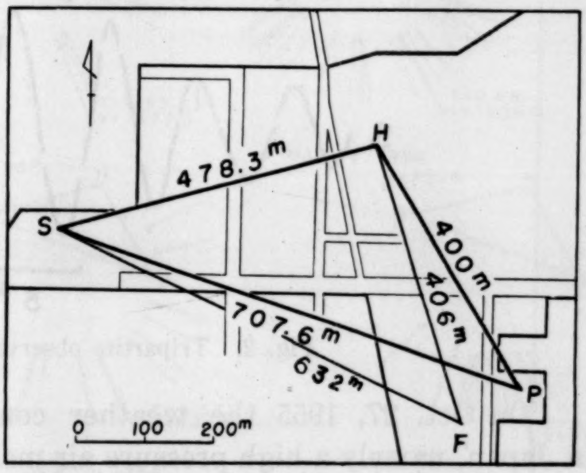

Fig. 1. Observation net in the grounds of Mitaka Branch of the Transportation Technical Research Institute, Mitaka, Tokyo.

The observations were made on the occasions of large microseisms (Fig. 2), and the results are shown in the following diagrams (Figs. 3 and 4).

On Sept. 26 and 27, 1955, a violent typhoon (called Typhoon No. 22 of 1955) was about 800 km from the stations on the southern sea. Air pressure at the centre was about 940 mb. The propagation direction of the microseismic waves was southerly on Sept. 26 and northerly on Sept. 27. So the results in the first day were favourable for the theory that microseismic waves are generated in the storm area, but those on the next day were the opposite.

---

[1] F. KISHINOUYE, *Bull. Earthq. Res. Inst.*, **20** (1942), 215-219.

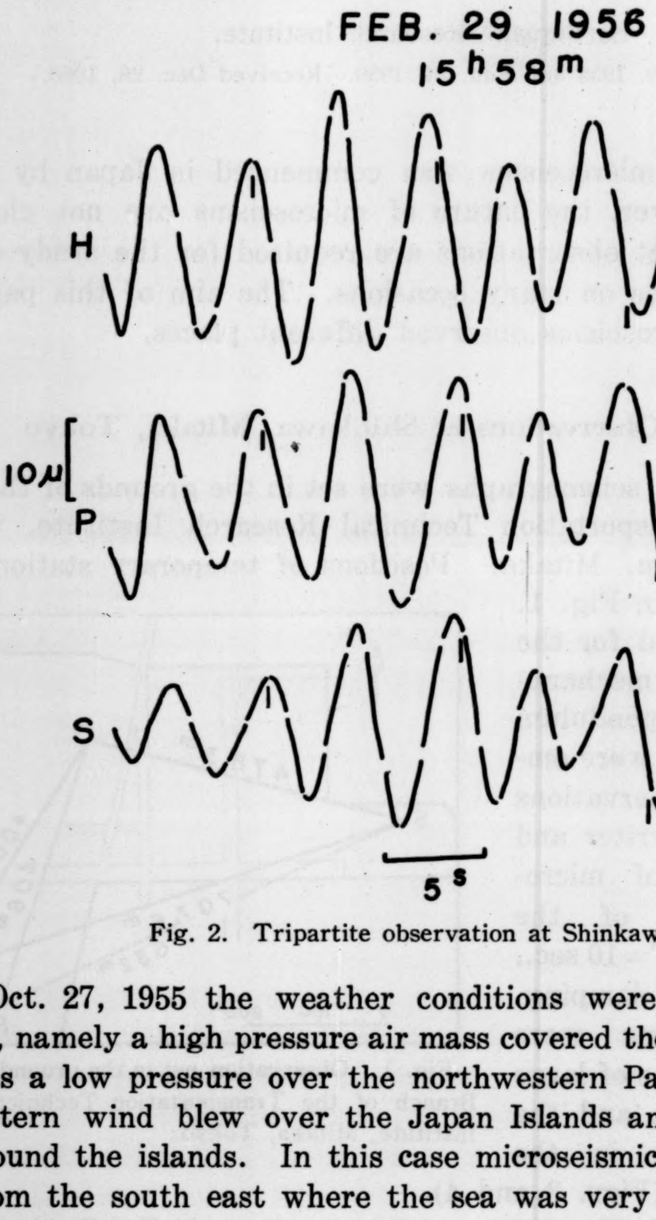

Fig. 2. Tripartite observation at Shinkawa.

On Oct. 27, 1955 the weather conditions were typical for winter in Japan, namely a high pressure air mass covered the eastern Siberia and there was a low pressure over the northwestern Pacific Ocean. Strong northwestern wind blew over the Japan Islands and the sea was very rough around the islands. In this case microseismic waves were propagated from the south east where the sea was very rough.

Throughout Feb. 29 and March 1, 1956, there was a cyclone on the sea northeast of from Japan and a small cyclone on the Japan sea. Microseismic waves were propagated from the south east, and the sea to the southeast was rough.

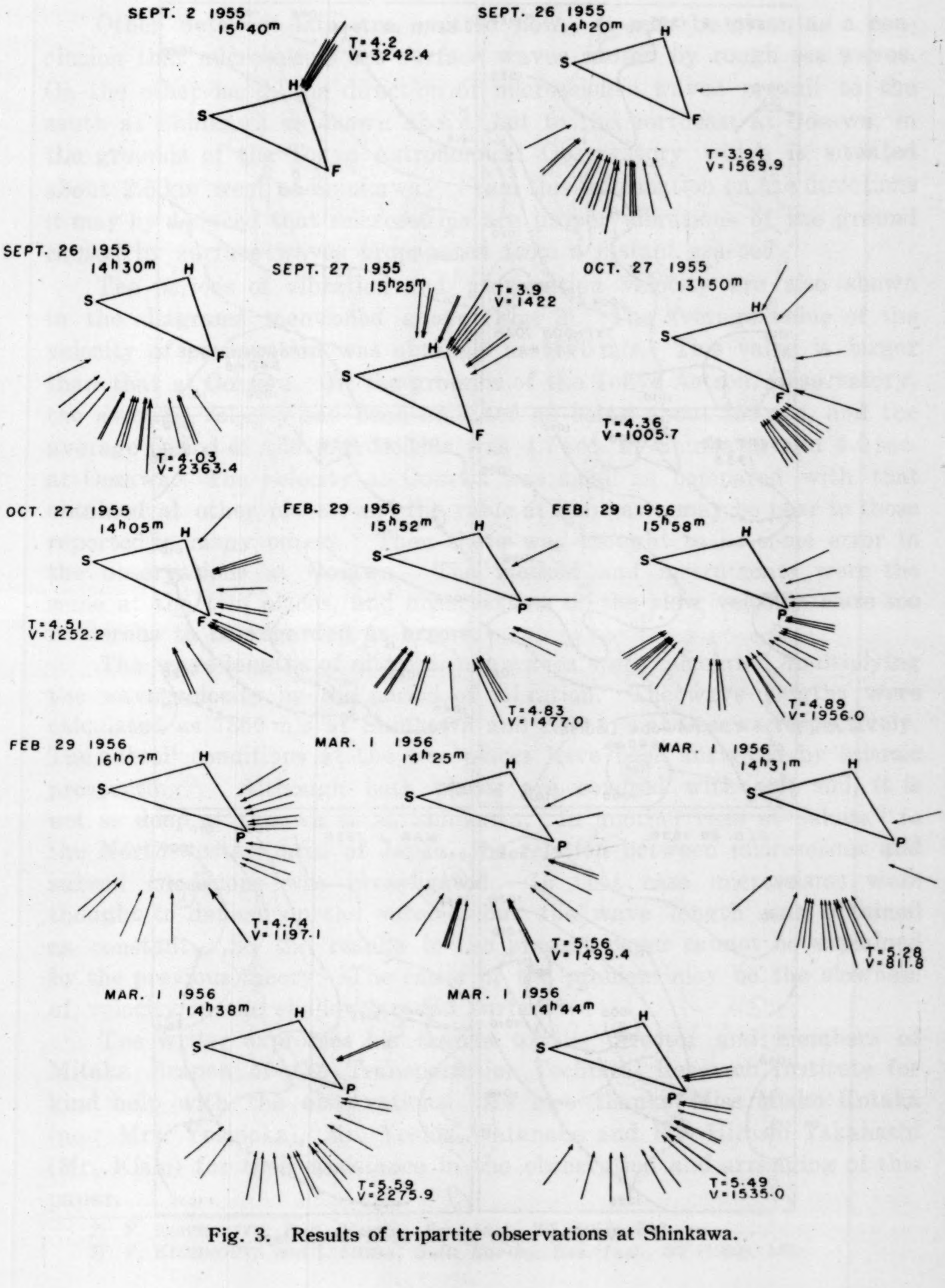
SEPT. 2 1955
$15^{h}40^{m}$
T=4.2
V=3242.4
H
S
F
SEPT. 26 1955
$14^{h}20^{m}$
H
S
F
T=3.94
V=1569.9
SEPT. 26 1955
$14^{h}30^{m}$
H
S
F
T=4.03
V=2363.4
SEPT. 27 1955
$15^{h}25^{m}$
T=3.9
V=1422
H
S
F
OCT. 27 1955
$13^{h}50^{m}$
H
S
F
T=4.36
V=1005.7
OCT. 27 1955
$14^{h}05^{m}$
H
S
F
T=4.51
V=1252.2
FEB. 29 1956
$15^{h}52^{m}$
H
S
P
T=4.83
V=1477.0
FEB. 29 1956
$15^{h}58^{m}$
H
S
P
T=4.89
V=1956.0
FEB 29 1956
$16^{h}07^{m}$
H
S
P
T=4.74
V=1197.1
MAR. 1 1956
$14^{h}25^{m}$
H
S
P
T=5.56
V=1499.4
MAR. 1 1956
$14^{h}31^{m}$
S
H
P
T=5.28
V=811.8
MAR. 1 1956
$14^{h}38^{m}$
S
H
P
T=5.59
V=2275.9
MAR. 1 1956
$14^{h}44^{m}$
H
S
P
T=5.49
V=1535.0

Fig. 3. Results of tripartite observations at Shinkawa.

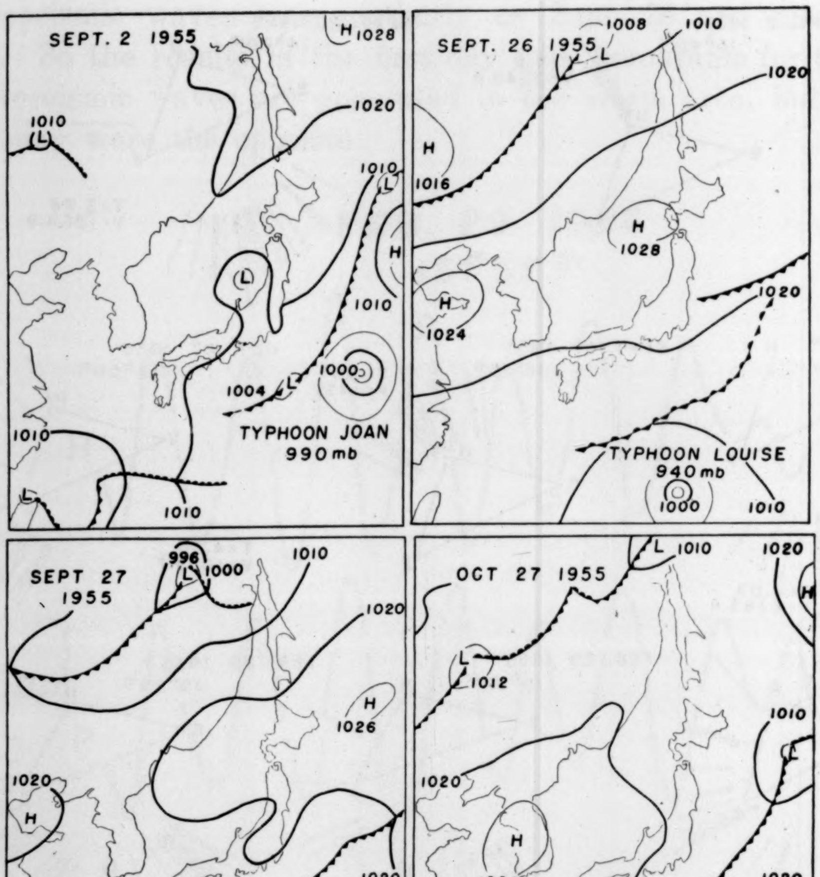
SEPT. 2 1955
H 1028
1010
L
1020
1010
L
H
L
1010
1004
L
1000
TYPHOON JOAN
990 mb
1010
L
1010
SEPT. 26 1955
1008
1010
L
1020
H
1016
H
1028
H
1024
1020
TYPHOON LOUISE
940 mb
1000
1010
SEPT 27
1955
996
L
1000
1010
1020
H
1026
1020
H
1020
TYPHOON LOUISE
940 mb
1000
1010
OCT 27 1955
L 1010
1020
H
L
1012
1010
L
1020
H
1024
1020
1020
H
FEB. 29 1956
1030
1030
1020
1010
L
996
1000
L
996
1000
1010
1030
1018
H
1020
MAR 1 1956
1020
1010
1040
H
1044
1000
990
L
1022
1010
1030
1020

Fig. 4. Weather maps on the observation days.

Other detailed data are omitted now. It may be given as a conclusion that microseisms are surface waves caused by rough sea waves. On the other hand, the direction of microseismic waves prevail to the south at Shinkawa as shown above, but to the northeast at Oosawa, in the grounds of the Tokyo Astronomical Observatory which is situated about 2.5 km west of Shinkawa. From this information on the directions it may by deduced that microseisms are proper vibrations of the ground caused by surface waves propagated from a distant sea-bed.

The periods of vibration and propagation velocity are also shown in the diagrams mentioned above (Fig. 3). The average value of the velocity of propagation was obtained as 1670 m/s. This value is larger than that at Oosawa. In the grounds of the Tokyo Astron. Observatory, the average velocity had been obtained as being about 550 m/s, and the average period of the microseisms was 4.7 sec. at Shinkawa and 4.0 sec. at Oosawa. The velocity at Oosawa was small as compared with that obtained at other places, and the value at Shinkawa may be near to those reported in many papers. Then there was thought to be some error in the observations at Oosawa. The method and instruments were the same at the two places, and observations of the slow velocity were too numerous to be regarded as errors.

The wave lengths of microseismic waves were calculated, multiplying the wave velocity by the period of vibration. The wave lengths were calculated as 7860 m/s at Shinkawa and 2200 m/s at Oosawa respectively. The subsoil conditions at the two places have been surveyed by seismic prospecting[2]. Although both places are covered with soft soil, it is not as deep at Oosawa as at Shinkawa. In another case at Sakata[3] in the North-western area of Japan, the relation between microseisms and subsoil conditions was investigated. In that case microseisms were thought to depend on the subsoil, but the wave length was obtained as constant. So the results in the present paper cannot be explained by the previous theory. The cause of the problem may be the slowness of velocity in the shallow ground surface.

The writer expresses his thanks to the director and members of Mitaka Branch of the Transportation Technical Research Institute for kind help with the observations. He also thanks Miss Mieko Kotaka (now Mrs. Yoshioka), Mr. Yoshio Watanabe and Mr. Hiroshi Takahashi (Mr. Kishi) for their assistance in the observation and arranging of this paper.

---

[2] F. KISHINOUYE, *Bull. Earthq. Res. Inst.*, **35** (1957), 542.

[3] F. KISHINOUYE and I. SHIDA, *Bull. Earthq. Res. Inst.*, **37** (1959), 187.

Tripartite Observations of Microseisms at Tateno

For the purpose of obtaining more data about microseisms near Tokyo, tripartite observations were carried out in the ground of the Aerological Observatory at Tateno, Ibaraki Prefecture. It is situated in the Kwantō Plain about 80 km NE from Tokyo. The observations were made in August and September, 1958. This was the International Geophysical Year, then this data may have served as to supplement the world-wide observations.

In the previous studies the writer had used mechano-optical seismographs, and the present observations were made with electric seismographs[4] designed to investigate of microseisms at the start.

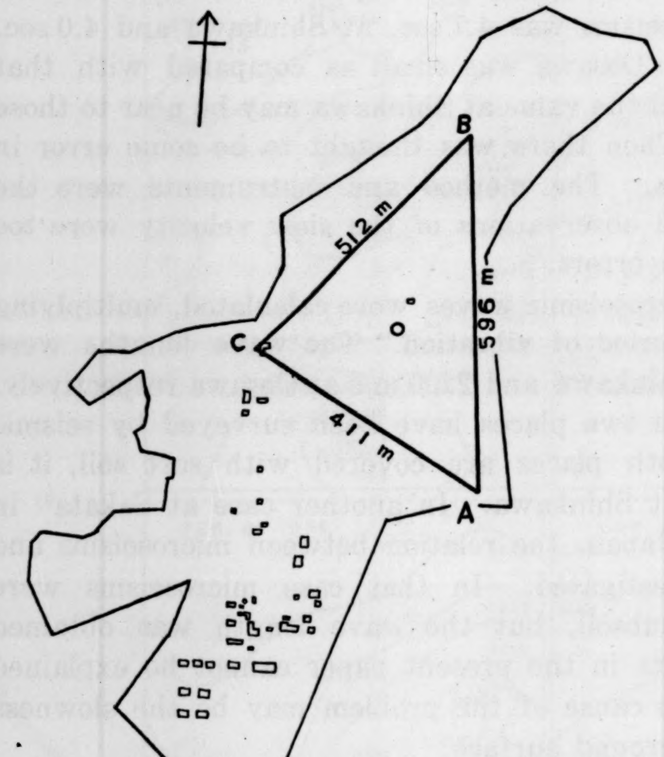

Fig. 5. Tripartite stations at Tateno.

The results of the observations are shown in the inserted diagrams (Figs. 5–8), and it will not be necessary to describe then in detail. As shown in Fig. 7, microseismic waves came mostly from the southeast. The direction of propagation did not point the position of the cyclone centre which in a northerly direction. The mean velocity of propagation was obtained as 1978 m/s, and the average period of vibration 3.67 seconds. The value of velocity is high as compared with those previously obtained by the writer near Tokyo.

The velocity of the microseisms may depend on the subsoil condition as stated before, and to support such an opinion the writer is endeavouring to obtain more data about microseisms by observations at as many places as possible.

---

[4] F. KISHINOUYE and Y. WATANABE, *Bull. Earthq. Res. Inst.*, **37** (1959), 327-335.

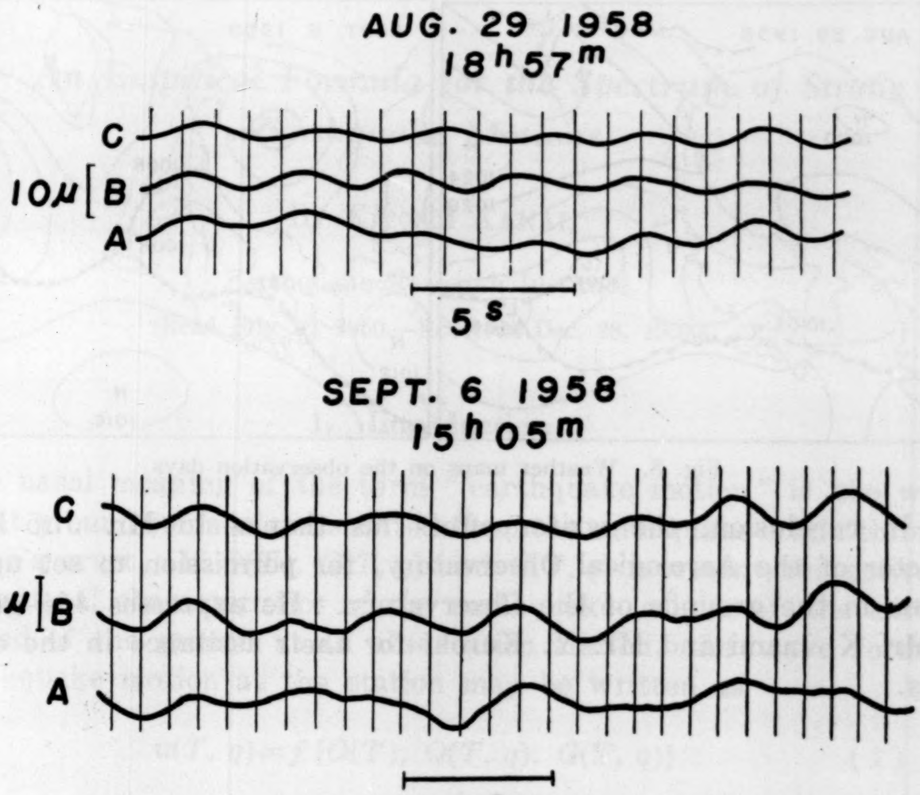

Fig. 6. Tripartite observations at Tateno.

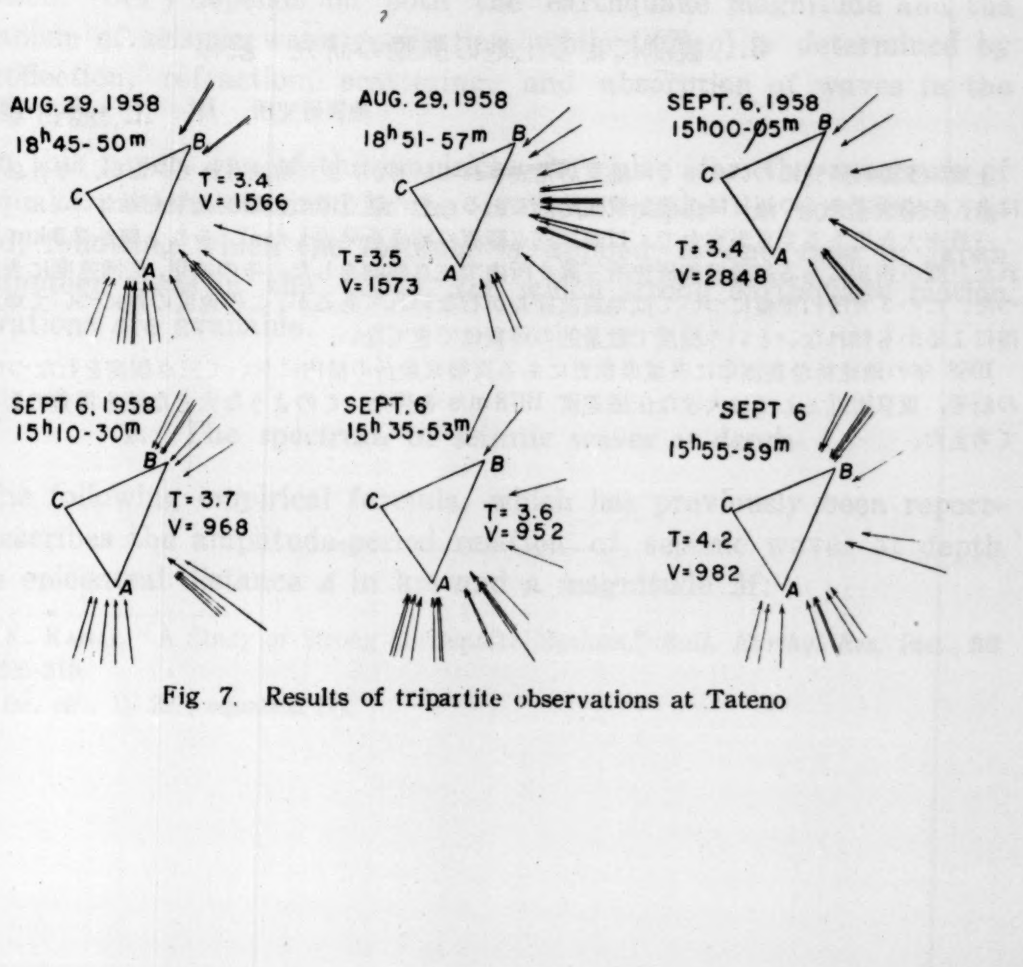
AUG. 29, 1958
18h45-50m
T = 3.4
V = 1566
C
B
A
AUG. 29, 1958
18h51-57m
T = 3.5
V = 1573
C
B
A
SEPT. 6, 1958
15h00-05m
T = 3.4
V = 2848
C
B
A
SEPT 6, 1958
15h10-30m
T = 3.7
V = 968
C
B
A
SEPT. 6
15h 35-53m
T = 3.6
V = 952
C
B
A
SEPT 6
15h55-59m
T = 4.2
V = 982
C
B
A

Fig 7. Results of tripartite observations at Tateno

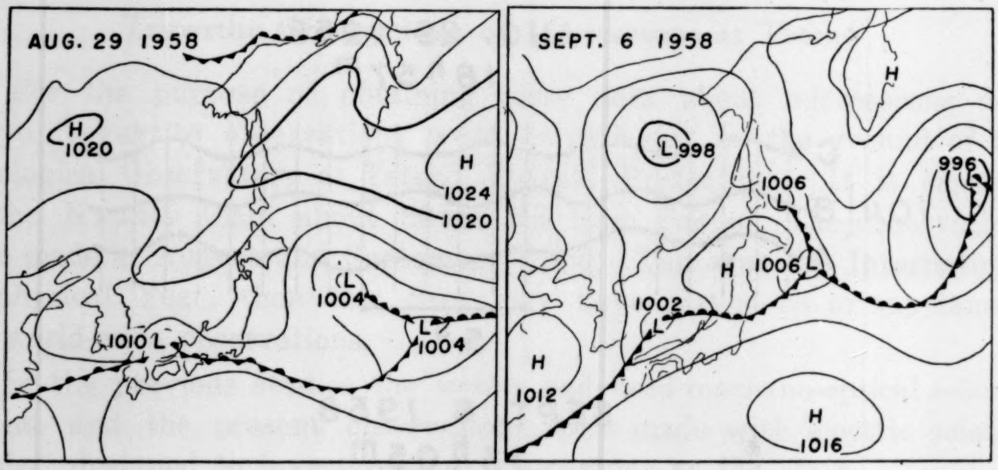
AUG. 29 1958
H
1020
H
1024
1020
L
1004
L
1004
1010 L
SEPT. 6 1958
L 998
H
996
L
1006
L
H
1006
1002
L
H
1012
H
1016

Fig. 8. Weather maps on the observation days.

In conclusion, the writer offers his thanks to Mr. Jirō Kawase, director of the Aerological Observatory, for permission to set up observation in the grounds of the Observatory. He expresses his gratitude to Mr. K. Inami and Mr. Y. Kuroki for their assitance in the observations.

---

3. 観測による土地の脈動の研究　続報

地震研究所　岸上冬彦

土地の脈動の研究について多くの論文が発表されているが，まだ解決されていない，今日必要なのは多くの場所で多くの時日に正確な観測結果である．その観点でこの観測結果を見たい．

三鷹市大沢にある東京天文台で，以前，三点観測の結果を発表したが，そこと僅か 2.5 km 東に離れた三鷹市新川にある運輸技術研究所三鷹支所内で三点観測をした．その結果，伝播速度に大差があつた．この 2 カ所の地盤については地震波探査が行なわれてあるが，この速度の差について地質的の差によるかも知れないという程度で数量的の解釈はできてない．

1958 年の地球物理観測年に茨城県館野にある高層気象台の構内において三点観測を行なつた．その結果，東京附近としては大きな伝播速度 1978 m/s を得た．このような大きな値も地盤の影響として考えた．

Bulletin of the Earthquake
Research Institute
Vol. 39 (1961), pp. 85-95

4. An Empirical Formula for the Spectrum of Strong Earthquake Motions.

By Kiyoshi KANAI,

Earthquake Research Institute.

(Read July 26, 1960.—Received Dec. 28, 1960.)

1. Introduction

The usual meaning of the term " earthquake motion " is the wave motion at ground surface transmitted from the earthquake origin through the earth's crust. If $O(T)$, $Q(T, q)$ and $G(T, q)$ represent, respectively, the vibrational characteristics of the earthquake origin, of the earth's crust, and of the ground at an observation station, the wave form of the earthquake motion at the station may be written as

$$u(T, q)=f\{O(T),\ Q(T, q),\ G(T, q)\} \qquad (1)$$

in which T and q represent, respectively, wave period and wave attenuation. $O(T)$ depends on both the earthquake magnitude and the mechanism of seismic wave generation, while $Q(T, q)$ is determined by the reflection, refraction, scattering, and absorption of waves in the earth's crust.

In this paper, one of the empirical formulae for the spectrum of earthquake motions obtained in the previous paper[1] is somewhat improved, following which the formula is applied to one case in Japan and nineteen cases in the U.S.A. for which strong earthquake motion observations are available.

2. The spectrum of seismic waves at depth

The following empirical formula, which has previously been reported[2] describes the amplitude-period relation of seismic waves at depth of the epicentral distance Δ in km and a magnitude M:

---

[1] K. KANAI, " A Study of Strong Earthquake Motions," *Bull. Earthq. Res. Inst.*, **36** (1958), 295-310.

[2] *loc. cit.*, 1), 297, equation (7).

$$\bar{u}=10^{0.61\,M-1.73\log\varDelta-1.47}T \qquad (2)$$

$$[0.05,\ 0.1\,\mathrm{sec}<T<T_m]$$

in which u and T represent, respectively, the displacement amplitude in cm and the period in second of seismic waves at depth and 0.05, 0.1 sec and T_m[3] are represented schematically in Fig. 1.

It follows directly from (2) that

$$\bar{v}=10^{0.61M-1.73\log\varDelta-0.67}, \qquad (3)$$

$$\bar{a}=\frac{10^{0.61M-1.73\log\varDelta+0.13}}{T}, \qquad (4)$$

where $\bar{v}$ is the spectral velocity in cm/sec and $\bar{a}$ is the spectral acceleration in cm/sec^2 of seismic waves at depth.

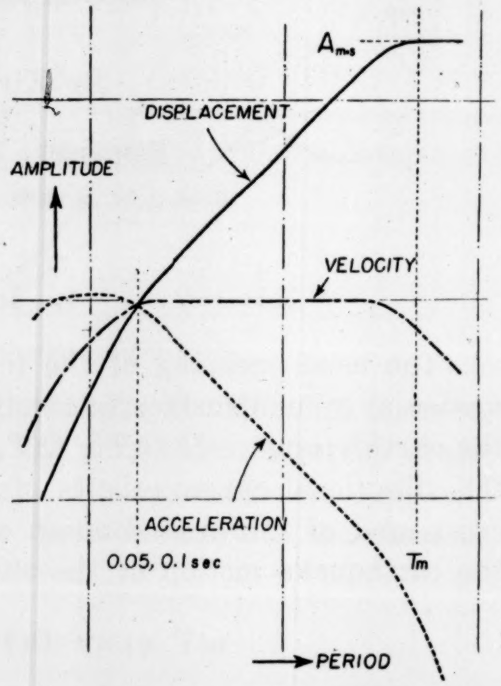

Fig. 1. Schematic figure of the displacement, the velocity and the acceleration spectra of seismic waves at depth.

3. The vibrational characteristics of the ground

Understanding of the seismic characteristics of the ground surface is being clarified as a result of observational investigations of earthquakes and microtremors, statistical analyses of earthquake damage and theoretical studies of seismic waves. Based on earthquake and microtremor observations, and adding theoretical considerations, it has been obtained a semi-empirical formula (5)[4], for the seismic characteristics of the ground consisting of a layer overlying a semi-infinite medium:

$$G(T,\,q)=\frac{1}{\sqrt{\left\{1-\left(\frac{T}{T_0}\right)^2\right\}^2+\left\{\frac{0.2}{\sqrt{T_0}}\frac{T}{T_0}\right\}^2}} \qquad (5)$$

---

3) K. KANAI and S. YOSHIZAWA, "The Amplitude and the Period of Earthquake Motions. II," *Bull. Earthq. Res. Inst.*, **36** (1958), 278, equation (5).

loc. cit., 1), 295, equation (1).

4) K. KANAI, "Semi-empirical Formula for the Seismic Characteristics of the Ground," *Bull. Earthq. Res. Inst.*, **35** (1957), 309-325.

K. KANAI, R. TAKAHASI and H. KAWASUMI, "Seismic Characteristics of Ground," *Proc. World Conf. Earthq. Engg., Berkeley* (1956), 31.

in which T and T_0 represent, respectively, in seconds, the period of seismic waves and the predominant period of the ground.

Strictly speaking, the stratum alone cannot be regarded as a conservative system, but the vibrations in that stratum should be considered as taking place in a dissipative system.

The expression of the following formula, (6), has been modified from (5) in order to make it more closely analogous to the expression for motion of a stratified visco-elastic body:

$$G(T, q)=1+\frac{1}{\sqrt{\left[\frac{1+\alpha}{1-\alpha}\left\{1-\left(\frac{T}{T_0}\right)^2\right\}\right]^2+\left\{\frac{0.3}{\sqrt{T_0}}\left(\frac{T}{T_0}\right)\right\}^2}} \tag{6}$$

in which

$$\alpha=\sqrt{\frac{\rho_1\mu_1}{\rho_2\mu_2}}\left(\equiv\frac{\rho_1 V_1}{\rho_2 V_2}\right) \tag{7}$$

and ρ_1, μ_1, V_1 and ρ_2, μ_2, V_2, are respectively the densities, elastic constants and velocities of the layer and the subjacent medium.

The following special cases are presented as illustrations of (6).

(i) Cases of no surface layer or extremely long wave periods:

$$T_0 \rightarrow 0 \text{ or } T \rightarrow \infty\,;\; G(T, q) \rightarrow 1\,.$$

(ii) Cases of a thick surface layer or very short wave periods:

$$T_0 \rightarrow \infty \text{ or } T \rightarrow 0\,;\; G(T, q) \rightarrow \frac{2}{1+\alpha}\,.$$

(iii) The case of resonance:

$$T=T_0;\; G(T, q)=1+\frac{\sqrt{T_0}}{0.3}\,.$$

In cases (i) and (ii) the ground magnifies the wave motion only very slightly. In case (iii) the values from (6) correspond very closely with those obtained from the previous formula (5).

4. Comparisons of computed and observed spectral values

Combining equations (2), (3) and (4) with (6) yields the following empirical formulae for ground surface earthquake motion spectra:

$$u=10^{0.61M-1.73\log\Delta-1.47}T\left[1+\frac{1}{\sqrt{\left[\frac{1+\alpha}{1-\alpha}\left\{1-\left(\frac{T}{T_0}\right)^2\right\}\right]^2+\left\{\frac{0.3}{\sqrt{T_0}}\left(\frac{T}{T_0}\right)\right\}^2}}\right], \tag{8}$$

$$v=10^{0.61M-1.73\log\Delta-0.67}\left[1+\frac{1}{\sqrt{\left[\frac{1+\alpha}{1-\alpha}\left\{1-\left(\frac{T}{T_0}\right)^2\right\}\right]^2+\left\{\frac{0.3}{\sqrt{T_0}}\left(\frac{T}{T_0}\right)\right\}^2}}\right], \tag{9}$$

$$a=\frac{10^{0.61M-1.73\log\Delta+0.13}}{T}\left[1+\frac{1}{\sqrt{\left[\frac{1+\alpha}{1-\alpha}\left\{1-\left(\frac{T}{T_0}\right)^2\right\}\right]^2+\left\{\frac{0.3}{\sqrt{T_0}}\left(\frac{T}{T_0}\right)\right\}^2}}\right], \tag{10}$$

$[0.05,\ 0.1\,\mathrm{sec}<T<T_m]$

where u, v and a are, respectively, the spectral displacement in cm, velocity in cm/sec and acceleration in cm/sec^2 of earthquake motions at the ground surface.

There are some records of destructive earthquakes in Japan including the 1923 Kwanto earthquake, but none of them was successful. They are either incomplete or unreliable.

A comparison of the values of acceleration calculated by (10) with the analytical results obtained from the incomplete seismogram of the 1923 Kwanto earthquake which was recorded at the University of Tokyo is shown in Table 1.

Table 1. The values of acceleration of the 1923 Kwanto earthquake.

Earthquake		Station (Univ. of Tokyo)		Period (sec)	Acceleration (cm/sec^2)	
Date	M	Δ (km)	Orientation		Observed	Calculated
Sept. 1, '23	7.9	100	EW	1.35	100	110
				0.3	>250	290

Table 1 tells us that the agreement between calculated and observed values is rather good.

Table 2. Instrumental data of fourteen stations in U.S.A.

Station			Instrument		
No.	Location	No. of stories	Location	Orientation	Period (sec.)
I	Vernon, Calif., Centr. Manuf. Dist. Term.	6	basement	N08E	0.065
				N98E	0.065
II	Los Angeles, Calif., Subway Terminal Bldg.	13	subbasement	N39E	0.065
				N129E	0.065
III	El Centro, Calif., Irrig. Dist. Sub-station	1	ground level, slab	NS	0.065
				EW	0.065
IV	Helena, Montana, Carroll College	5	basement	NS	0.080
				EW	0.080
V	Ferndale, Calif., City Hall	2	slab	N45E	0.066
				N135E	0.065
VI	Santa Barbara, Calif., Court House	2~4	basement	N42E	0.064
				N132E	0.065
VII	Hollister, Calif., City Library	1	basement	N01E	0.066
				N91E	0.066
VIII	Olympia, Washington, Highway Test Lab.	1	slab	N80E	0.080
				N170E	0.081
IX	Seattle, Washington, Army Deport	1	shed	N02E	0.085
				N92E	0.085
X	San Francisco, Calif., Alexander Bldg.	16	basement	N81E	0.063
				N171E	0.065
XI	San Francisco, Calif., S. Pacific Bldg.	14	basement	N45E	0.067
				N135E	0.067
XII	San Francisco, Calif., State Bldg.	6	basement	N81E	0.065
				N171E	0.065
XIII	San Francisco, Calif., Golden Gate Park	1	slab	N10E	0.075
				N100E	0.077
XIV	Oakland, Calif., City Hall	16	basement	N26E	0.066
				N116E	0.068

Table 3. The values of periods of twelve destructive earthquakes in U.S.A.

Earthquake			Station		Period (sec.)	
No.	Date	M	No.	Δ(km)	Max. accel. recorded	Max. accel. of spectrum
1	Mar. 10, '33	6.3	I	45	0.3	0.3
			II	53	0.65	0.65, 0.3
2	Oct. 2, '33	5.3	I	27	0.35	0.3
			II	35	0.65	0.65, 0.3
3	Dec. 30, '34	6.5	III	56	0.5	0.5, 0.2
4	Oct. 31, '35	6.0	IV	24	0.4	0.4, 0.25
5	Sept. 11, '38	5.5	V	56	0.2	0.2, 0.4
6	May 18, '40	7.0	III	48	0.5	0.5, 0.2
7	Feb. 9, '41	6.6	V	121	0.3	0.3, 0.6
8	June 30, '41	5.9	VI	24	0.3	0.3, 0.6
9	Oct. 3, '41	6.4	V	80	0.3	0.3, 0.6
10	Mar. 9, '49	5.3	VII	16	0.35	0.35
11	Apr. 13, '49	7.1	VIII	72	0.35	——
			IX	88	0.9	0.9, 0.3
12	Mar. 22, '57	5.3	X	17	0.3	0.6
			XI	18	0.2	1.25
			XII	16	0.3	0.5
			XIII	13	0.2	0.5
			XIV	28	0.2	0.7

The instrumental records and spectra[5] of twelve United States earthquakes recorded by the United States Coast and Geodetic Survey in the period from 1933 to 1957 have been examined. The seismograph

---

[5] J. L. Alford, G. W. Housner and R. R. Martel, "Spectrum Analysis of Strong-motion Earthquakes," *1st Tech. Rep. Office Nav. Res., Contr. No. 6onr-244, Task Order 25, Project Design, NR-081-091*-(1951).

D. E. Hudson and G. W. Housner, "An Analysis of Strong-motion Accelerometer Data from the San Francisco Earthquake of March 22, 1957, " *Bull. Seism. Soc. Amer.*, **48** (1958), 253-268.

Table 4. The values of accelerations of twelve destructive earthquakes in U.S.A.

Earthquake		Station		Orientation	Acceleration (g)	
					Observed	Calculated
1	Mar. 10, '33	I	Vernon	N08E	0.10	0.12
				N98E	0.12	
		II	Los Angeles	N39E	0.04	0.06
				N129E	0.03	
2	Oct. 2, '33	I	Vernon	N08E	0.07	0.07
				N98E	0.08	
		II	Los Angeles	N39E	0.03	0.03
				N129E	0.02	
3	Dec. 30, '34	III	El Centro	NS	0.14	0.08
				EW	0.12	
4	Oct. 31, '35	IV	Helena	NS	0.11	0.19
				EW	0.12	
5	Sept. 11, '38	V	Ferndale	N45E	0.07	0.04
				N135E	0.06	
6	May 18, '40	III	El Centro	NS	0.28	0.21
				EW	0.17	
7	Feb. 9, '41	V	Ferndale	N45E	0.05	0.04
				N135E	0.03	
8	June 30, '41	VI	Santa Barbara	N42E	0.16	0.20
				N132E	0.12	
9	Oct. 3, '41	V	Ferndale	N45E	0.07	0.05
				N135E	0.07	
10	Mar. 9, '49	VII	Hollister	N01E	0.10	0.16
				N91E	0.14	

(To be continued)

(Table 4. Continued)

Earthquake		Station		Orientation	Acceleration (g)	
					Observed	Calculated
11	Apr. 13, '49	VIII	Olympia	N80E	0.18	0.15
				N170E	0.15	
		IX	Seattle	N02E	0.05	0.06
				N92E	0.05	
12	Mar. 22, '57	X	Alexander	N81E	0.04	0.08
				N171E	0.04	
		XI	S. Pacific	N45E	0.03	0.05
				N155E	0.03	
		XII	State Bldg.	N81E	0.05	0.10
				N171E	0.08	
		XIII	Golden Gate	N10E	0.07	0.14
				N100E	0.08	
		XIV	Oakland	N26E	0.03	0.04
				N116E	0.02	

constants and earthquake data appear in Tables 2 and 3. The resonance values of acceleration have been computed from (10), using as T_0 the periods of the maximum trace accelerations from Table 3. The calculated values are compared with values of the maximum recorded accelerations in Table 4 and Fig. 2. (The maximum recorded acceleration is the average of two waves in the vicinity of the maximum.) Again it will be seen in Table 4 as well as Fig. 2 that the comparison of the calculated and observed values is good.

In order to serve as a reference, the displacement, the velocity and the acceleration spectra in the cases where T_0 (predominant period of ground)$=0.2, 0.4, 0.6, 0.8, 1.0$ sec, Δ (epicentral distance)$=50, 100, 150$ km and M (magnitude)$=7, 8$, besides the condition where α (the impedance ratio of the surface layer to the subjacent medium)$=1/5$, are shown in Fig. 3. (The value of $\alpha=1/5$ is a plausible value in consideration of the average condition of the observation points in Japan and, in this case, the value of α has a slight influence upon the amplitude of the reso-

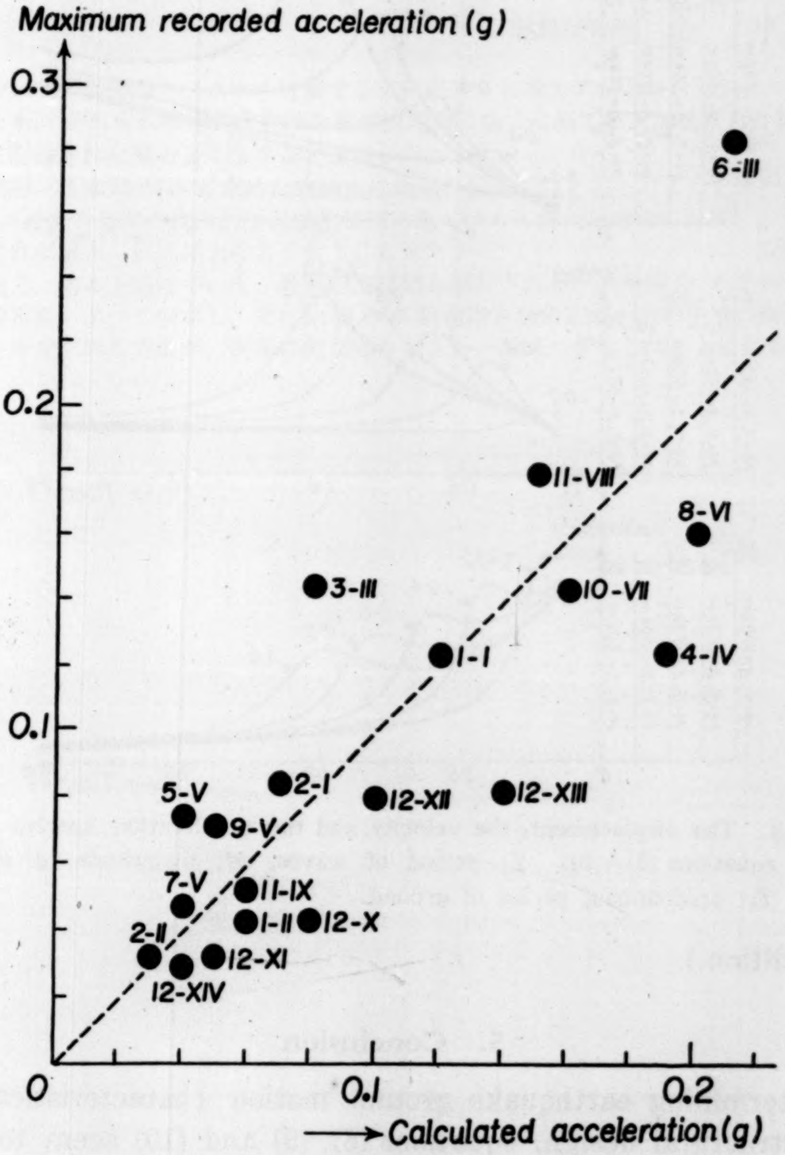

Fig. 2. Relation between the maximum recorded accelerations and the values of calculated accelerations obtained by using the empirical formula.

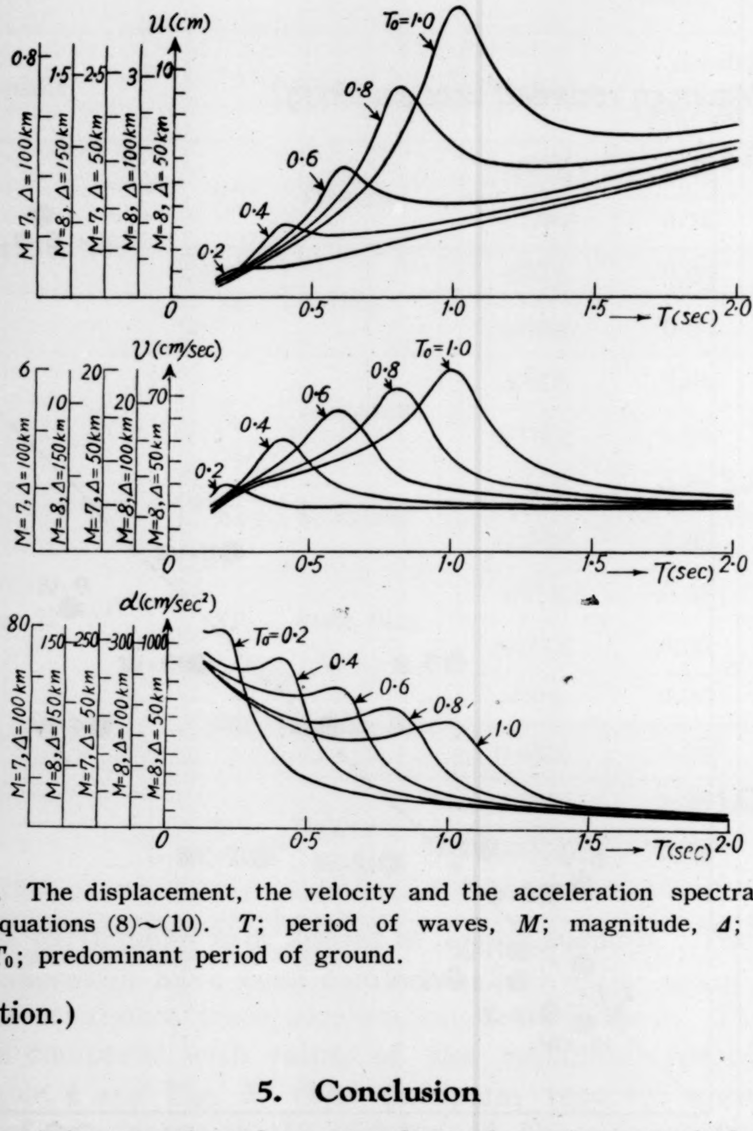

Fig. 3. The displacement, the velocity and the acceleration spectra obtained by using equations (8)∼(10). T; period of waves, M; magnitude, Δ; epicentral distance, T_0; predominant period of ground.

nance condition.)

5. Conclusion

In determining earthquake ground motion characteristics for purposes of structural design, equations (8), (9) and (10) seem to be applicable. The magnitudes and epicentral distances of anticipated earthquakes may be estimated by the application of engineering judgment to statistical analyses of the seismicity, and there can be thus obtained an approximate spectrum of seismic waves in the bed rock. If this spectrum is combined with the vibration characteristics of the ground at the structure, the lateral force coefficient can be determined.

The author wishes to thank Professor C. M. Duke, University of California, Los Angeles, and Miss S. Yoshizawa who have assisted him in preparing this paper.

4. 強震動スペクトルに関する実験式

地震研究所 金井 清

前論文において，地震動スペクトルに関する実験式を，日本とアメリカ合衆国について，別々に求め，それらを，それぞれの国の代表的な破壊的地震にあてはめて最大加速度を計算し，それらの値が，実際に記録された値とよく合うことを示した．

今回は，前回，日本について求めた実験式に地盤の振動特性を加えたものを求め，関東地震および12ケのアメリカ合衆国の代表的な破壊的地震にあてはめて最大加速度を計算し，それらの値が，実際に記録された値と，前回以上によく合うことを示す．

今回の研究で，ある土地について，最悪の地震動と期待される，大地震のマグニチュードと震央距離を工学的判断によつて仮定し，更に地盤の卓越周期を加味して，その土地の耐震工学上の強震地動スペクトルを求める方法が，実用に供し得ることが一層はつきりしたことになる．

Bulletin of the Earthquake Research Institute
Vol. 39 (1961), pp. 97-114

5. *On Microtremors. VIII.*

By Kiyoshi KANAI and Teiji TANAKA,

Earthquake Research Institute.

(Read Apr. 24, 1956; Jan. 27, Apr. 28 and July 21, 1959.—Received Dec. 28, 1960.)

Contents

1. Introduction.
2. The period distribution of microtremors.
3. The amplitude and the period of microtremors for time.
4. Microtremors in the underground.
5. Microtremors on the sea-bottom.
6. Local geology and microtremors.
7. Earthquakes and microtremors.
8. Classification of the ground by microtremors.
9. Conclusion.
10. Appendix.

1. Introduction

In an ordinary place, a seismograph which has more than about a thousand times magnification, records the ground motions continuously.

Usually, the amplitudes of the motions are 0.1~1 microns, and the range of their periods are from 0.05, 0.1 sec to 1, 2 sec.

Such ground vibrations are called microtremors.

Microtremors are chiefly caused by artificial disturbances such as traffic, industrial machines and so on. Therefore, generally speaking, the larger the city, the greater the amplitudes of microtremors.

The study concerning microtremors was started soon after seismology had been established as a branch of science[1]. Otherwise, little research have been done intermittently, until several years ago[2], because it had been considered as a slight interest of phenomena in the study of natural science. In recent years, some investigations of microtremors were carried out in order to develop the studies relating to not only natural microearthquakes but also explosion seismic waves[3].

---

[1] F. OMORI, "On Micro-tremors", *Bull. Earthq. Inv. Comm.*, **2** (1908), 1-6.

[2] U. INOUYE, "Comparison of Earth Shakings Above-ground and Underground", *Bull. Earthq. Res. Inst.*, **12** (1934), 712-741 (in Japanese).

M. ISHIMOTO, "Observations sur des secousses d'une petite Amplitude", *Bull. Earthq. Res. Inst.*, **15** (1937), 697-705.

From systematic measurements of microtremors which have been carried out at several thousands places in Japan, it was found that the properties of the ground as inferred from the characteristics of microtremors are utilizable for determining the seismic factor relating to earthquake-proof construction designs[4].

2. The period distribution of microtremors

The period distribution curve of microtremors shows a definite form for respective kinds of subsoils.

That is, when the formation of the ground relating to vibration characteristics is simple, as for instance, in the case of a simple stratified layer, a relatively sharp peak appears at about 0.1~0.6 sec on the period distribution curve of the microtremors.

---

[3] Y. TOMODA and K. AKI, "Frequency Analysis of Local Tremors of the Ground by means of a Magnetic Microseismic Spectrometer", *Journ. Seism. Soc. Japan, Ser. 2*, **5** (1952), 17-22 (in Japanese).

C. D. V. WILSON, "The origins and nature of microseisms in the frequency range 4 to 100 c/s", *Proc. Roy. Soc. London*, **217** (1953), 176-188.

C. D. V. WILSON, "An analysis of the vibrations emitted by some man-made sources of microseisms", *Proc. Roy. Soc. London*, **217** (1953), 188-202.

K. AKAMATU, "On Microtremors", *Journ. Seism. Soc., Japan, Ser. 2*, **9** (1956), 21-39 (in Japanese).

K. AKI, "Space and Time Spectra of Stationary Stochastic Waves with Special Reference to Microtremors", *Bull. Earthq. Res. Inst.*, **35** (1957), 415-456.

K. AKAMATU, "On Microtremors II", *Journ. Seism. Soc., Japan, Ser. 2*, **11** (1958), 40-48 (in Japanese).

[4] K. KANAI and T. TANAKA, "Measurement of the Microtremor", *Bull. Earthq. Res. Inst.*, **32** (1954), 199-209.

Subsoil Research Team, the Earthquake Research Institute, "Investigation into Seismic Characteristics of Subsoils in Tokyo", *Bull. Earthq. Res. Inst.*, **33** (1955), 492-495 (in Japanese).

K. KANAI, T. TANAKA and K. OSADA, "Measurement of the Microtremor. II. (Tokyo Metropolis)", *Bull. Earthq. Res. Inst.*, **35** (1957), 109-133 (in Japanese).

K. KANAI, T. TANAKA and K. OSADA, "Measurement of the Microtremor. III. (Yokohama City)", *Bull. Earthq. Res. Inst.*, **35** (1957), 135-148 (in Japanese).

K. KANAI, N. NASU, T. TANAKA and K. OSADA, "Measurement of the Microtremor. IV. (Sakata and Tsuruoka)", *Bull. Earthq. Res. Inst.*, **35** (1957), 149-162 (in Japanese).

K. KANAI, H. KAWASUMI, T. TANAKA and K. OSADA, "Measurement of the Microtremor. V. (Osaka City)", *Bull. Earthq. Res. Inst.*, **35** (1957), 163-180 (in Japanese).

K. KANAI, T. TANAKA, T. MORISHITA and K. NAKAGAWA, "Measurement of the Microtremor. VI. (Ichinomiya City, Aichi Prefecture)", *Bull. Earthq. Res. Inst.*, **35** (1957), 181-190 (in Japanese).

K. KANAI, T. TANAKA and K. OSADA, "Measurement of the Microtremor. VII. (Kawasaki City)", *Bull. Earthq. Res. Inst.*, **35** (1957), 191-200 (in Japanese).

On the other hand, when the formation of the ground is complex, more than two peaks appear at the periods between shorter than 0.2sec and longer than 1 sec on the curve mentioned above.

In fact, on a mountain a sharp peak appears at the period 0.1~0.2 sec, while on firm diluvial ground such as up-town in Tokyo the peak is at the period 0.2~0.4 sec. On the soft alluvial ground such as down-town in Tokyo the curve is irregular in shape and a number of peaks appear in the range of the period 0.4~0.8sec. On especially thick soft ground the curve is flat, the period ranging from 0.05, 0.1sec to 1, 2sec.

Microtremors recorded on various kinds of ground by the microtremor recorder, with the corresponding period distribution curves are shown in Fig. 1.

The period distribution curve is, in many cases, influenced greatly by the properties of the first medium of layered ground. On the other hand, the curves on fresh rock as well as on bed rock are flat at periods ranging from less than 0.1 sec to larger than 1 sec.

From these facts, we can consider that the amplitudes of microtremors at ground surface become larger at such periods as are synchronous with the natural period of the subsoil from the feature of selective resonance.

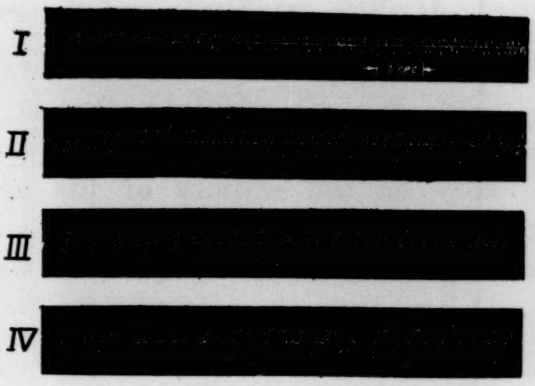

Fig. 1-a. Representative records of microtremors observed at the various kinds of ground. The symbols of I, II, III and IV represent the kinds of ground used in the Building Code of Japan.

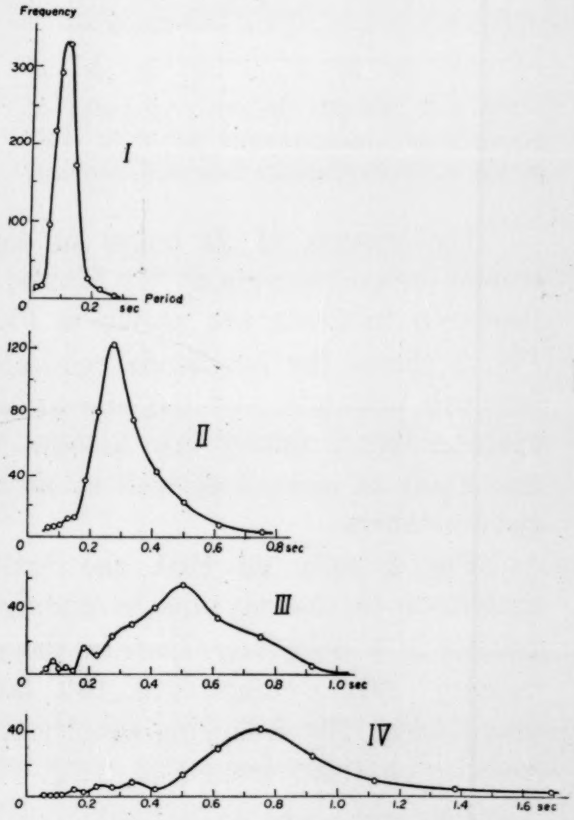

Fig. 1-b. Representative period distribution curves of microtremors at the various kinds of ground. (A part of the each record of them are shown in Fig. 1-a.)

3. The amplitude and the period of microtremors for time

The largest amplitude of microtremors during the daytime is much greater than at midnight, that is to say, the ratio of daytime to midnight is 2~10 times, because the amplitude of the microtremors depends greatly on the activity of the artificial vibration source surrounding the measuring place. Here, the largest amplitude is used to mean the average of the large amplitudes which often appear.

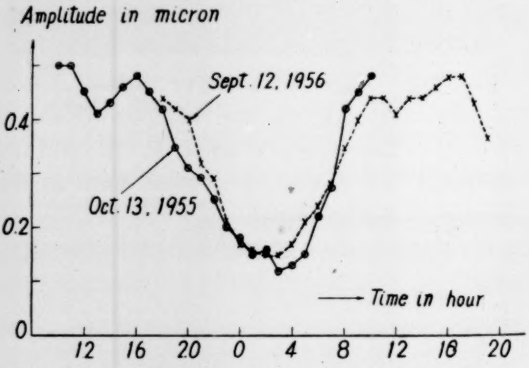

Fig. 2-a. Results (largest amplitudes) of microtremor measurements for a 24 hour period at the Earthquake Research Institute.

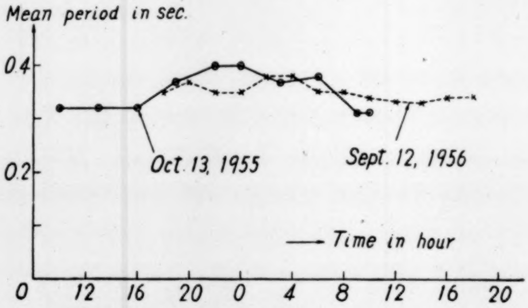

Fig. 2-b. Results (mean periods) of microtremor measurements for a 24 hour period at the Earthquake Research Institute.

The results of 24 hours of microtremor measurements at the Earthquake Research Institute are shown in Fig. 2. Fig. 3 shows the amplitude relationship between midnight and daytime at thirty spots in Japan, taking into amount various kinds of subsoil as well as artificial circumstances.

Fig. 3 tells us that the ratio of amplitude in the daytime to midnight is smaller in a noisy city than in the quiet country side. Regarding the largest amplitudes, the following empirical formula is obtained from Fig. 3:

$$(\text{midnight}) = 0.3 \times (\text{daytime})^{1.5} \quad (1)$$

Fig. 4 shows the predominant, the mean and the largest period relations between midnight and daytime at twenty spots

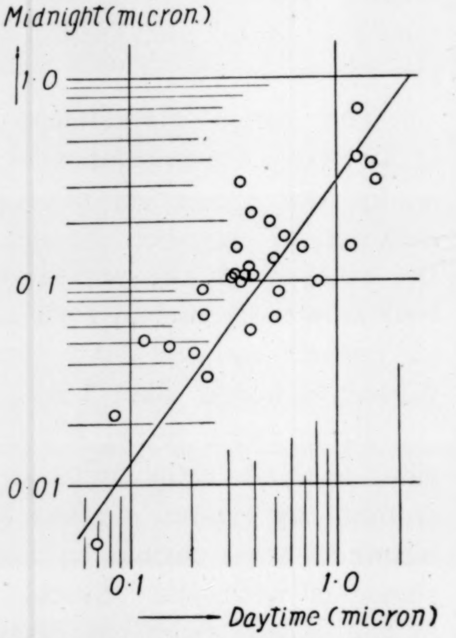

Fig. 3. Amplitude relation of microtremors between midnight and daytime.

in Japan with various kinds of subsoil.

Fig. 4 as well as Fig. 2 shows us that the predominant, the mean and the largest periods of microtremors change slightly with time and depend greatly on the vibration characteristics of the subsoil. Here, the largest and the predominant periods mean, respectively, the longest period of waves recorded by the microtremor recorder (1 sec natural period and proper damping) and the peak period of the period distribution curve.

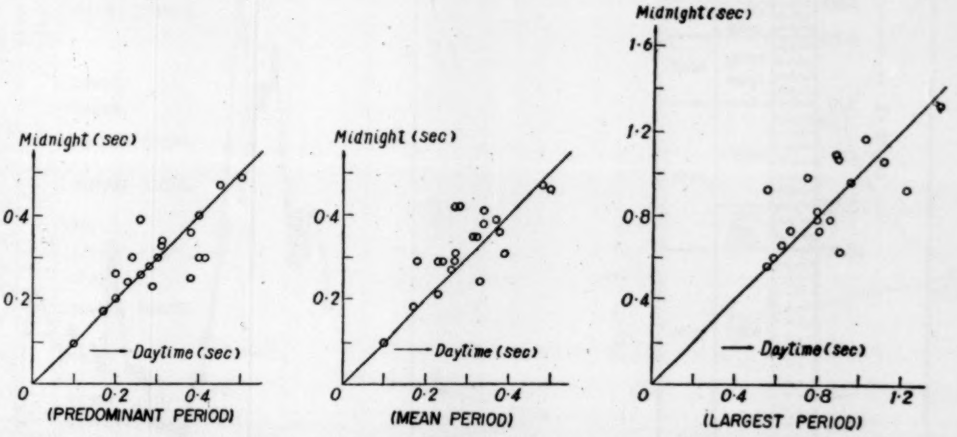

Fig. 4. Period relations of microtremors between midnight and daytime.

4. Microtremors in the underground

Simultaneous observations of microtremors, using the bored-hole self-levelling vibrograph[5], at different depths at several places with different kinds of subsoil have been carried out by us.

(i) At Komaba, Tokyo.

Figs. 5 and 6 show, respectively, the boring log and the amplitude ratios of the ground surface to the 13.4 m depth at Komaba in Tokyo. It can be seen from Fig. 6 that the amplitude ratio mentioned above reaches its maximum at 0.25～0.30 sec period and its minimum at 0.35～0.40 sec period. On the other hand, Fig. 7, shows the period distribution curves at ground surface and at a depth of 13.4 m. It will be seen in Fig. 7 that the periods of 0.25～0.30 sec and 0.35～0.40 sec mentioned above, just correspond respectively, to the peak periods of period distribution curves at the respective places.

The amplitudes of microtremors of such periods as are synchronous

---

[5] K. KANAI and T. TANAKA, "Self-levelling Vibrograph", *Bull. Earthq. Res. Inst.*, **36** (1958), 359-368.

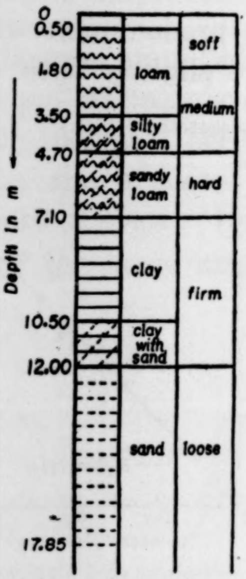
0
0.50
1.80
3.50
4.70
7.10
10.50
12.00
17.85
Depth in m
loam
silty loam
sandy loam
clay
clay with sand
sand
soft
medium
hard
firm
loose

Fig. 5. Boring log at Komaba, Tokyo.

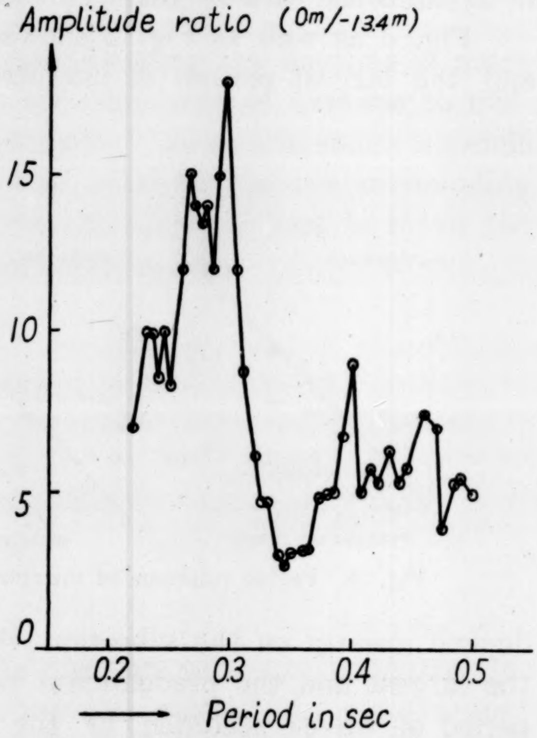

Fig. 6. Amplitude ratios of microtremors of the ground surface to the 13.4 meters depth at Komaba, Tokyo.

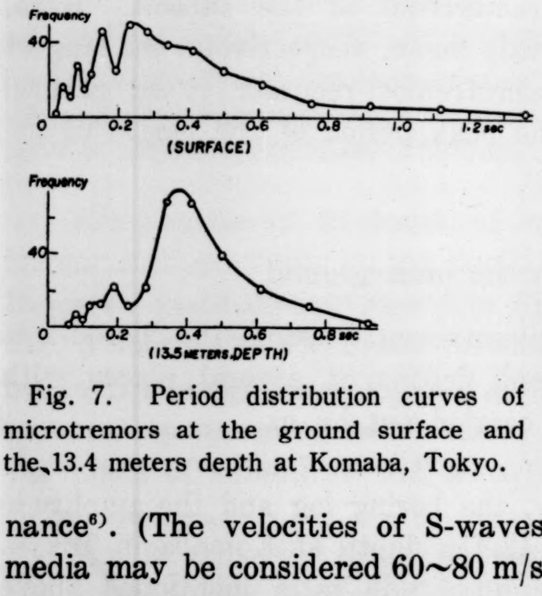

Fig. 7. Period distribution curves of microtremors at the ground surface and the 13.4 meters depth at Komaba, Tokyo.

with the natural ones of the strata, the superficial soft media of 4.70 m thickness and the intermediate loose sand layer of 5.6 m thickness, are relatively preponderant owing to the feature of selective resonance[6]. (The velocities of S-waves in the soft as well as the loose media may be considered 60~80 m/sec)

(ii) At Ōtemachi, Tokyo

Figs. 8-a and 8-b show respectively, the boring log and the relationship of the largest amplitudes to depths at Ōtemachi, Tokyo. On the other hand, the period distribution curves at the different depths are shown in Fig. 9.

It will be seen from Figs. 8-b, 9 and 8-a that, at a depth of 11.5 m, the largest amplitude is remarkably large, a very sharp peak

---

[6] K. KANAI and S. YOSHIZAWA, "Relation between the Amplitude of Earthquake Motions and the Nature of Surface Layer. III", *Bull. Earthq. Res. Inst.*, **31** (1953), 275-279.

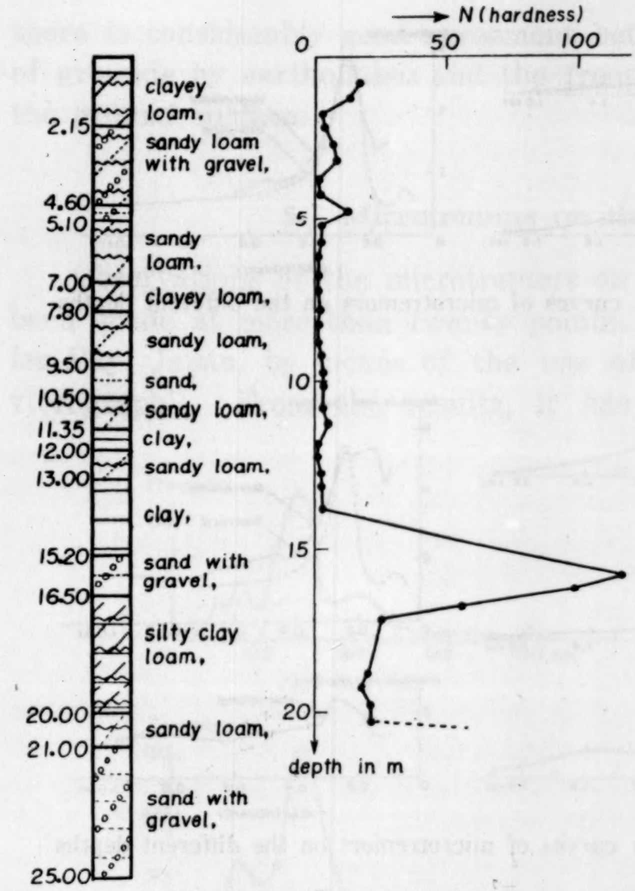

Fig. 8–a. Boring log at Ōtemachi, Tokyo.

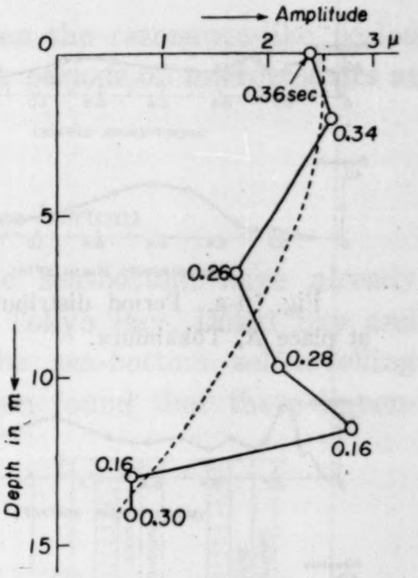

Fig. 8–b. Relation of the largest amplitude of microtremors to the depth at Ōtemachi, Tokyo.

appears in the period distribution curve and the hardness of the soil is not considerable. Then, from the above facts, it is possible to consider that amplitudes of about 0.1 second per period which are synchronous with natural ones of a clay layer of about 12 m in depth are considerably preponderant, owing to the selective resonance. It seems that the broken line in Fig. 8–b probably means the amplitude distribution of waves of about 0.35 sec per period which synchronize with the natural period of the surface layer overlying the

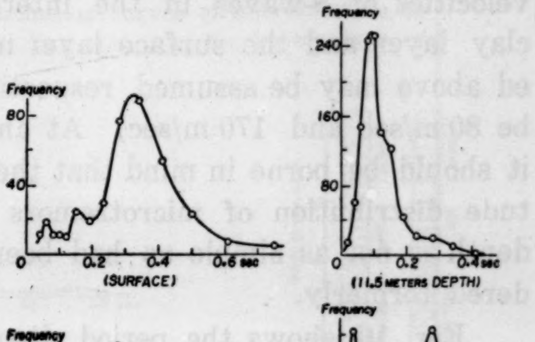

Fig. 9. Period distribution curves of microtremors on the different depths at Ōtemachi, Tokyo.

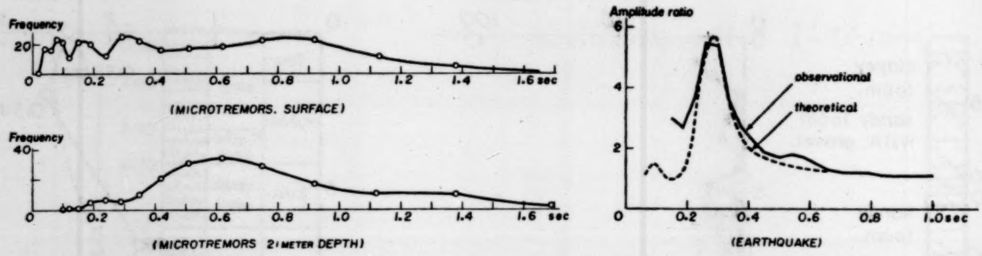

Fig. 10-a. Period distribution curves of microtremors on the different depths at place A, Tōkaimura.

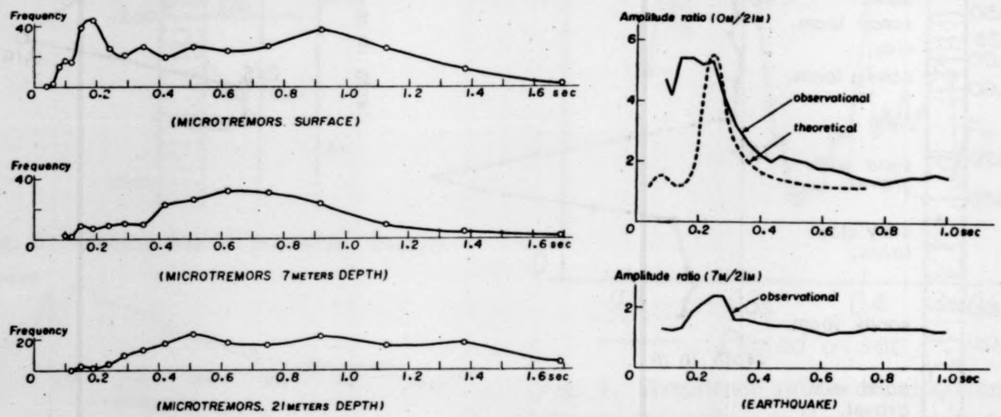

Fig. 10-b. Period distribution curves of microtremors on the different depths at place B, Tōkaimura.

15.20 m deep gravel layer. (The average velocities of S-waves in the intermediate clay layer and the surface layer mentioned above may be assumed, respectively, to be 80 m/sec and 170 m/sec) At any rate, it should be borne in mind that the amplitude distribution of microtremors to the depth is not as simple as had been considered formerly.

Fig. 10 shows the period distribution curves of microtremors at different depths at two places at Tokaimura, Ibaraki prefecture, together with the average amplitude ratios of the ground surface to the depth of the seismic waves observed at the same places.

It will be seen from Fig. 10 that

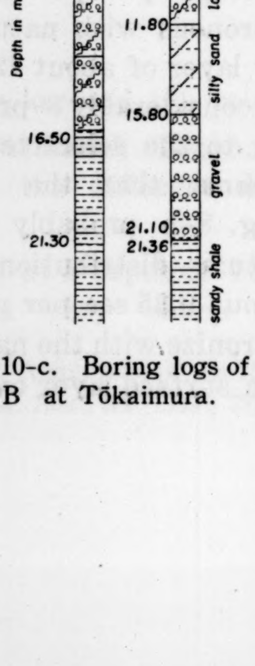
(B)
(A)
W.L.
4.26
W.L.
4.25
sand
7.00
7.30
7.20
7.55
Depth in m
loam with gravel
11.80
silty sand
15.80
16.50
gravel
21.10
21.30
21.36
sandy shale

Fig. 10-c. Boring logs of places A and B at Tōkaimura.

there is considerably good agreement between the resonance-like period of grounds by earthquakes and the frequent periods of microtremors at the ground surface.

5. Microtremors on the sea-bottom

Observations of the microtremors on the sea-bottom have already been made at more than twenty points, in Tokyo Bay, Dōkai Bay and Ise Bay, Japan, by means of the use of the sea-bottom self-levelling vibrograph[7]. From the results, it has been found that there is con-

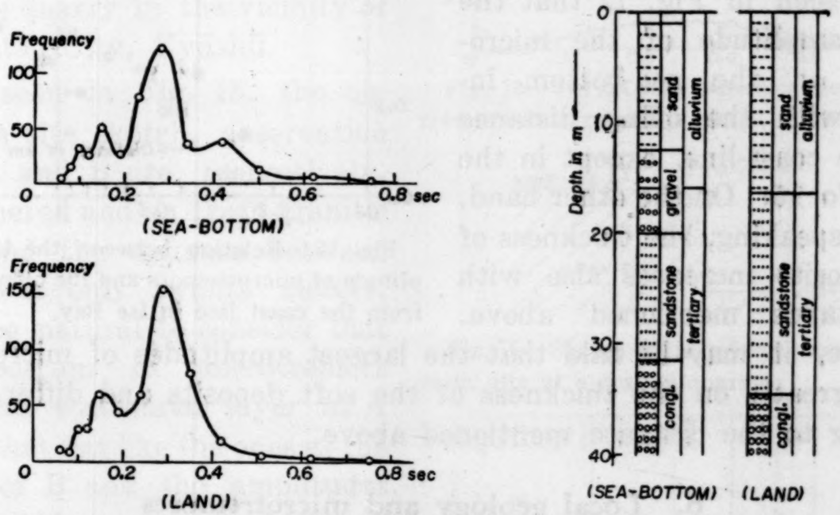

Fig. 11-a. Comparative period distribution curves of microtremors on the sea-bottom and on the land in Dōkai Bay area, and the boring logs of these places, respectively.

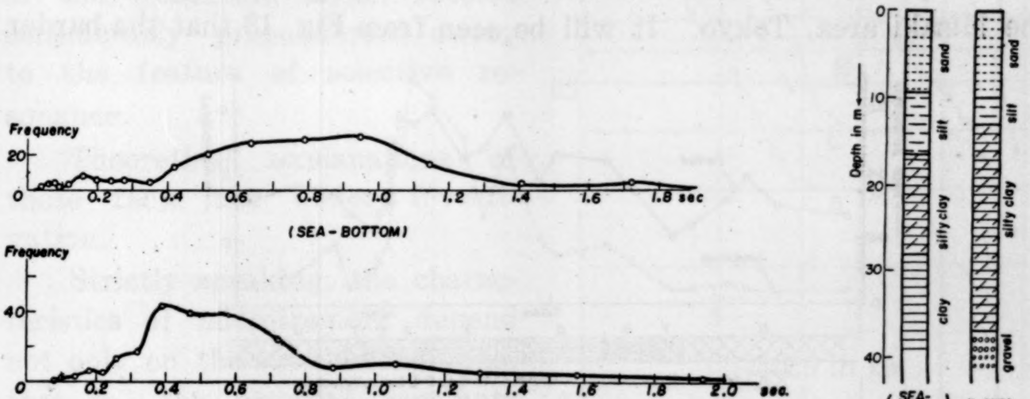

Fig. 11-b. Comparative period distribution curves of microtremors on the sea-bottom and on the land in Ise Bay area, and the boring logs of these places, respectively.

---

[7] *loc. cit.*, 5).

siderably good similarity between the characteristics of the microtremors on the sea-bottom and the ones on the land.

Fig. 11 shows some examples of the comparative period distribution curves of microtremors observed on the sea-bottom and on the land. Fig. 12 represents the relation between the largest amplitudes of the microtremors and the offing distances from the coast-line of Ise Bay[8]. Roughly speaking, it will be seen in Fig. 12 that the largest amplitude of the microtremors on the sea-bottom increases with the offing distance from the coast-line, except in the case of No. 15. On the other hand, roughly speaking, the thickness of soft deposits increases also with the distance mentioned above. Therefore, it may be said that the largest amplitudes of microtremors depend greatly on the thickness of the soft deposits and differ slightly according to the distance mentioned above.

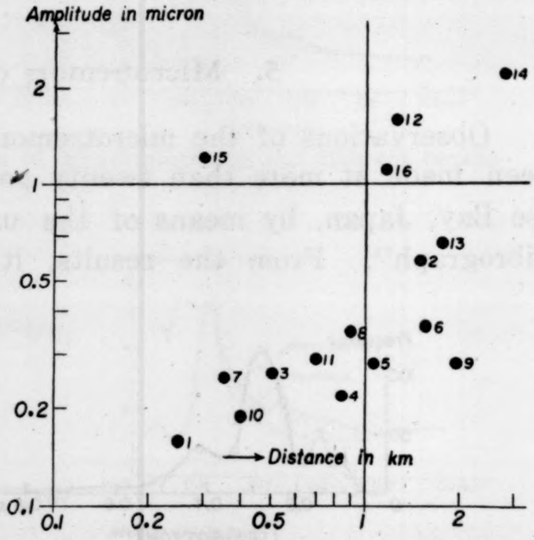

Fig. 12. Relation between the largest amplitude of microtremors and the offing distance from the coast line in Ise Bay.

6. Local geology and microtremores

Fig. 13 shows the relations among the mean periods as well as the largest amplitudes of microtremors and the local geological formations at the Misaki area, Tokyo. It will be seen from Fig. 13 that the harder

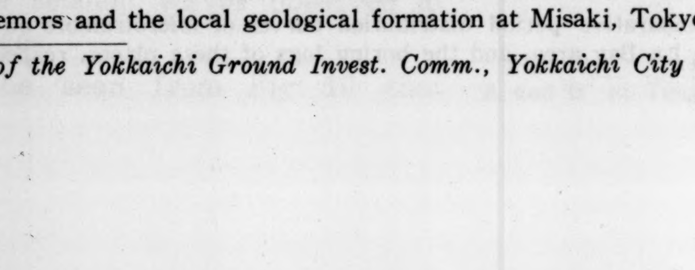

Fig. 13. Relation among the mean period and the largest amplitude of microtremors and the local geological formation at Misaki, Tokyo.

---

[8] *Report of the Yokkaichi Ground Invest. Comm., Yokkaichi City* (1959), 105–111 (in Japanese).

the subsoil, the longer the period and the larger the amplitude of the microtremors. Otherwise, in Fig. 13, the correlations among the periods as well as the amplitudes of the microtremors and the local geological formations seem surprisingly close because the distances between the observation points were rather short.

Fig. 14 shows typical comparative figures of the period distribution curves of microtremors at a granite quarry in the vicinity of Wakamatsu City, Kyūshū.

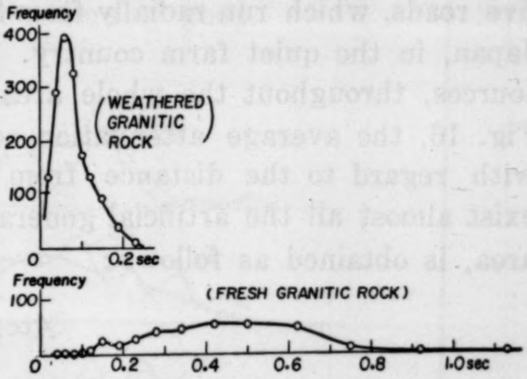

Fig. 14. Period distribution curves of microtremors at a granite quarry.

As seen in Fig. 15, the observation site sketch, observation points A and B are, respectively, on weathered and on fresh granitic rocks, and the distance between A and B is only twenty meters. It will be natural to consider that the spectrum of microtremors under the weathered layer at A is somewhat flat like the ones at the surface of B and the amplitudes at A of 0.06 sec period which are synchronous with the natural ones of the weathered layer, become considerably preponderant owing to the feature of selective resonance.

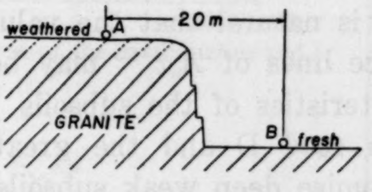

Fig. 15. Sketch of the microtremor measurement site at a granite quarry.

Theoretical explanations of these facts are under investigation.

Strictly speaking, the characteristics of microtremors depend not only on the subsoil conditions, that is, the physical constants and the dimensions of each material and the disposition of the materials which are made up of

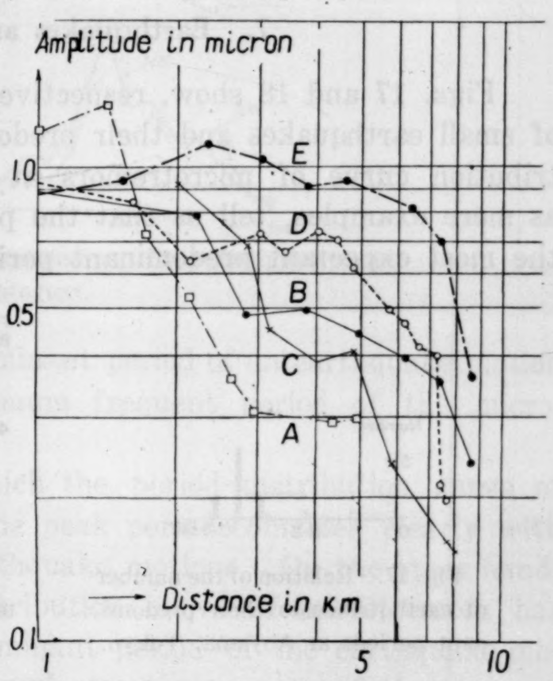

Fig. 16. Largest amplitude distributions of microtremors observed along the quiet roads which run from Sakata City.

so-called subsoil, but also on the activity conditions of artificial disturbances, that is, traffic, industrial machines, etc. Fig. 16 represents the largest amplitude distributions of microtremors observed along the five roads, which run radially from Sakata City in Yamagata prefecture, Japan, in the quiet farm country. There are few artificial disturbance sources, throughout the whole area where the five roads run. From Fig. 16, the average attenuation coefficient of microtremor amplitude, with regard to the distance from the margin of Sakata City, where exist almost all the artificial generation sources of microtremors in the area, is obtained as follows:

$$A \propto x^{-1.3} \qquad (2)$$

where A and x are, respectively, the maximum amplitude and the distance mentioned above.

It is natural that the values of the deviations from the amplitude-distance lines of $A_0 x^{-1.3}$ may be considered as the effects of the vibration characteristics of the subsoils themselves. Therefore, the middle part of the road D and the greater part of the road E are considered to compromise deep weak subsoils.

7. Earthquakes and microtremors

Figs. 17 and 18 show, respectively, the relation between the number of small earthquakes and their predominant periods and the period distribution curve of microtremors at Aoyama in Tokyo. These figures, as mere examples, tell us that the peak period of microtremors will be the most expectant predominant period for earthquakes.

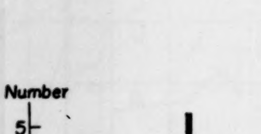

Fig. 17. Relation of the number of earthquakes to their predominant periods at Aoyama, Tokyo.

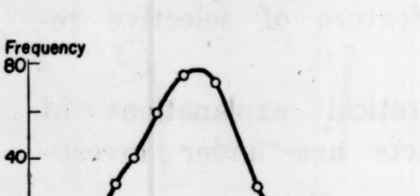

Fig. 18. Period distribution curve of microtremors at Aoyama, Tokyo.

Figs. 19 and 20 show, respectively, the period distribution curves of earthquakes observed with strong motion seismographs as well as of microtremors at San José, California, and Seattle, Washington, in the U.S.A. Figs. 19 and 20, are also mere examples which show us that the correlations between the period distribution curves of earthquakes and the ones of microtremors are considerably good.

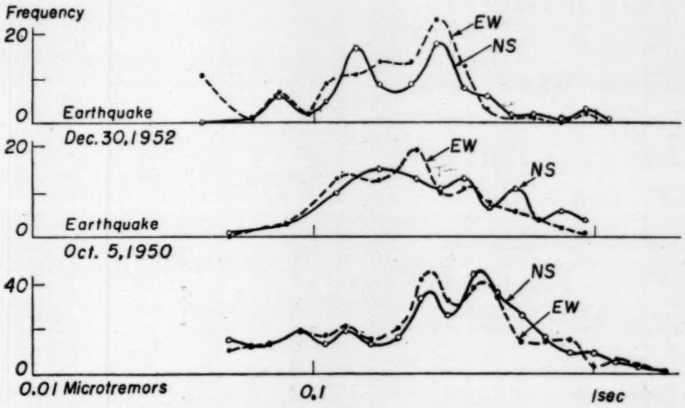

Fig. 19. Period distribution curves of the earthquakes and microtremors at San José, California.

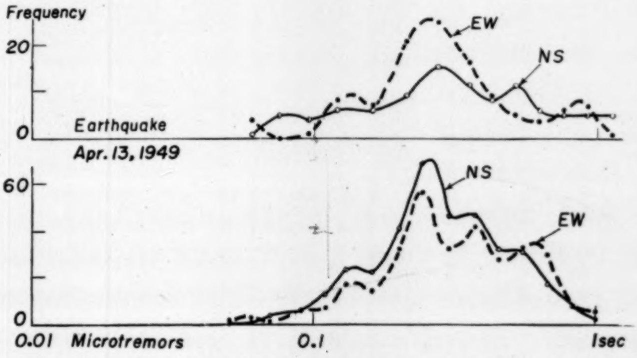

Fig. 20. Period distribution curves of the earthquake and microtremors at Seattle, Washington.

Generally speaking, the predominant period of an earthquake motion is closely connected with the maximum frequent period of the microtremors.

Furthermore, in a place in which the period distribution curve of microtremors has a single peak, the peak period coincides clearly with the predominant period of the earthquake motions. On the other hand, in a place in which the period distribution curve of microtremors has more than two peaks, the predominant period of the earthquake motions takes usually either of them and sometimes many of them.

8. Classification of the ground by microtremors

(i) The first proposal in ground classification. It has been stated, in Section 3, that the predominant, the mean and the largest periods change their values slightly whenever they are measured. (Here, the largest period means the largest wave recorded by the microtremor recorder which has a one second natural period and proper damping.) It is convenient to use the largest and the mean periods in a practical classification of the ground even though their physical purports have not as yet been made clear.

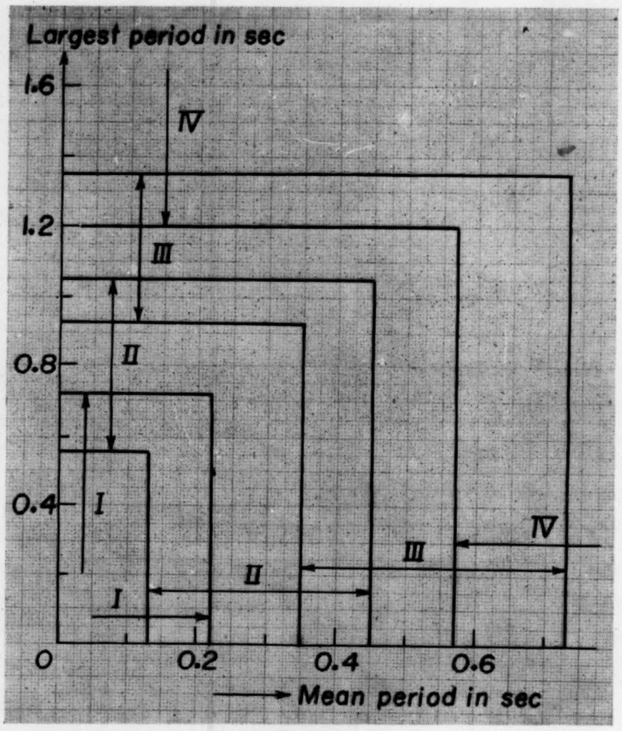

Fig. 21. The first proposal in the classification of the ground by microtremor measurement. Symbols I, II, III and IV represent the kinds of ground used in the Building Code of Japan.

Therefore, a diagram as shown in Fig. 21, which has been obtained after the trial and error method, considering the results of microtremor measurement as well as the subsoil conditions, is taken as the first proposal in a classification of the ground. The symbols I, II, III and IV in Fig. 21 represent the kinds of ground the same as used in the Building Code of Japan, and the standards for a designation of these kinds are presented in Section 10.

(ii) The second proposal in ground classification. We have experienced many cases in which the results of ground classification by the first proposal alone are considered to be unnatural. Now, some of them are described as follows :

(a) The predominant period of the short period appeared on a very thick soft ground, because such ground consisted of plural layers and the influence of the uppermost layer is remarkable.

(b) The period distribution curves on fresh rock, bed rock and sand hill take a very flat form.

Thereupon, it is inevitable that the largest amplitude of the microtremors should be taken into consideration in a classification of the ground even though the largest amplitudes change their values not only with time but also through artificial circumstances.

Consequently, the diagram of the relation of the largest amplitude to the predominant period, which has also been obtained after the same method as the first proposal as shown in Fig. 22 is adopted auxiliarily.

It is called the second proposal in ground classification.

(c) Earthquake damage and the types of ground classified by microtremors.

The relation between the percentage of earthquake damage to Japanese wooden houses in the case of the 1944 Tōkai earthquake at the Kikugawa River district, Shizuoka prefecture obtained by Ooba⁹⁾ and the kind of ground classification at each place arising from the first proposal together with the second one is shown in Fig. 23.

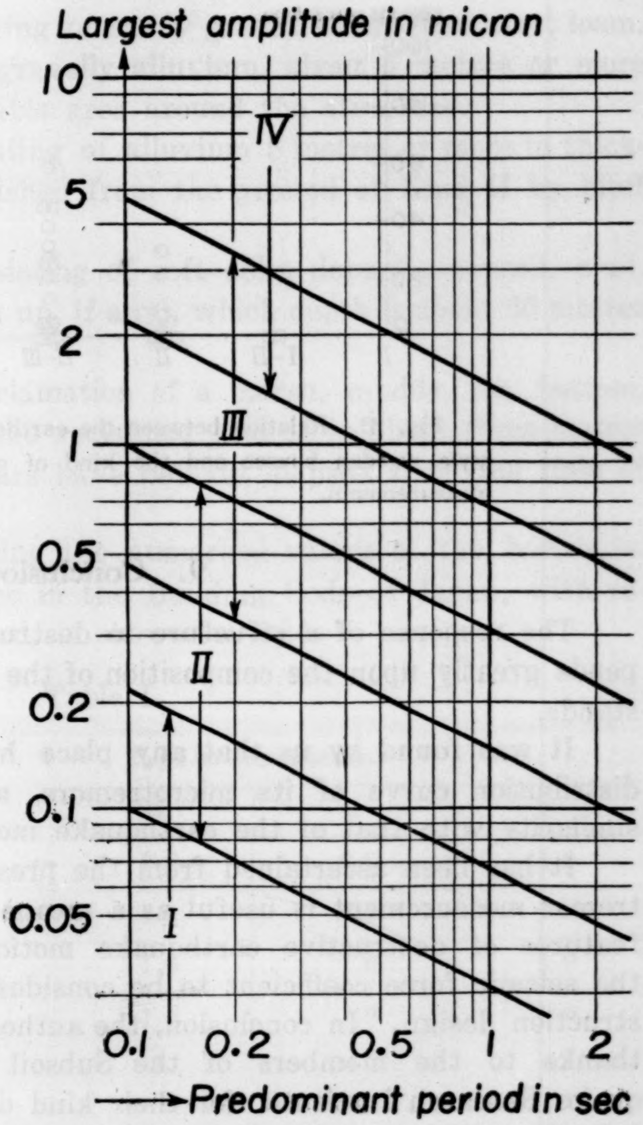

Fig. 22. The second proposal in the classification of the ground by microtremor measurement. Symbols I, II, III and IV represent the kinds of ground used in the Building Code of Japan.

It will be seen in Fig. 23 that the correlations between the earthquake damage ratios and the kinds of ground determined by the results of microtremor measurements are satisfactory.

---

9) S. OOBA, "Study of the Relation between the Subsoil Conditions and the Distribution of the Damage Percentage of Wooden Dwelling Houses in the Province of Totomi in the case of the Tonankai Earthquake of December 7th, 1944", *Bull. Earthq. Res. Inst.*, **35** (1957), 201-295 (in Japanese).

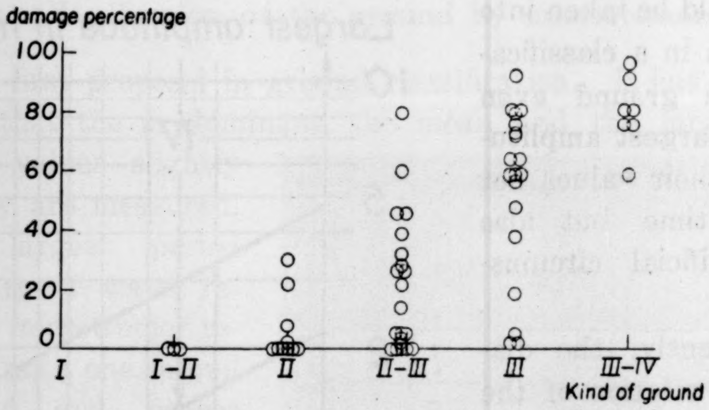

Fig. 23. Relation between the earthquake damage to Japanese style wooden houses and the kind of ground after microtremor measurements.

9. Conclusion

The response of a structure to destructive earthquake motions depends greatly upon the composition of the ground on which the structure stands.

It was found by us that any place has a definite type of period distribution curve of its microtremors, and it has considerably good similarity with that of the earthquake motions at the same place.

It has been ascertained from the present investigations that microtremor measurement is useful as a means not only for anticipating the features of destructive earthquake motions but also for determining the seismic force coefficient to be considered in earthquake proof construction design. In conclusion, the authors wish to express their hearty thanks to the members of the Subsoil Research Team, the Earthquake Research Institute, for their kind discussion in the course of this investigation and to the U. S. Coast and Geodetic Survey for co-operation in using the strong motion seismograms. The authors are much obliged to Messrs. T. Suzuki and K. Osada and to Miss S. Yoshizawa without whose help this work could not have been done.

10. Appendix

(i) The standards for the designation of four kinds of ground according to the Building Code of Japan are as follows:

Kind I: Ground consisting of rock, hard sandy gravel, etc., classified as tertiary or older strata over a considerable area around the structure.

Kind II : Ground consisting of sandy gravel, sandy hard clay, loam, etc. classified as diluvial, or gravelly alluvium, about 5 metres or more in thickness, over a considerable area around the structure.

Kind III : Ground consisting of alluvium 5 metres or more in thickness, which can be distinguished from the ground of Kind II by bluff formation.

Kind IV : Alluvium consisting of soft delta deposits, topsoil, mud, or the like (including heaping up, if any), which depth is about 30 metres or more.

Land obtained by the reclamation of a marsh, muddy sea bottom, etc., of which the depth of the reclaimed ground is about three metres or more and where thirty years have not yet elapsed since the time of reclamation.

(ii) Standerds for reducing the numerical values of the horizontal coefficient of the seismic force in the Building Code of Japan, with reference to the kinds of ground, is shown in Table I.

Table I.

Kind of ground	Type of construction			
	A	B	C	D
I	0.6	0.6	0.8	1.0
II	0.8	0.8	0.9	1.0
III	1.0	1.0	1.0	1.0
IV	1.5	1.0	1.0	1.0

A : Wooden construction.
B : Steel framed construction.
C : Reinforced concrete construction, steel frame and reinforced concrete construction, or steel-concrete composite construction.
D : Masonry, brick, concrete block and other constructions.

5. 常時微動について 第8報

地震研究所 金井 清
地震研究所 田中 貞二

常時微動の測定結果については，現在までに，19 回にわたつて地震研究所談話会で発表し，そのうち，東京，横浜，庄内，大阪，一宮，川崎の測定結果は，すでに，地震研究所彙報に第1報～第7報として掲載した．

本報告では，常時微動の一般的性質を，第1章～第8章で述べ，第9，10章では，常時微動の測定結果を地震工学上の地盤種別判定に利用する方法について述べる．

常時微動の頻度曲線と，同じ場所での地震動の頻度曲線および振巾スペクトルとに密接な関係のあることは，われわれの研究によつて，非常にはつきりしてきたが，日本では，まだ，強震動の満足な記録が得られていないので，それらの相関性が果して破壊的地震動にもあてはまるかどうか，いい換えると，常時微動によつて求められた地盤の振動的性質が地震工学上の構造物設計資料として，果して，役立つかどうかという点では，必らずしも，明確な答えが出されたとはいえなかつた．

筆者たちは，最近，アメリカ合衆国における強震計，普通地震計の設置場所，ならびに設置予定地の約 200 ヵ所で，常時微動の測定を行なつた．現在，それらの場所で得られた強震記録の各種方法の解析結果と常時微動の測定結果との比較検討を行なつているが，従来，地震動と常時微動には密接な関係があるという普通地震の比較で得られた結果が，強震動にもあてはまるという実例のごく一部を第7章で紹介した．

なお，東海地震の木造家屋の被害率と常時微動の性質からきめた地盤種別との間に，相当よい相関のあることもわかつた (第 23 図参照)．

強震動と常時微動との関係については，次回に詳しく報告するつもりである．

昭和36年3月25日印刷
昭和36年3月30日発行

東京都文京区本富士町一番地
東京大学構内
編纂兼発行者　東京大学地震研究所

東京都新宿区山吹町一八四番地
印刷者　笠井康頼

東京都新宿区山吹町一八四番地
印刷所　株式会社　国際文献印刷社

売捌所
東京都中央区日本橋通二丁目六番地
丸善株式会社

Sold by Maruzen Co., Ltd., Nihonbashi-dôri, Chûô-ku, Tôkyô.
Price of this copy: 328 Yen. (Postage exclusive.)